RELIABILITY ANALYSIS OF THE SPACE STATION FREEDOM ELECTRICAL POWER SYSTEM

by

Captain Michael C. Talbott

submitted in partial fulfillment of the requirements for the Degree of Master of Science

Thesis Advisor: Dr. Vira Chankong

Department of Systems Engineering
Case Western Reserve University

August 1989

RELIABILITY ANALYSIS OF THE SPACE STATION FREEDOM ELECTRICAL POWER SYSTEM

Abstract
by
Captain Michael C. Talbott

In space, the on-board electrical power system of a space station has to provide the power needed for scientific missions (discretionary loads) and everyday station housekeeping chores (non-discretionary loads). Due to size constraints of the spacecraft, the electrical power system's output, efficiency and reliability will be constrained producing a system that is imperfect.

This thesis applies traditional reliability techniques and modified methods to evaluate the reliability of the proposed NASA Space Station electrical power system. The modified methods take into account components and assemblies that have different levels of failure affecting the power output. These components and assemblies with failure levels other than "all or nothing" power outputs define each power output level between complete failure and expected nominal power. By applying this analysis approach to the proposed NASA Space Station electrical power system in conjunction with some reasonable assumptions, different levels of the electrical power output are identified along with the exceedance probability that each interval will occur at a specified time.

DEDICATION

I dedicate this thesis to my understanding wife, Navarre, who has endured through my anxieties and unusual schedules; and to my three children, Christopher, David and Nicole, who think their Daddy no longer has a job.

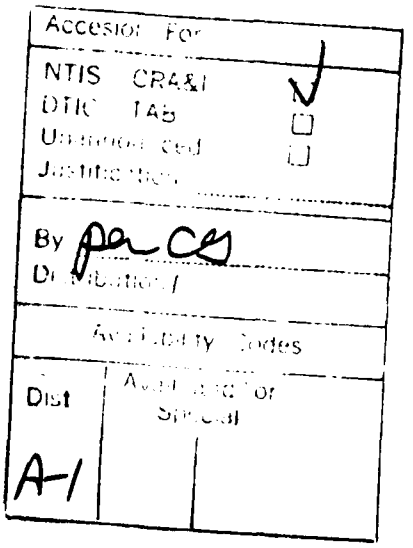

ACKNOWLEDGMENTS

We wish to thank Mr. David Hoffman, Systems Engineering and Integration Division of Space Station Systems Directorate at NASA Lewis Research Center, Cleveland, Ohio, who assisted and directed our efforts to model and analyze the Space Station electrical power system.

Thanks are also due to Dr. Karl Faymon and Mr. Jim Kish, Power Technology Division of the Aerospace Technology Directorate at NASA Lewis Research Center, Cleveland, Ohio, who assisted in obtaining related research materials and provided feedback on our efforts to produce a dynamic analysis tool useful to Space Station power system research.

Thanks are due to the Department of Mathematics, United States Military Academy, West Point, New York, who sponsored my attendance at Case Western Reserve University and allowed me the opportunity to pursue my Masters of Science degree.

Thanks are due to Ms. Denise DiFilippo, Lockheed, Houston, Texas, and Ms. Sylvia Washington, Engineering Directorate, NASA Lewis Research Center, whose assistance in providing research papers were instrumental in acquainting us with the Space Station electrical power system and whose research in the field of load scheduling provided us an initial objective to pursue.

Thanks are due to Igor Vaks, Case Western Reserve University, Cleveland, Ohio, who developed the Power System software that we used to do our analysis of the electrical power system.

Thanks are due to Dr. Vira Chankong, my thesis advisor, for his valuable guidance and advice and to Drs. Ken Loparo and Ben Hobbs for reviewing this work as members of my thesis committee.

Thanks are also due to my fellow students at Case Western Reserve University who helped me conquer that unforgiving invention - the computer.

Last, but not least, thanks are due to my family who have endured the long hours of concentrated effort necessary to keep my head above water and to produce this work.

TABLE OF CONTENTS

LIST OF FIGURES

LIST OF TABLES

CHAPTER 1 - INTRODUCTION

In any major product, resource constraints such as funding, time or space, limit our ability to provide an ideal end product. Instead, we seek an optimal use of our limited resources to provide the best possible product. In other words, we maximize the usage of our resources to achieve our desired end.

The problem of energy production in space is no different. On the surface, it appears that the energy source for space vehicles and satellites, the sun, is unlimited. It is the conversion of the sun's energy into usable electrical power, be it a photovoltaic, a solar dynamic, or some undiscovered process, that begins restricting the energy resource. The cost effectiveness of the energy conversion process and the overall objective of the space project further restrict the energy resource. As in the case of an orbiting space station, the shadow effects, caused by the earth's shadow falling over the space station, and the operational peak demands on board necessitate an energy storage system capable of supplying energy to compensate for these fluctuations. When deciding the type and capacity of the

energy storage system, its volume and weight requirements are weighed against the energy needs of the space station. Our present energy storage technologies have not produced a low cost system that overcomes the space and weight restrictions and simultaneously satisfies fluctuating energy demands and a space system's expansion of its power system.

Another constraining factor of the energy resource is the redundancy of the energy power system (EPS). Frequent system failures could call for a system that could handle greater fluctuations of energy input such as energy storage assemblies with larger capacities. On the other hand, the size of a perfect system with no failures is prohibitive, so a system whose design characteristics fall somewhere in between these two extremes must be designed. Since system failure, partial or total, is a real possibility, the probability of different types and magnitudes of failure becomes a key decision criteria in determining the amount of redundancy in the system.

Normally the size and weight of an assembly will increase as redundancy increases, thereby causing system engineers to balance these two factors against each other when designing the system. Inevitably, the amount of built-in redundancy will be restricted just as the amount of space for storage equipment or sleeping and eating

will be restricted. One way of quantifying the ability of a particular energy power system to satisfy its demand requirements is to calculate its capability to produce a certain amount of power that can be applied to its loads. Decisions then can be made on the size of the energy storage system or the amount of redundancy in each component. Given this information, decision makers and engineers can make intelligent compromises between weight, size and reliability.

One key objective for decision makers whenever any compromise is made concerning the EPS is the assurance that the minimum required electrical power will be available at any given time based on reliability models. Inevitably, each system on-board the Space Station including the EPS will be cut back near to its minimum acceptable level leaving little room for error or the luxury of spare resources. Careful decision makers will demand information on the effects of all options. Changes in the reliability of power outputs is just one common effect frequently examined. Thus, it is necessary to explore the reliability problem from several perspectives using as many applicable tools as possible.

One of these tools is to represent the reliability model as a series-parallel system and analyze this model's power output. However, since the Space Station

users will use as much energy as can be made available, there will be times when the demands will exceed nominal levels. These exceedances will be referred to as peak demands. At the other end of the spectrum, there will be times that available power will fail to meet the nominal level due to scheduled maintenance or component and assembly failures. Since the use of all energy will be closely managed, the probability of a certain output of power at a given time will be a key factor when deciding how to schedule the laboratory experiments or any preventive maintenance. The analysis of the series-parallel reliability model can provide insight into the possible "failure choke points" - components whose design specifications, if improved, would significantly enhance the reliability of the system. Since funding and other research resources are limited, identification of these "choke points" can direct decisionmakers toward the most efficient use of these resources. This translates into improving on redundancy of assemblies, improvement in mean-time-between-failures of components, increased energy production or storage capacities, or development of replacement and preventive maintenance policies.

Herein lie the objectives of this work: to develop a reliability model for the proposed EPS for the NASA Space Station Freedom; to break up the power spectrum of

the model into intervals where an exceedance probability can be determined for each interval; and to identify the components or assemblies that engineers and decisionmakers should focus on to most efficiently improve system reliability.

The remainder of this work will focus on discussing our effort in accomplishing the above objectives. After discussing the related works, we will begin identifying the assemblies and systems of the EPS. Then we will define the tools we used in forming our models. After identifying the assumptions essential to the feasibility of our model, we will discuss the methods we used in analyzing the model. We will note key results and conclude with a brief summary and concluding remarks.

CHAPTER 2 - RELATED WORK AND CURRENT RESEARCH OBJECTIVES

To date, most approaches on the reliability of the proposed Space Station electrical power system (EPS) have utilized simulation techniques for their analysis. Certainly, since this problem is so complex, Monte Carlo simulations work well. The shortcomings that exist in these works usually are found not in the simulation techniques used but in their ability to accurately model the EPS and simulate its operation.

Presently, the National Aeronautics and Space Administration (NASA), the architect of the Space Station Freedom project, is developing tools to analyze the power availability and reliability of the EPS. They have one analytic and two computer simulation approaches at their disposal.

The first approach is the UNIRAM methodology. ARINC Research Corporation [4], contracted by NASA to examine the EPS, used a UNIRAM reliability, availability, and maintainability (RAM) assessment methodology which incorporates an IBM, PC-based software package that employs an analytic technique to perform RAM analysis. It was developed primarily for determining the

availability of advanced power generation systems. UNIRAM builds a model of the power system in terms of the possible operating states it can be in [20]. Thus far, ARINC has used UNIRAM to examine the effects of different maintenance policies and has concentrated its efforts on availability over a time period rather than investigating strict reliability of the system or assemblies. They conducted a sensitivity analysis that produced a criticality ranking of components and subassemblies. ARINC had to model the insolar and eclipse cycles separately due to the dependencies between assemblies of each model. However, their simulation incorporated repairs and sparing (replacement of failed components with spares on-board the space station) to the system. Their model consisted of elements at different levels above and below the orbital replacement unit (ORU) level in an attempt to more realistically model the EPS. They did identify power levels between 100% and 0% by discretizing what is in reality a continuous power spectrum.

The second approach uses a program called TIGER. This program is one in a family of computer programs developed by the Naval Sea Systems Command to conduct RAM evaluation of complex systems [20]. This software was designed to be applied to ships and their on-board

systems. The TIGER output provides data on system reliability and average availability over a specified time period. To get reliability results, the program divides the number of successful runs ("success" is a simulation run that does not go below the designated minimum power level determined by the user) by the total number of simulation runs. This becomes quite cumbersome since the analyst has to determine the possible power output intervals and run the simulation for each interval. No extensive results on an EPS model are known using TIGER.

A third program called ETARA which uses the FORTRAN-based language APL, is also a RAM simulation model developed under the guidance of Hoffman [19] at NASA Lewis Research Center. It also is a Monte Carlo simulation that is primarily used for computing availability and reliability. It computes reliability by dividing the number of times the system or component did not fail over a specified time period by the total number of runs. It also computes the expected reliability based on the probability distribution function. This program determines the reliability for any power level in the same manner as the TIGER program does and has the same major drawback of being cumbersome. This program is extremely slow (100 one year runs take over twenty-four

hours on a PC) and, thus, very inconvenient. Also, like the two previous approaches, a combined insolar and eclipse model was not used.

Singh et al; [32] have taken a different approach by modeling the EPS as a continuous Markov process and conducting a frequency duration analysis. Using a transition rate matrix with a model of the photovoltaic and solar dynamic systems, they have one model that analytically examines both the insolar and eclipse cycles. The key element of their model is the transition rate matrix which takes into account only a few components but does allow for a repairable system. However, obtaining the transition rates is difficult since the systems have no data to derive these rates. For a complex model, which the EPS is, the implementation can become quite tedious and becomes a series of merging similar states to yield a state transition diagram for the system. Also, their models are inconsistent with the proposed design and do not consider the effects of the Power Management and Distribution (PMAD) system. Finally, only separate modeling of the PV and SD systems can be conducted.

Singh et al; [33] also used Monte Carlo simulation while modeling the EPS as a Markov process. They used the same models as they did in their analytic method;

however, in this simulation, they can assess a hybrid model that has both PV and SD systems. This method handles the charging/discharging effects of the energy storage assemblies well. Singh et al; were more concerned with developing the tool rather than a model; therefore, their results using their model have little value. This simulation was much quicker than the ETARA method; but for a more complex model of the EPS, simulation time would be much longer. This simulation method also does not consider the power levels between complete failure and maximum output.

These are the known related works but research is ongoing. ARINC is working on a combined insolar and eclipse model using the UNIRAM methodology. The Rocketdyne Division of Rockwell International is working on a reliability analysis as part of their contracted commitment to the Space Station EPS. However, no specific information concerning the techniques they are employing nor any results they have derived have been made public. Their contributions on the EPS's reliability will be the primary non-NASA work produced.

Each of the above works are the initial attempts to develop tools to analyze the reliability of the evolving EPS. Although each approach taken has merit, no one approach has been sufficient to accurately analyze the

EPS as it will operate. In this work, a different approach is taken in an attempt to provide another tool to use and expand upon in the pursuit of reliability information. The objective is to determine the reliability of the Space Station's EPS at the different power levels using analytical techniques. This reliability takes into account design specifications such as mean-time-between-failure (MTBF), failure distributions of components, the operating age of the system, and the interconnections that define the reliability model.

This model contributes to the expansion of the knowledge base that will be used for fault detection, fault prediction, scheduling of loads, and system and component reliability analysis. Since it is a analytical tool, its greatest value is to provide a prior probability distribution for the power output spectrum.

The reliability model that is developed in Chapter 3 must determine and account for the different power levels based on the interconnections and the components' effects on the power output. Since the Space Station electrical power system has been designed to prohibit total failure and to minimize the probability of catastrophic failure (where power requirements for minimal operation and life support cannot be satisfied), any useful power system

model has to provide information on the probability of the power levels between total success (maximum output) and complete failure (where the power output is zero).

This work describes the framework used in establishing the model; develops the reliability model for the Space Station electrical power system; identifies the assumptions it is based on; and identifies those components or assemblies that have the greatest impact on electrical power production on-board the proposed Space Station.

CHAPTER 3 - THE ELECTRICAL POWER SYSTEM MODEL AND ASSUMPTIONS

The Space Station electrical power system (EPS) is a hybrid configuration consisting of Photovoltaic (PV) and Solar Dynamic (SD) modules and a Power Management and Distribution (PMAD) system. Each PV module is designed to provide 18.75 kW net to the loads. Each SD module is designed to produce 25 kW net to the loads. In Phase 1 of NASA's plan, there will be four PV modules producing a net total of 75 kW. In Phase 2, two SD modules will be added giving the station a net total of 125 kW. Phase 1 also includes an unmanned polar sun synchronous (remains oriented towards the sun in the same position relative to the earth and sun) orbiting platform while Phase 2 augments the Space Station with an unmanned co-orbiting platform. The first Phase 1 launch is planned for 1994, and the phase should be complete by 1996, while Phase 2 should be completed in 1998. In the Growth Phase, the space station's optimal power level will grow to 325 kW by adding three additional pairs of SD modules to its configuration. The electrical power produced by the PV and SD modules passes to the PMAD which distributes power at 440 volt, 20 kHz, single phase AC and converts it to 208 volt, 20 kHz, single phase AC prior to reaching the

user and the power distribution and control units (PDCUs).

The Space Station will use a low-earth orbit between 180-250 miles above earth. Each station orbit will take approximately 90 minutes to complete of which the station will be sunlit for 60 minutes (insolar cycle) and in the earth's shadow for 30 minutes (eclipse cycle). During the eclipse cycle of each orbit an energy storage facility will provide the power for the station. A detailed description of the Space Station EPS can be found in the Primary Source Description Document (PSDD) [30].

In the next three sections a brief explanation of the different assemblies is provided along with their respective reliability diagrams (RBDs) to illustrate the model building process used.

PHOTOVOLTAIC MODULE

Since PV technology is proven, it will be deployed first to provide power to initiate Space Station operations in Phase 1. Four PV modules will be constructed for the Space Station, all during Phase 1. Two PV modules will be starboard and two will be port enabling power to enter the PMAD from two input sources.

The PV module consists of six assemblies: the solar array assembly (SAA), the beta gimbal assembly (BGA), the

integrated equipment assembly (IEA), the thermal control assembly (TCA), the electrical equipment assembly (EEA), and the energy storage assembly (ESA). A diagram of the proposed PV module is shown in Figure 3-1.

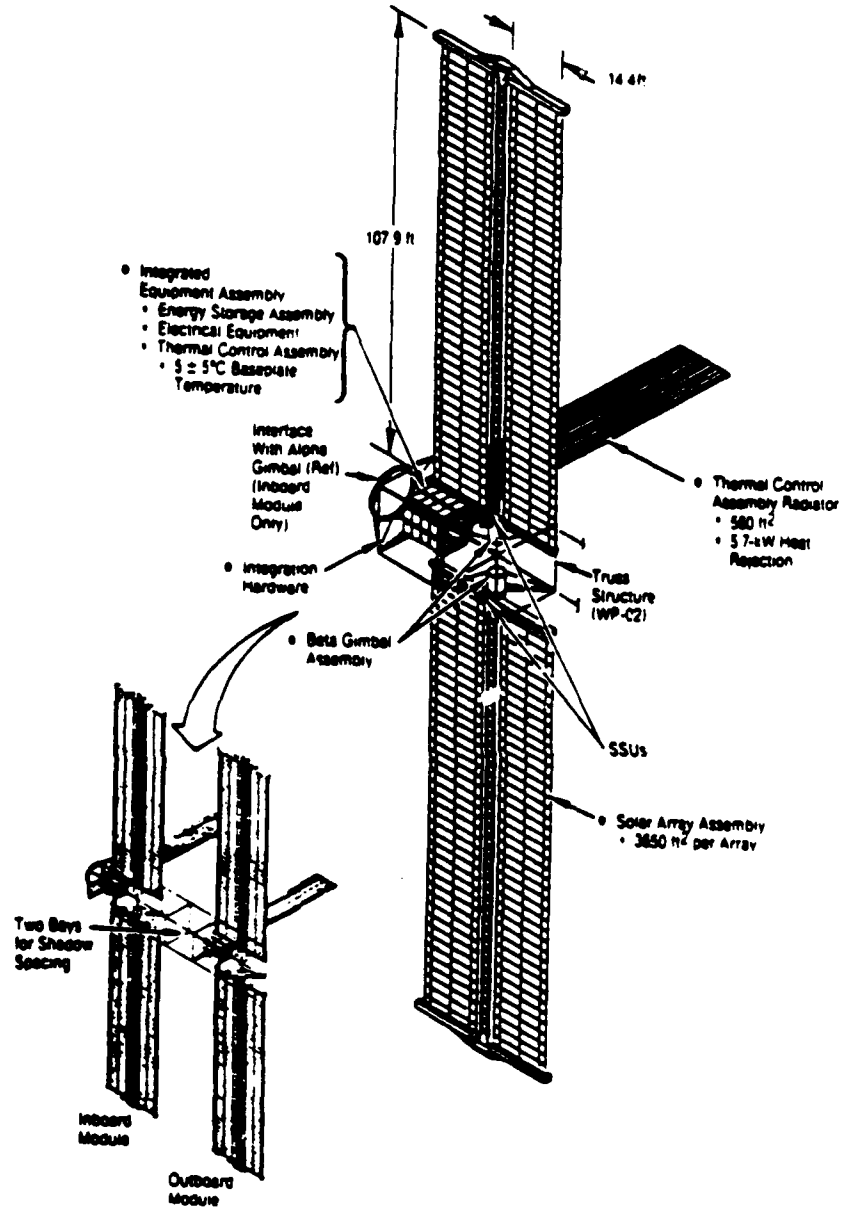

Figure 3-1. PV Module System.

Source: Power System Description Document, Rocketdyne, 1988.

There are two solar array assemblies in each PV module. Each has two solar array blankets that independently convert the solar energy into DC electrical power during the insolar cycle. The SAA includes the electrical hardware needed to manage the electrical power out of the PV wing. Each SAA consists of four ORUs (see Figure 3-2).

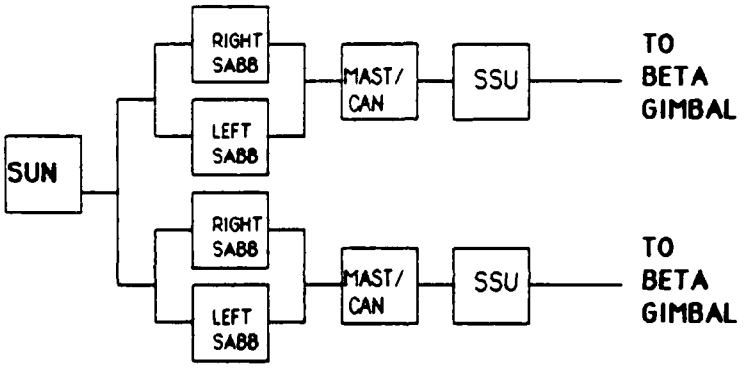

Figure 3-2. Solar Array Assembly RBD.

The beta gimbal assembly provides the beta angle solar orientation for each SAA, so each PV module has two BGAs. It also transfers data from the SAA across the rotating surface to the EEA. Each BGA consists of five ORUs (see Figure 3-3).

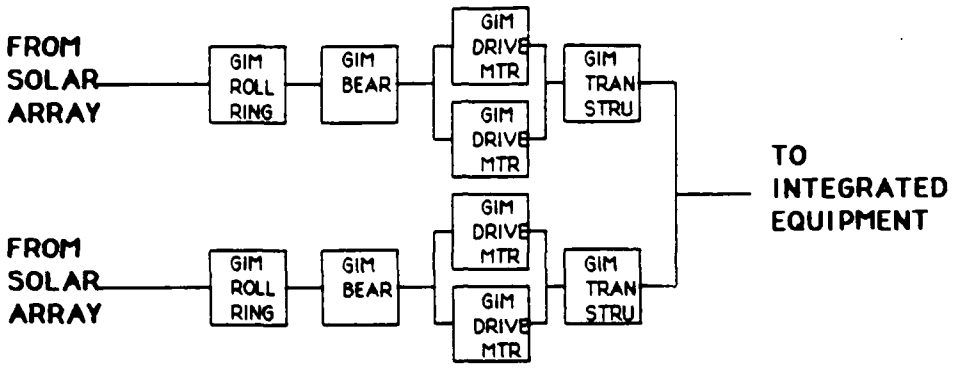

Figure 3-3. Beta Gimbal Assembly RBD.

The integrated equipment assembly is a box structure that provides mechanical support for the energy storage assembly, the electrical equipment assembly, and some components of the thermal control assembly. It is located between the bases of each solar array assembly. The IEA consists of two ORUs (see Figure 3-4).

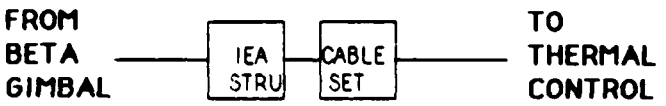

Figure 3-4. Integrated Equipment Assembly RBD.

The thermal control unit acquires, transports and rejects excess heat generated by the energy storage and electrical equipment assemblies. The eight utility plates are fastened to the four long sides of the IEA and

provide the surface for 32 ORUs from the ESA, EEA and TCA. If a utility plate fails, the four ORUs mounted on it will all overheat and fail. The heat rejection section consists of nine radiator subassemblies of which seven must work to ensure that the PV module components maintain temperatures within safe operational limits. The heat transport subassembly consists of two redundant series of six ORUs each. In total there are 47 ORUs in the TCA (see Figure 3-5).

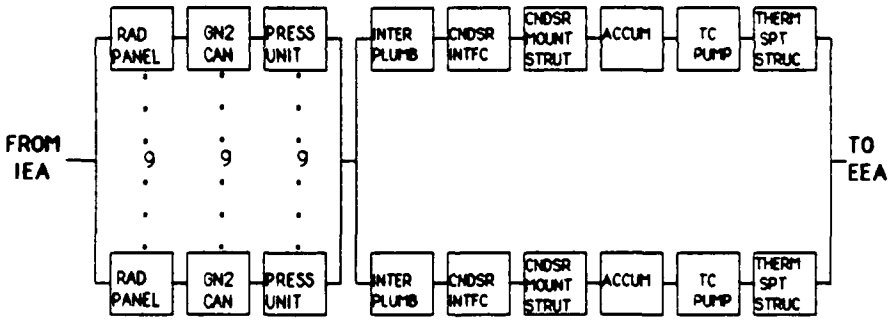

Figure 3-5. Thermal Control Assembly RBD.

Note: Utility plates are colocated with the ORUs mounted to them.

Among its many functions, the electrical equipment assembly accepts DC power from the solar array and energy storage assemblies and converts it to AC power. The EEA ORUs are mounted on utility plates. For our reliability

model, the main inverter units (MIUs) appear to be part of the energy storage assembly but are EEA ORUs. The EEA consists of ten ORUs (see Figure 3-6).

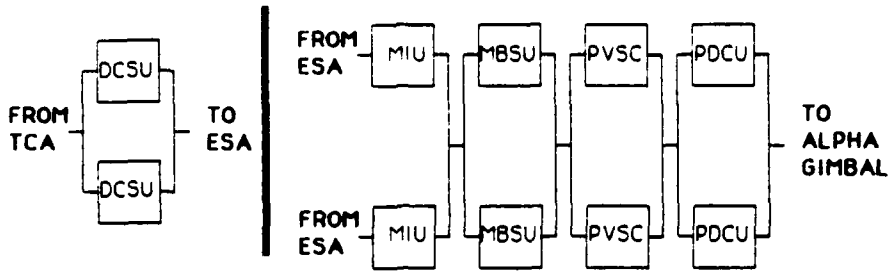

Figure 3-6. Electrical Equipment Assembly RBD.

The energy storage assembly, by far the heaviest assembly in the PV module, consists of 20 ORUs - five battery charge/discharge units (BCDUs) and 15 nickel-hydrogen battery packs. One BCDU and three battery pack ORUs are mounted on one utility plate. The ESA provides DC power during the eclipse cycle and peak demands and possesses the electrical hardware needed to manage the DC flows into and out of the batteries. (see Figure 3-7).

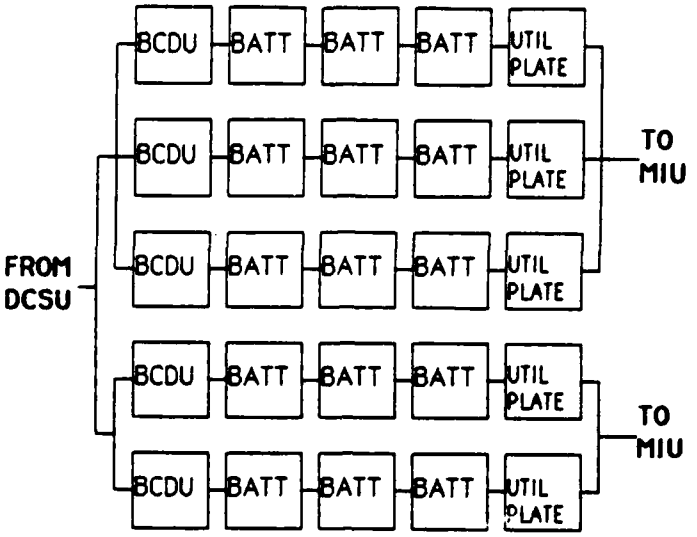

Figure 3-7. Energy Storage Assembly RBD.

The three battery packs are modeled in series since all three will be replaced if one fails. This policy is necessitated by thermal considerations.

The last major operational characteristic that had to be modeled was how the PV module operated during the insolar and eclipse cycles. Except during peak demands, the ESA does not provide power for the output. Likewise, during the eclipse cycle, the SAA and BGA do not affect the power output. Therefore, two models are needed, one for the insolar cycle and one for the eclipse cycle (see Figures 3-8 and 3-9). One of the major differences in our model from those presently used by NASA is we connect the insolar and eclipse models into one model. The "how" will be explained later in this work.

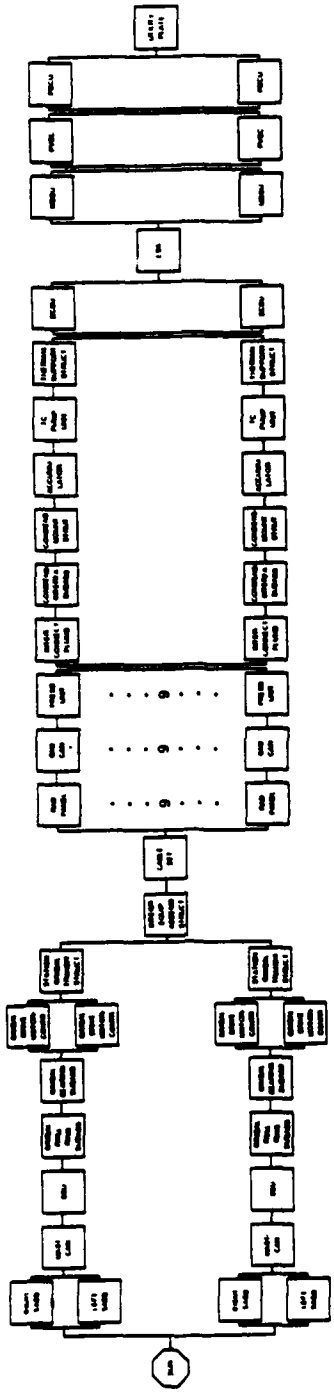

Figure 3-8. Insolar PV Model RBD.

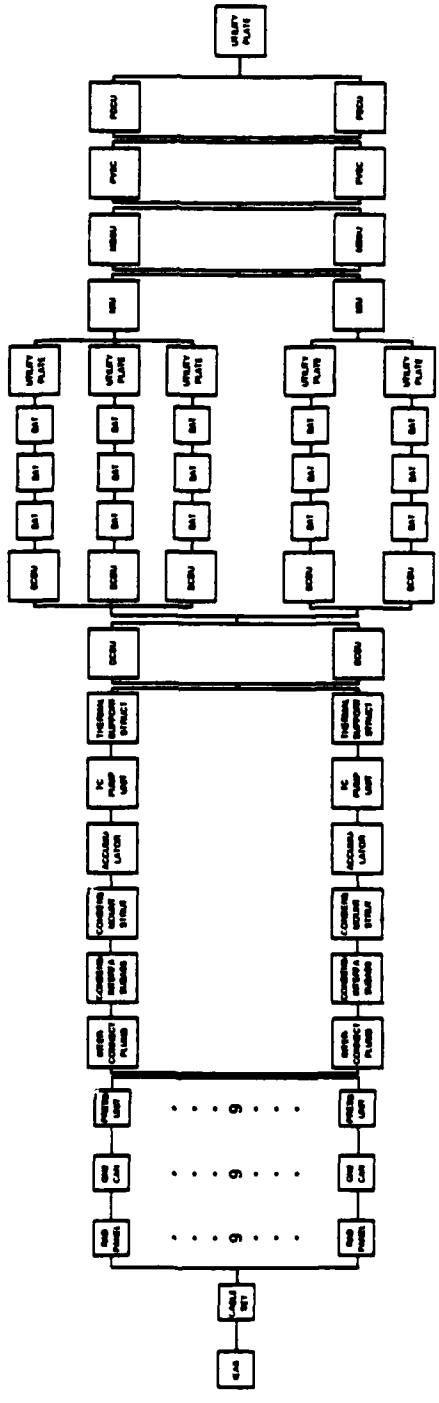

Figure 3-9. Eclipse PV Model RBD.

SOLAR DYNAMIC MODULE

The solar dynamic module collects solar insolation and converts it into usable electrical energy using a Closed Brayton Cycle system. The first two SD modules are not deployed until Phase 2. The SD technology has not been thoroughly tested in space, so this slight delay will allow for additional testing and analysis. The SD module should be much more efficient than the PV module, so NASA is planning to eventually deploy ten on the Space Station. The SD modules will be added to the Station in pairs, one starboard and one port, enabling power to enter the PMAD from two input sources. The SD module consists of six assemblies (we've combined two assemblies into one to have six in our model): the Concentrator Assembly, the Receiver/Power Conversion Unit (PCU) Assembly, the Heat Rejection Assembly (HRA), the Electrical Equipment Assembly (EEA), the Beta Gimbal Assembly (BGA), and the Interface Structure/Integration Hardware Assembly (IS/IHA). A diagram of the proposed SD module is shown in Figure 3-10.

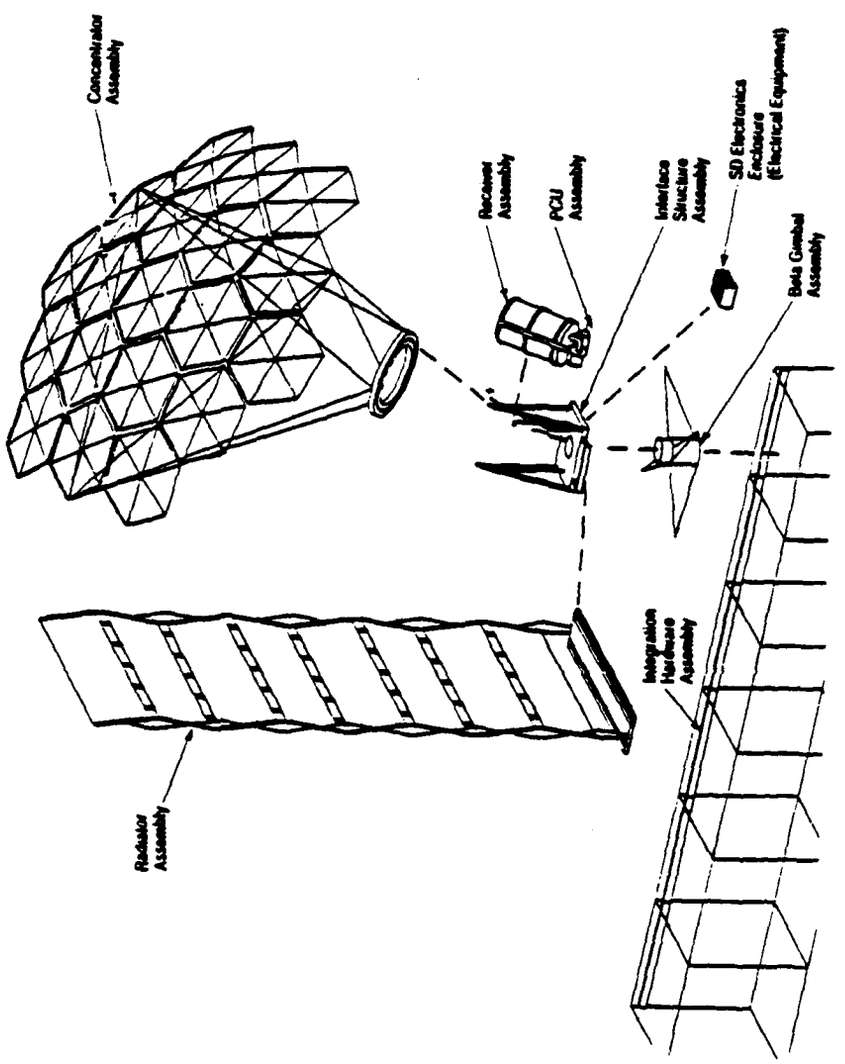

Figure 3-10. Solar Dynamic Module System.

Source: Power System Description Document, Rocketdyne, 1988.

The concentrator assembly collects the solar insolation and concentrates it at the receiver aperture. It has a fine-pointing mechanism that allows the concentrator to optimize the energy flow into the aperture. The concentrator assembly consists of seven ORUs (see Figure 3-11).

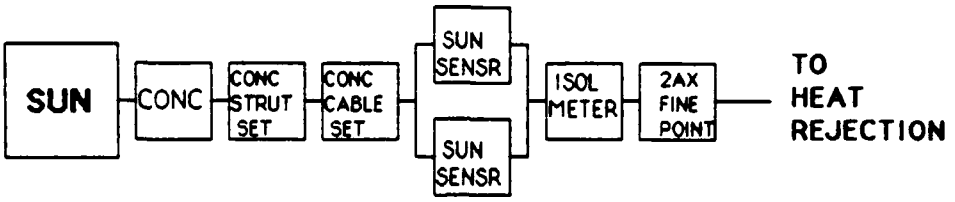

Figure 3-11. Concentrator Assembly RBD.

The heat rejection assembly collects the excess heat much like the PV module's TCA and radiates it into space. The radiator panel subassembly, unlike the radiator panels of the PV module, is one ORU. Along with it, the HRA has redundant interconnect lines that transports the excess heat from the PCU and EEA to the radiator panels. The utility plate, mounted on the interface structure assembly, serves as the surface for EEA components. The HRA consists of nine ORUs (see Figure 3-12).

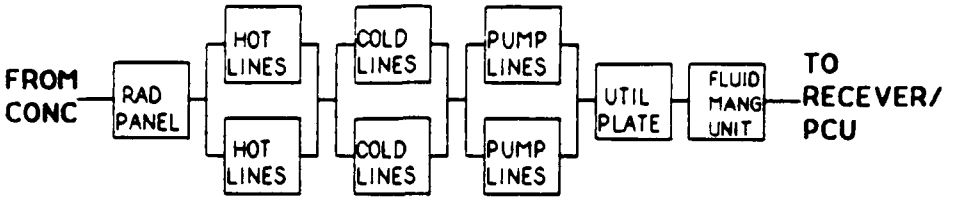

Figure 3-12. Heat Rejection Assembly RBD.

The receiver/power conversion unit receives the solar energy from the concentrator; transfers it to the PCU working fluid (He/ Xe mixture) and to a thermal energy storage material for use during the eclipse cycle; and converts the thermal energy into AC electrical power. The receiver/PCU assembly consists of six ORUs (see Figure 3-13).

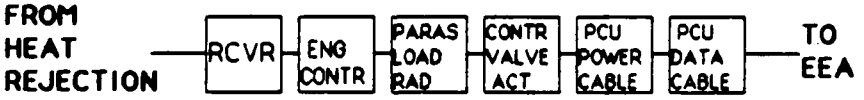

Figure 3-13. Receiver/Power Conversion Unit RBD.

The electrical equipment assembly converts the AC power produced by the PCU to usable AC power, manages the entire SD module, and provides fault isolation and detection within the SD module. The EEA is mounted to the interface structure assembly and consists of four ORUs (see Figure 3-14).

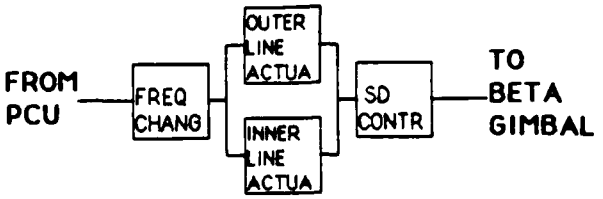

Figure 3-14. Electrical Equipment Assembly RBD.

The beta gimbal assembly functions just as its counterpart functions in the PV module keeping the SD module oriented for optimal solar intake along the beta axis and transfers data from the EEA and SD controller across the rotating surface to the PV module. The BGA consists of five ORUs (see Figure 3-15).

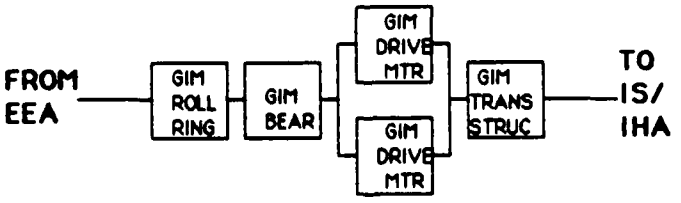

Figure 3-15. Beta Gimbal Assembly RBD.

The interface structure/integration hardware assembly provides the structural interface for the SD assemblies and the needed cabling and truss supports. The IS/IHA consists of two ORUs (see Figure 3-16).

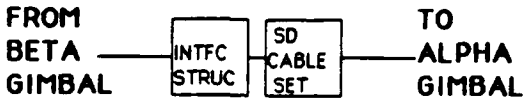

Figure 3-16. Interface Structure/Integration Hardware Assembly RBD.

In actuality, the electrical power from the SD module combines with the power of the PV module outboard of the alpha gimbal joint. However, no additional components are provided for this interface. Our model shows this mixing just prior to the alpha gimbal joint.

POWER MANAGEMENT AND DISTRIBUTION SYSTEM

The PMAD system, in conjunction with the Data Management System found within the operational element of the Space Station, orchestrates the EPS to ensure power is provided to the station loads as it is demanded. Since NASA has just made the switch from a Dual Ring architecture to the Star Hybrid structure, not much specific information is available. It is known that the PMAD is now designed to provide a network of paths that allows for rerouting of power to the loads in the event of component failures within the PMAD system. The PMAD consists of the following ORUs: a pair of power management controllers (PMCs), two pairs of main bus switching units (MBSUs), approximately 40 AC to DC

switching units (ADCUs) and an equal amount of power distribution and control units (PDCUs). Electrical power flows through the two alpha gimbal joints, one starboard and one port, and enters the PMAD through two separate pairs of MBSUs. The AC power is converted to DC power in the ADCU and then flows to a PDCU where a load is connected. The PMCs orchestrate the management of the EPS through the PV source controllers and the SD controllers.

THE OVERALL EPS

Now that the three different systems have been briefly explained, a description of the blocks and connections used in putting all parts of the EPS together is needed. Understanding what reliability means is addressed first.

In general, reliability is a measure of a system's performance for some time period under established operating conditions. In this work, reliability is defined to be the probabilistic measure of a power system's performance for a designated time period under the condition that there are no external disturbances to degrade or enhance any component's or assembly's performance. Traditionally, reliability analysis has focused on determining the expected length of time a system can operate without failure. In this work, we have

different levels of failure as defined by the interconnections of the components and assemblies. Therefore, we focus on these finite number of power levels and vary the time to establish power profiles.

Closely associated with reliability is availability. Availability is the probability of a system being operable at time t [27]. Availability is the same as reliability for a system without repairs. Therefore, the terms reliability and availability are interchangeable when analyzing our model since we consider it non-repairable.

MODEL BLOCKS

Orbital replacement units (ORUs) are the basic building blocks of the Space Station EPS. Our work is unique in that it builds a model that represents each ORU of the EPS and does not break any ORU down further. This is logical since present maintenance policies prohibit on-line internal repairs of ORU subassemblies. Though ORUs may consist of one component or several components, the term component in the remainder of this work will refer to an ORU. A brief description of the proposed ORUs and assemblies of the EPS is given in Appendix A.

Four types of reliability blocks are used to model each ORU: normal, quasi-normal, conditional and dummy

blocks. Each block has two key bits of data that define each ORU and are needed to conduct our reliability analysis: 1) the power throughput when the ORU works (W_R) and when it fails (W_Q), and 2) the probability of the block still working at time t. Since all failures are random and the MTBFs are constant, the ORUs are assumed to fail exponentially; therefore, the following equations are used to calculate the probabilities:

$$P(\text{Works at time } t) = R = \exp[-t/MTBF] \qquad (1a)$$

$$P(\text{Fails by time } t) = Q = 1 - \exp[-t/MTBF]. \qquad (1b)$$

Although the exponential distribution is used, an extension to the Weibull distribution which can be used to provide a more general capability for modeling the failure distribution is straight forward. Each ORU has a corresponding MTBF design specification which is stated in the PSDD.

A normal block is characterized by $W_R = 1$ and $W_Q = 0$ and uses equations (1a) and (1b) to obtain the probabilities for R and Q. A quasi-normal block also uses equations (1a) and (1b) but has power throughputs of $W_R = 1$ and $W_Q = k$ where $0<k\leq 1$. In our model, only the beta gimbal bearing subassembly (ORU 112 and ORU 242) is quasi-normal where $W_Q = 0.3$. This occurs because in the worst case scenario three-tenths of the maximum solar energy can still be collected by either the PV or SD

module.

The conditional block has the power levels $W_R = 1$ and $W_Q = 0$ but a one-way dependence exists between two or more blocks which causes a conditional probability relationship to be used instead of equations (1a) and (1b). In our model, only the DC switching units (DCSUs)(ORU 141), the MBSUs (ORU 143), the PVSCs (ORU 144) and the MIUs (ORU 142) are conditioned on the status of the utility plates they are mounted on. However, since the respective MTBFs of the eight electrical equipment assembly ORUs are at least four times greater than the MTBF of the utility plate, the conditional probability relationship is not derived and equation (1a) and (1b) are used to calculate R and Q.

If the conditional probabilities had to be computed, the following set of relationships would be used to find the reliability of the conditional blocks:

$$R_{140}(A) = \text{Prob(both A and 140 working at time t)} = R_A * R_{140} \qquad (2a)$$

$$Q_{140}(A) = \text{Prob(140 not working)} + \text{Prob(140 working but A not working)} = Q_{140} + R_{140} * Q_A, \qquad (2b)$$

where $R_{140}(A)$ is the probability that ORU A works when mounted on ORU 140 (the utility plate); $Q_{140}(A)$ is $1 - R_{140}(A)$; R_A is the reliability of ORU A independent

of other ORUs; and $Q_A = 1 - R_A$. $W_R = 1$ is paired with equation (2a) and $W_Q = 0$ is paired with equation (2b).

The fourth block, the dummy block, is used to represent an element or component that is important to the output of the EPS although it is not part of the EPS. Computationally, the dummy block has no impact on the models' results. Our representation of the sun and the alpha gimbal joints are examples of the use of dummy blocks. For this block the power levels are $W_R = 1$ and $W_Q = 1$ and the probabilities are represented using equations (1a) and (1b).

The connections are the next ingredients needed to allow us to define our model.

MODEL CONNECTIONS

There are five types of connections in our model: series, normal parallel (fully redundant), k-out-of-n parallel (partially redundant), partitioned parallel (proportionally redundant), and summation. Each connection defines the power level W_i and its corresponding probability.

Before describing the connections, a brief explanation about the power output levels is needed. In reality, the power output spectrum is continuous from zero to 100% output (maximum output). However, as was the

case with the UNIRAM, TIGER and ETARA approaches, the power output spectrum is discretized to enable analysts to apply different techniques and present data that is easier to interpret. In our model, our final output seemingly implies that the system is discrete, but it really represents a continuous power spectrum segmented into several intervals. Therefore, the probability at a specific power level, W_i, at some intermediate stage in the analysis of a module or system is actually the probability that the power output will fall in the interval between W_{i-1} and W_i (the next lower power level and the specified power level, respectively). This concept will be demonstrated later in this work. It is necessary to introduce this concept at this point since certain connections define different power levels and might seem to imply a discrete system exists.

The first connection is the standard series connection. The RBD for a series system is given below:

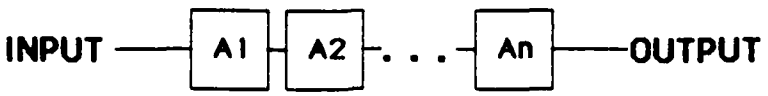

Figure 3-17. Series RBD.

A series system is used when the failure of any one component of an n-component system results in the system's failure [28]. We assumed each ORU failure was independent except the eight EEA ORUs in the PV module;

therefore, the following standard reliability relationships can be used to analyze an RBD:

$$R(t) = \prod_{i=1}^{n} R_i(t) \qquad (3a)$$

$$Q(t) = 1 - \prod_{i=1}^{n} R_i(t) \qquad (3b)$$

All series connections in our models are normal series connections. The number of power levels do not change when simplifying a series connection unless a quasi-normal block is involved in the simplification. If a quasi-normal block is involved, then each power level is reduced by a factor of W_Q when analyzing the series which represents that blocks failure mode. This is no different than when analyzing a normal block because in the normal case, W_Q = 0 and all series power levels would be zero in the event of that block's failure.

The second connection type is the normal parallel or fully redundant connection. The RBD of a parallel system is given in Figure 3-18.

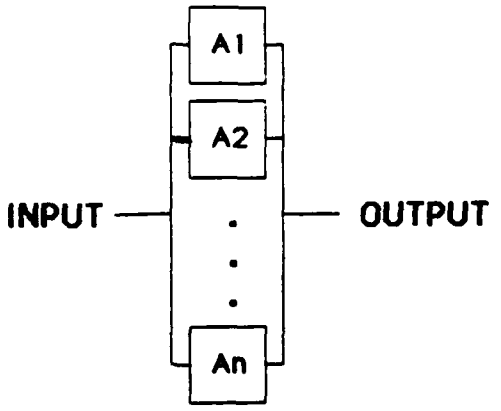

Normal parallel connection: (Fully redundant)

Power W is delivered to OUTPUT if at least one of n units $A_1, \ldots, A_n$ works.

Figure 3-18. Normal Parallel Connection.

The normal parallel system is a system where all components of the system have to fail for the system to fail [28]. The standard reliability relationships can be used:

$$R(t) = 1 - \prod_{i=1}^{n} Q_i(t) \qquad (4a)$$

$$Q(t) = \prod_{i=1}^{n} Q_i(t) \qquad (4b)$$

Examples of normal parallel connections occur in the SAA of the PV module and the HRA of the SD module. Like the series system, power output is $W_R = 1$ or $W_Q = 0$. No quasi-normal blocks are involved in any parallel connection.

The third connection is the k-out-of-n parallel connection. The RBD for the general case is given in Figure 3-19.

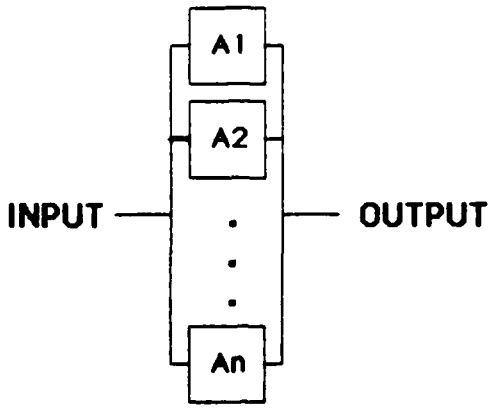

k-out-of-n parallel connection: Power W is delivered to OUTPUT if at least of n units $A_1,\ldots,A_n$ work.

Figure 3-19. k-out-of-n Parallel Connection.

The k-out-of-n parallel system occurs when k components have to work in an n-component parallel system for the system to work. The following binomial reliability relationships are used:

$$R(t) = \sum_{i=k}^{n} \binom{n}{i} (R(t))^i (Q(t))^{n-i} \qquad (5a)$$

$$Q(t) = 1 - \sum_{i=k}^{n} \binom{n}{i} (R(t))^i (Q(t))^{n-i} \qquad (5b)$$

where $\binom{n}{i}$ *is defined as* $\frac{n!}{i!(n-i)!}$

The k-out-of-n parallel connection is only used in the TCA of the PV module. The corresponding power levels are $W_R = 1$ and $W_Q = 0$.

The fourth and most unique connection is the partitioned parallel, or proportionally redundant, connection. Billinton [7] discusses this phenomenon in his description of capacity outage probability tables although he does not refer to it in terms of a type of series-parallel connection. In essence, the partitioned parallel connection is a generalized form of the recursive technique Billinton discusses. The RBD for the partitioned parallel connection is identical to the normal parallel system's but is analyzed differently. A thorough explanation of this connection is needed since it is unique.

Traditional series-parallel analysis recognizes only two output states - success or failure. These two states in our problem would be 100% (or maximum) output and 0% output. This analogy will be referred to as "all or nothing" outputs. In fact, in our first attempt at this problem, we came up with probabilities for "all or nothing" power outputs at time t. This produced no useful results although the reliability block diagrams for each system remained useful. We realized the key issue with our problem was not determining the "all or nothing" output reliabilities. We restarted with the basic assumption that a catastrophic power loss was highly unlikely to occur. This precluded further study on the

"all or nothing" problem. Therefore, we began examining the components and assemblies that had an effect on the power levels.

Initially, the obvious candidates were those components which converted the solar energy into power for the Space Station. The solar array blankets in the photovoltaic (PV) system and the concentrator and receiver assemblies of the solar dynamic (SD) system "produced" power for the EPS. "Produced" here refers to the capability of a component to capture solar energy. In the PV system model (see Figure 3-20), the left and right solar array blankets are in parallel, yet "produce" power independently from the other.

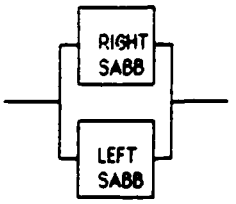

Figure 3-20. Solar Array Blanket and Box Subassembly.

If interpreted using traditional series-parallel connections, this system would be analyzed as a fully redundant system and maximum power would flow through the solar array blanket and box subassembly whenever either or both blankets were functioning. In reality, since we

are analyzing the EPS at the ORU level, fifty percent of the maximum power output of the blanket subassembly will flow from the subassembly if just one of the blanket ORUs works; 100% will flow if both work; and no power will flow if neither works. Mathematically, the significance of the difference between these approaches is shown using series-parallel reduction methodologies.

R_A is defined to be the probability that component A works, Q_A is the probability that A fails, and $R_A(X\%)$ is the probability that component A is at the X% power level. Using traditional series-parallel techniques, the probability that the solar array blanket and box subassembly (designated "01-02") will produce power is:

$$R_{01-02} = R_{101}*R_{102} + R_{101}*Q_{102} + Q_{101}*R_{102},$$

$$Q_{01-02} = Q_{101}*Q_{102},$$

where R_{01-02} is maximum power (one power level). In the case of a partitioned parallel system, we use the same techniques, but we break down R_{01-02}:

$$R_{01-02}(100\%) = R_{101}*R_{102},$$

$$R_{01-02}(50\%) = R_{101}*Q_{102} + Q_{101}*R_{102}, \text{ and}$$

$$R_{01-02}(0\%) = Q_{01-02} = Q_{101}*Q_{102}.$$

As can be seen, the probability of getting no power, Q_{01-02}, is the same in both cases. Further inspection discovers that $R_{01-02}(100\%) + R_{01-02}(50\%) = R_{01-02}$. Therefore, all we have done by highlighting $R_{01-02}(100\%)$

and $R_{01-02}(50\%)$ is to break down R_{01-02} into different states. Now, we have three output states instead of two. In order to generalize this phenomenon, which we call a partitioned parallel connection, for those subassemblies this pertains to, we use the following illustration:

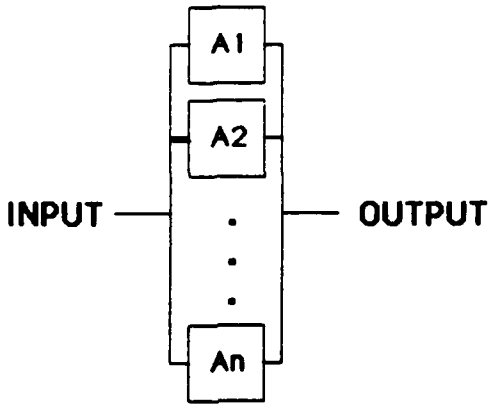

Partitioned parallel connection: Power kW/n is delivered to OUTPUT if k units of the n units $A_1,\ldots,A_n$ work.

Figure 3-21. Partitioned Parallel Connection.

Examples of subassemblies with partitioned parallel connections include: the solar array blankets and boxes (ORUs 101 and 102); the upper and lower battery series subassemblies consisting of a BCDU (ORU 151), battery (ORU 152), and utility plate (ORU 140); and the energy storage assembly consisting of the upper and lower battery series subassemblies in series with the main inverter unit (ORU 142). The power levels depend on the number of components in parallel, and all components are

identical.

The fifth connection, which is a generalization of the partitioned parallel connection, is the summation. This connection was needed to combine the system's power output with other systems also providing power. The summation adds all combinations of the combining systems' power outputs while multiplying their corresponding probabilities together. All identical power outputs are then combined and their corresponding probabilities are summed. The following example is used for illustration.

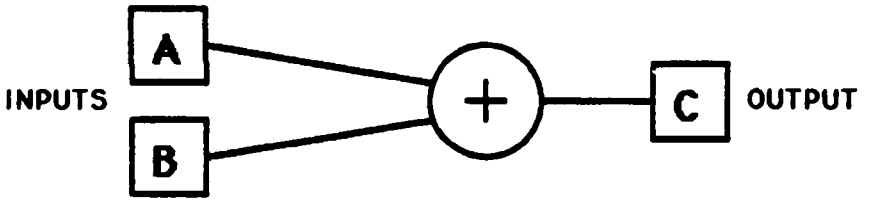

Figure 3-22. Summation Connection Example.

In this example, the output states for the input A are defined as $R_A(10kW) = 0.8$, $R_A(8kW) = 0.15$ and $R_A(0kW) = 0.05$. TThe output states for the input B are defined as $R_B(5kW) = 0.9$ and $R_B(0kW) = 0.1$.

All inputs are combined at the summation connection, or node. The resulting output states for C are defined in Table 3-1.

POWER LEVEL	RELIABILITY
15 kW	0.72
13 kW	0.135
10 kW	0.08
8 kW	0.015
5 kW	0.045
0 kW	0.005

Table 3-1. Resulting Output States for Summation Example.

As can be seen, the Law of Total Probability is satisfied since the sum of the probabilities of the outputs is one.

The latter two types of connections, although not complicated, do present a minor problem - as the number of power levels increase, the successive partitioned parallel or summation connections cause the number of power levels to grow at less than or equal to a combinatorial rate. This phenomenon is demonstrated by our previous example. Prior to the summation connection, three and two power output states existed. In comparison, there are 3*2, or 6, resulting power output states. This phenomenon also occurs for the partitioned parallel connection. Obviously, for input systems with several power output states, the resulting power output states can be very cumbersome. The solution to this problem is

discussed later in this work.

THE PHOTOVOLTAIC MODEL

With the modeling framework established, we can put our assembly models together to form models at the module and EPS level, which is one of our original objectives. The first model is the PV module (see Figure 3-23). [Note: The numbering system is unique to our models and are designed to organize the models into assemblies.] It is the most interesting since it has elements of each type of block and connection. As can be seen, the PV module consists of an insolar and an eclipse models which are connected by a summation connection. The heat rejection subassembly is modeled as a k-out-of-n parallel system. As stated earlier, the beta gimbal bearing subassembly is modeled as a quasi-normal block with W_Q = 0.3. The following are partitioned parallel connections: between the solar array blankets, between the starboard SAA-BGA series and port SAA-BGA series, between the three BCDU-battery-utility plate (upper) series, between the two BCDU-battery-utility plate (lower) series, and between the upper ESA-MIU series and the lower ESA-MIU series. The insolar model has ten power levels and the eclipse model has six power levels. Combined together, there are sixty power levels which, as

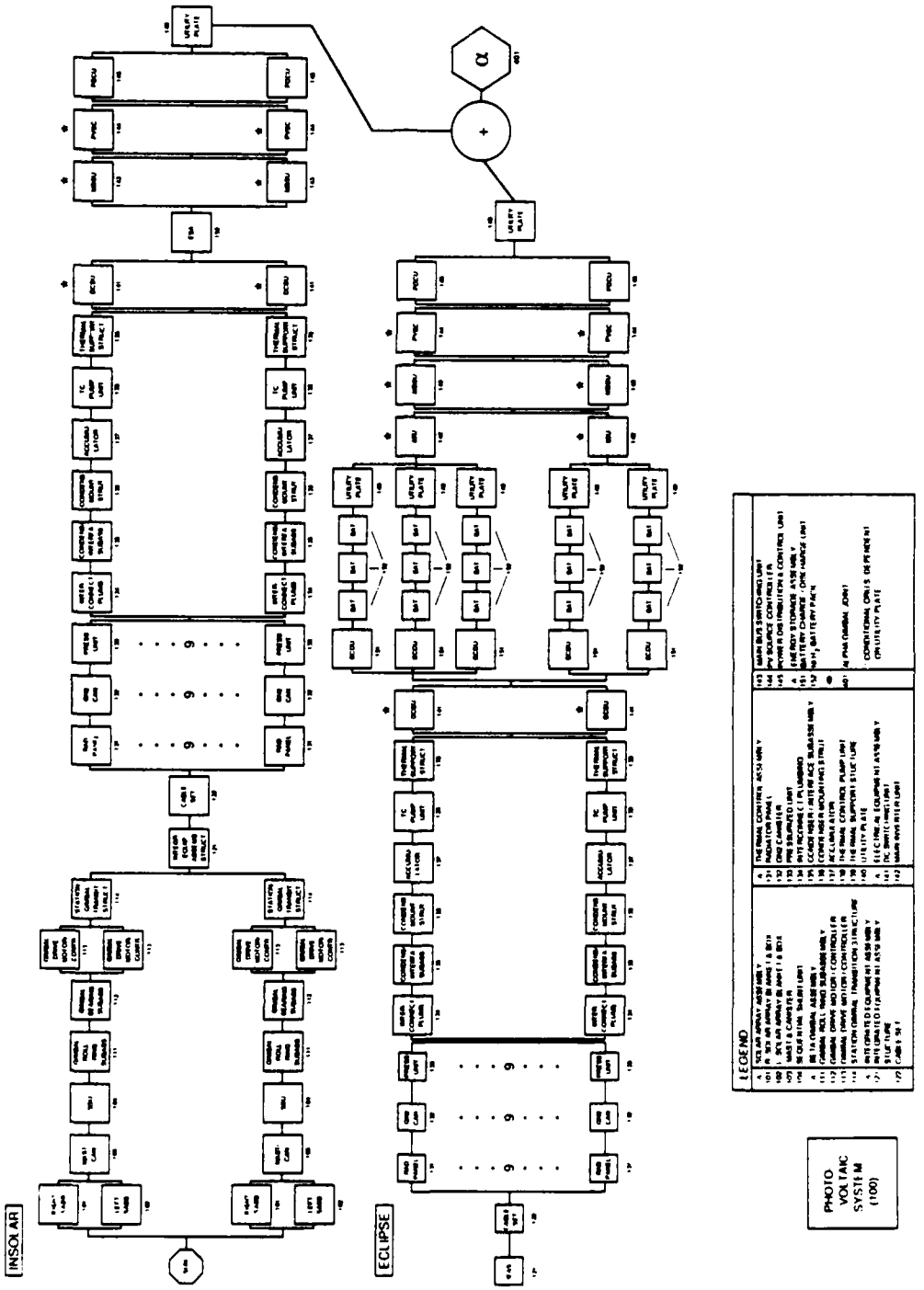

Figure 3-23. Photovoltaic Model.

mentioned earlier, are really 59 power output intervals of varying lengths and one specific power level where $W_Q = 0$.

THE SOLAR DYNAMIC MODEL

The SD module is much simpler as it is primarily a series system (see Figure 3-24). There are no k-out-of-n or partitioned parallel systems within it. In fact, since the beta gimbal bearing subassembly ORU is quasi-normal, there are only two power intervals ($0.3<W_1<1$ and $0<W_2<0.3$) and one specific power level where $W_Q = 0$. All the parallel systems have normal parallel connections. Although the SD module has a thermal storage capability, this same system is used during both the insolar and eclipse cycles. This reason coupled with the existence of only one concentrator and receiver eliminates the need to use a partitioned parallel connection.

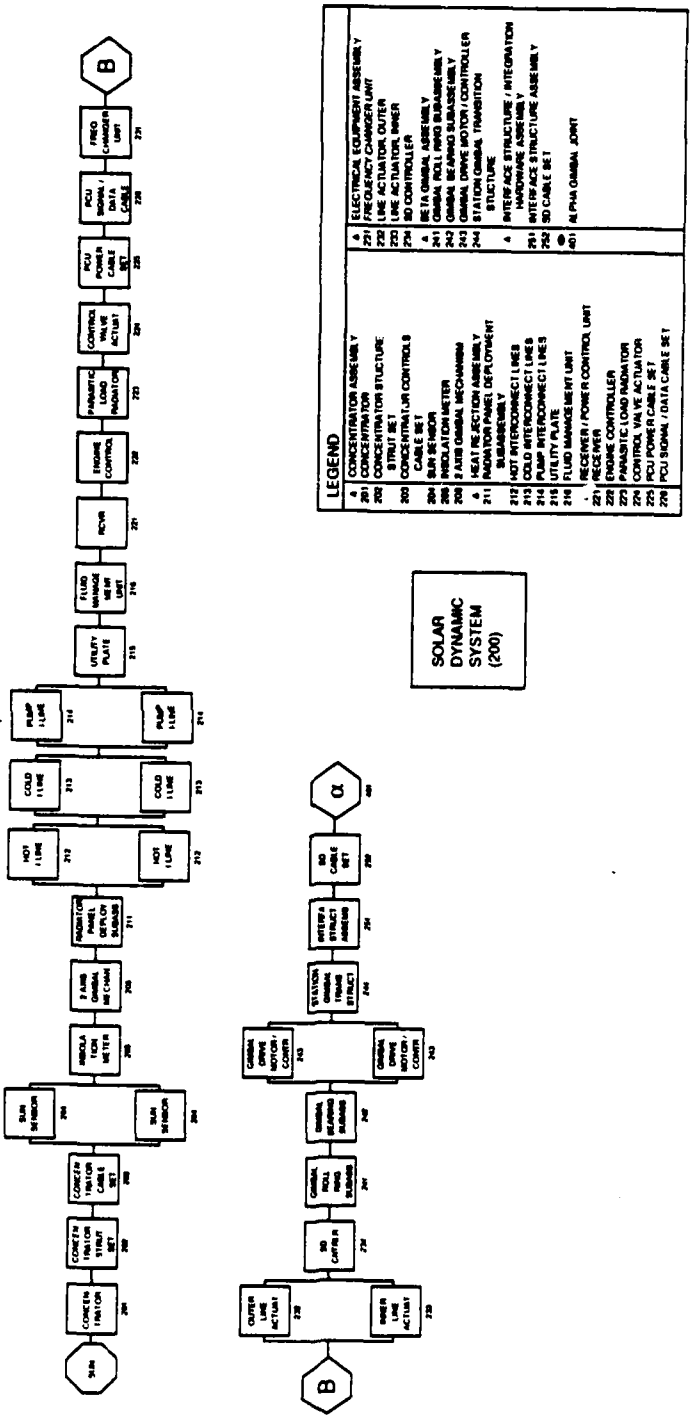

Figure 3-24. Solar Dynamic Model.

THE POWER MANAGEMENT AND DISTRIBUTION MODEL

The PMAD system is the simplest of the systems in terms of an RBD (see Figure 3-25). The power output to each load is the same, so the diagram could be traced to any of the loads to analyze the power output. The PMAD system, since it does not produce power in any manner, does not have a partitioned parallel system. Additionally, it does not have any other special feature. All blocks and connections are normal.

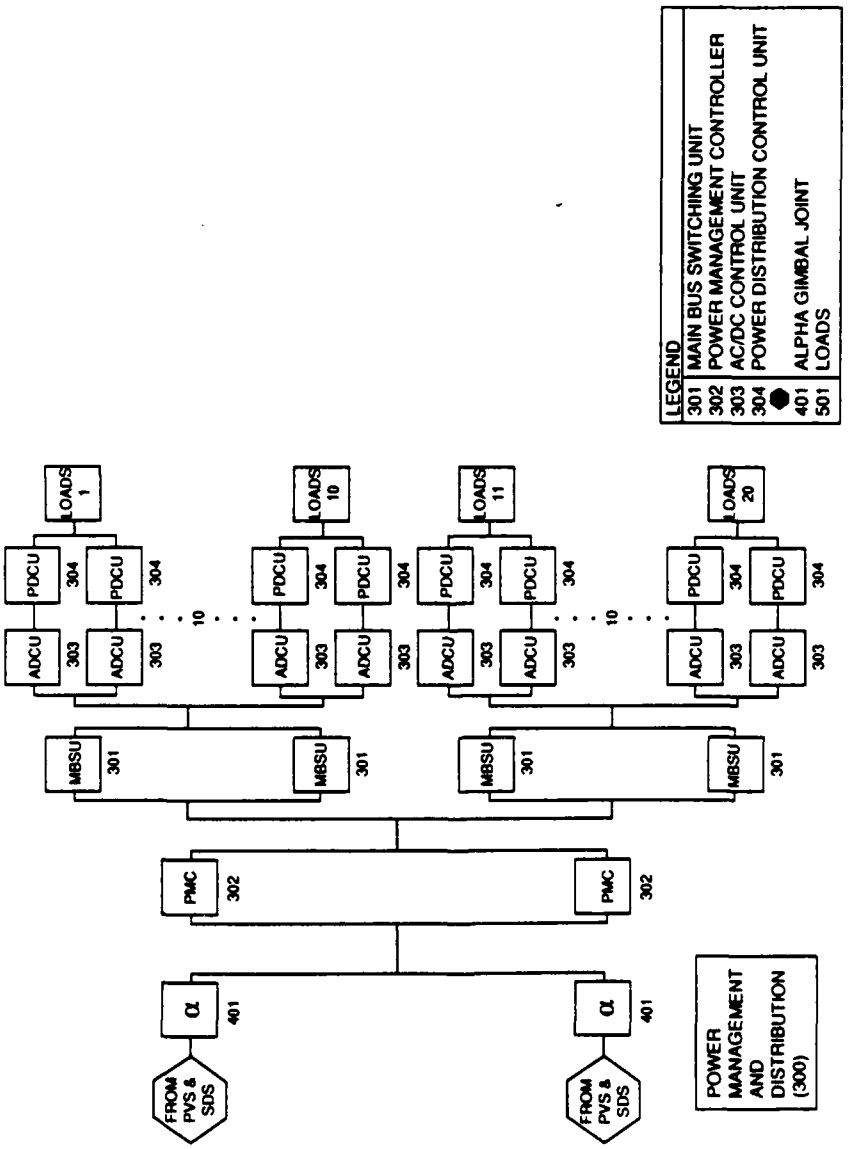

Figure 3-25. Power Management and Distribution Model.

THE EPS MODEL

The last model is the overall EPS model (see Figure 3-26). It models the Phase 2 EPS system with four PV modules and two SD modules. There are two alpha gimbal joints which are assumed to be perfectly reliable. All the modules are connected using summation connections because each power module adds to the power output of the EPS.

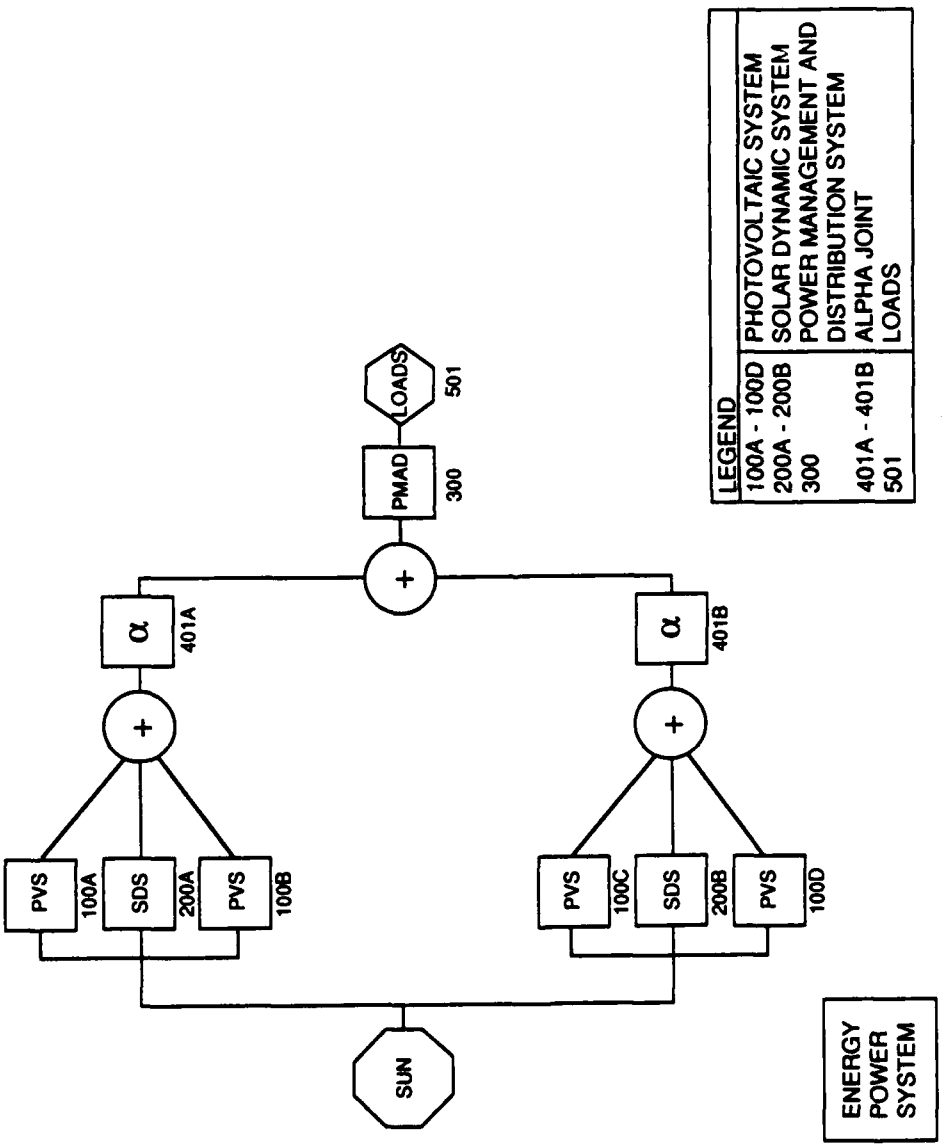

Figure 3-26. EPS Model.

MODEL ASSUMPTIONS

With this last model, the assumptions, previously mentioned and unmentioned, need to be stated together. There are several conditions that have to be assumed to allow the models to be constructed and analyzed. The assumptions are:

(1) During any orbit, the insolar cycle lasts 60 minutes and the eclipse cycle lasts 30 minutes when, in reality, the length of each cycle varies with the seasons.

(2) These are steady state models. When a module is evaluated at time t, we assume the system is operating at its designed nominal level. That is, the batteries are fully charged no matter which cycle of the orbit it's in. This also means that since the eclipse cycle lasts 30 minutes, then on the average one-third of the power being produced by the PV module is provided directly by the ESA. This assumption is vital to the feasibility of our PV model. Without this assumption, the proportion of the power being provided by the insolar and eclipse models would vary over time and we could not combine these them into an analytic model.

(3) At t = 0, all ORUs are brand new. Aging has not been incorporated into the model.

(4) The ORU is the level used for modeling the EPS

since when components are replaced, they are replaced at the ORU level. An ORU is a self-contained box which will not be repaired in place.

(5) ORU failures are independent except for the conditional blocks.

(6) Since the MTBF for the utility plates is at least four times that of the EEA ORUs mounted on them, the conditional probability is dropped and the two utility plates are assumed not to have a significant effect on the power levels.

(7) The configuration of the heat rejection subassembly of the PV module consisting of the nine radiator panels (ORU 131), gaseous nitrogen canisters (ORU 132), and pressurization units (ORU 133) is assumed. When the PV model was constructed, the available information indicated that the HRA was a 7-out-of-9 parallel system. However, subsequent information provided in the PSDD gave reference to there being either ten radiator panels or twelve radiator panels. Since verification one way or the other could not be made, we stayed with a 7-out-of-9 HRA. Once the actual configuration is determined, the model can be easily modified to accommodate the changes.

(8) When all four PV modules are operating, the power for the outboard module's thermal control pumps (ORU 138)

are regulated by the inboard module's PDCUs. This is due the fact the outboard modules do not have PDCUs. Since this design seemingly reduces the reliability of the EPS, discussion is ongoing as to whether PDCUs should be added to the outboard PV modules or some other configuration is better. For this reason, our PV models all contain one pair of PDCUs. If the final PV module design does not include PDCUs in the outboard modules, an outboard PV model can easily be built using the computer package designed to support this works computational analysis.

(9) The MTBFs used are the design specifications given in the initial Space Station design document and given in the PSDD. They are provided in Table 3-2.

ORU Mean-Time-Between-Failures

Photovoltaic		Solar Dynamic		PMAD	
ORU #	MTBF (hours)	ORU #	MTBF (hours)	ORU #	MTBF (hours)
101	131,400	201	131,400	301	87,600
102	131,400	202	262,800	302	43,800
103	131,400	203	262,800	303	87,600
104	87,600	204	87,600	304	87,600
111	262,800	205	87,600		
112	131,400	206	262,800		
113	87,600	211	87,600		
114	262,800	212	262,800		
121	525,000	213	262,800		
122	525,000	214	262,800		
131	350,400	215	262,800		
132	727,080	216	113,880		
133	727,080	221	131,400		
134	262,800	222	87,600		
135	876,000	223	87,600		
136	262,800	224	262,800		
137	262,800	225	262,800		
138	280,320	226	262,800		
139	262,800	231	87,600		
140	350,400	232	87,600		
141	87,600	233	87,600		
142	87,600	234	43,800		
143	87,600	241	262,800		
144	43,800	242	131,400		
145	87,600	243	87,600		
151	87,600	244	262,800		
152	103,400	251	262,800		
		252	262,800		

Table 3-2. MTBF Data for EPS ORUs.

(10) No external forces can cause a component to fail, i.e., meteors, spacecraft collisions, etc.

(11) All failure distributions are exponential because we are evaluating the normal operating time of a system which has a constant hazard rate or MTBF, and all failures are purely random [6]. We found no evidence to

contradict this assumption. Additionally, the memoryless property of the exponential distribution is well suited for this problem.

(12) In the worst case scenario, a failure of any beta gimbal bearing subassembly results in 30% of the power still being produced.

(13) Repair, replacement, and preventive maintenance are not allowed.

(14) All electronic ORUs in parallel are capable of handling any output power they might encounter. At this time, this assumption is needed to establish the performance capabilities of the electronic components' power capacities in the absence of definitive information for each ORU.

(15) The alpha gimbal joint is not a component of the EPS but is vital to its operation. No information was available on its reliability, so perfect reliability is assumed.

(16) There are 15 battery pack ORUs. Three battery packs make a battery. In the event one battery pack fails, the entire battery (three battery packs) are considered failed. In fact, the battery is considered failed if their collective storage capacity drops below 90% because thermal complications arise. In our model, all three battery packs can fail, but the output power is

"all or nothing."

(17) Unlike previous attempts, we treat the power spectrum as continuous. The way we will accomplish this is to represent the power spectrum by a finite number of intervals. There is one major difference between previous attempts and our approach. Earlier efforts either identified discrete power levels, such as in the "all or nothing" case (see Figure 3-27), or represented the power spectrum by fixing the power level intervals (see Figure 3-28).

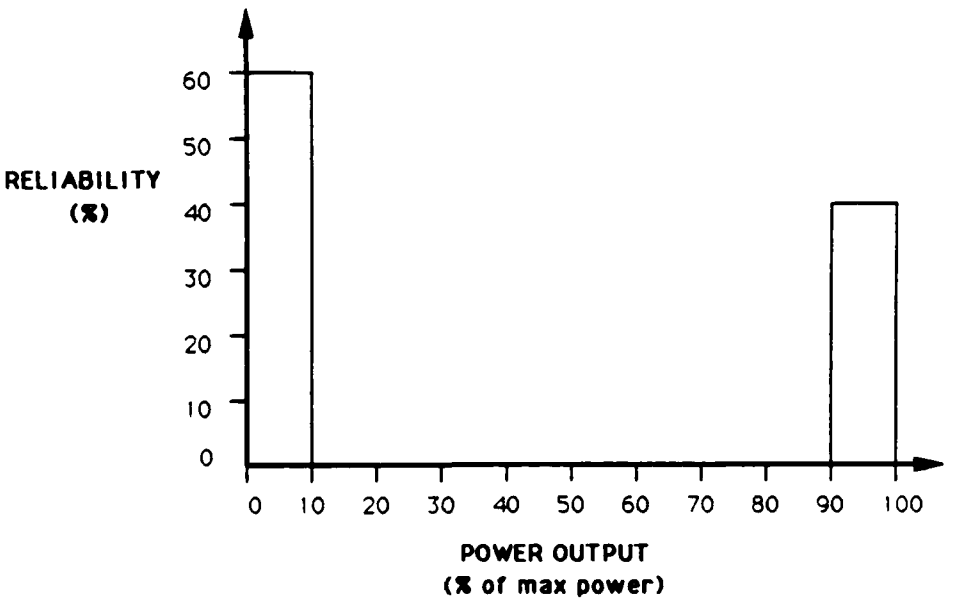

Figure 3-27. "All or Nothing" Power Spectrum.

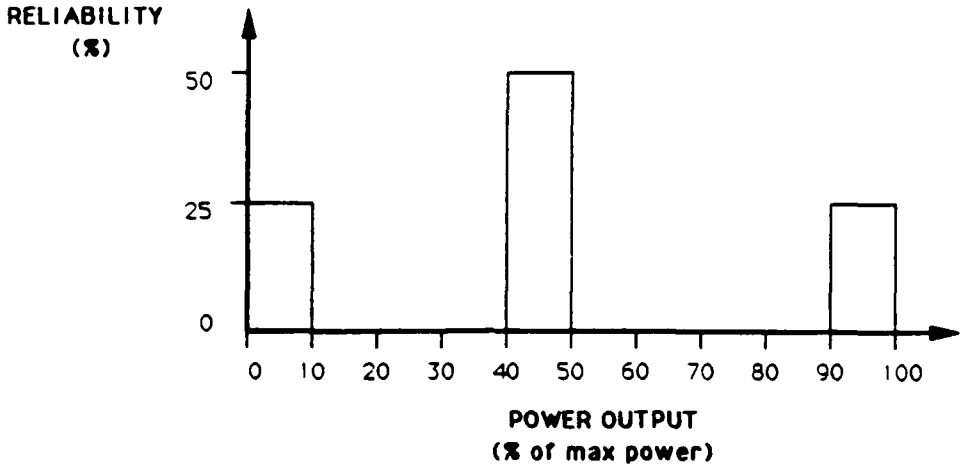

Figure 3-28. Fixed Interval Power Spectrum.

Our approach allows the model to determine the end points. The computations are influenced primarily by the use of partitioned parallel and summation connections. Figure 3-29 provides an example of this concept.

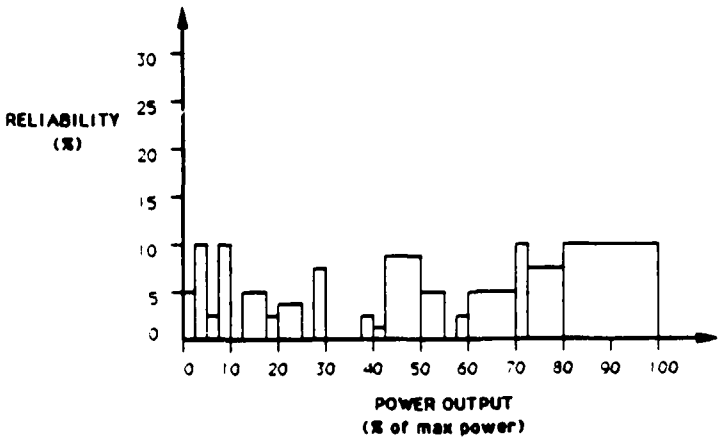

Figure 3-29. System-Determined Power Spectrum.

Note how the interval lengths are unequal.

(18) The exact positioning of the ORUs on the utility plates is not specified in the PSDD. The PV model is based on the assumed arrangement of the ORUs on the integrated equipment assembly structure shown in Figure 3-30.

At this point, the models have been developed and the assumptions have been stated. The last step of this work to determine potential uses of these RBDs of the space station, one of which is to identify the most critical ORUs in the EPS.

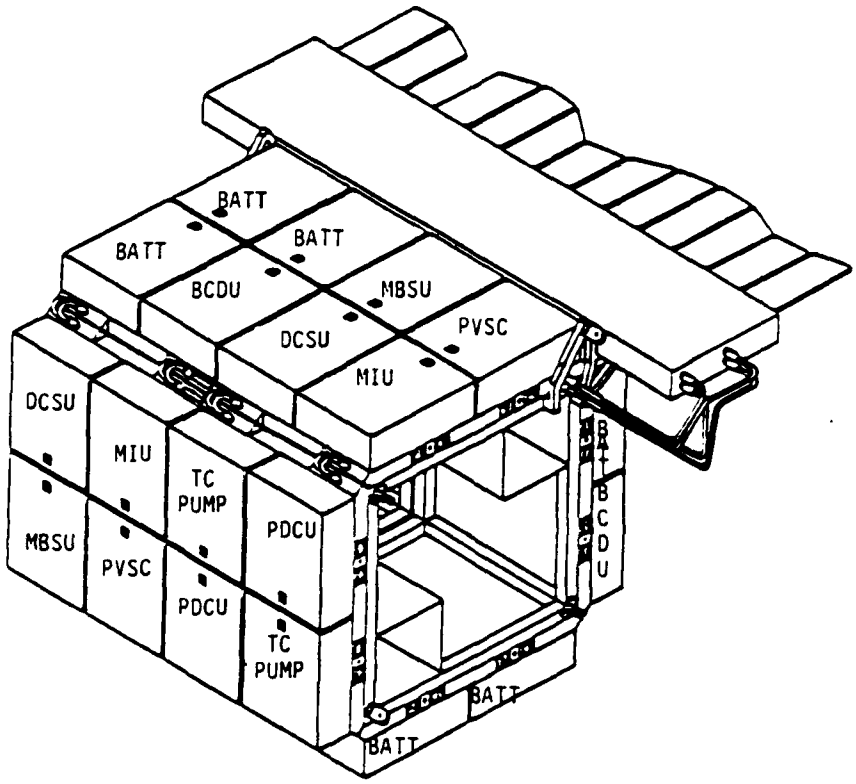

Source: Power System Description Document, Rocketdyne, 1988.

Figure 3-30. ORU Arrangement on Integration Equipment Assembly.

CHAPTER 4 - RESULTS

CRITICALITY RANKING

To determine the most critical ORUs and assemblies, we analyzed each module by varying the reliability of the ORUs. Two different analyses were conducted. The first, making each ORU and assembly perfectly reliable, would demonstrate the positive impact each ORU makes on the power output if it did not fail. The second, increasing the ORU MTBFs by 50% and 100%, would demonstrate the positive impact each ORU makes on the power output if its own individual performance improved; first by 50% and, then, by 100%. By dividing the probability of each power output of the adjusted case by the same output's probability in the nominal case, we get a sensitivity ratio. For example, if R(100% power when t = 8760 hours for the nominal case) = 0.065 and R(100% power when t = 8760 hours when only the battery pack is perfectly reliable) = 0.13, the sensitivity ratio equals 0.13/0.0.65 = 2. The magnitude of the ratios indicates the change in the power output when the adjusted ORU never fails. In the previous example, a sensitivity ratio equal to 2 means the reliability of achieving 100% power is improved by 100% when all battery packs are perfectly reliable and the remaining ORUs are the same as in the

nominal case. The higher the sensitivity ratio, the more critical that ORU is to the systems. Using the magnitude of the ratios, the ORUs are ranked from most critical to least critical. This is called the criticality ranking. For the PV module, we evaluated each case at one month (720 hours), six months (4380 hours), one year (8760 hours), two years (17520 hours), and five years (43,800 hours). For the SD module and the PMAD system, we evaluated each case at one month, one year, and five years. We examined the 100% and 50% power levels for t = 720 hours and t = 8760 hours to obtain the reliability of the output power being at a least 50% and 100%, respectively. For t = 43,800 hours, at 100% the probability approaches zero; thus, we chose 66.7% and 50% as the power levels examined. A summary of the conditions evaluated is provided in Tables 4-1 through 4-3.

	PHOTOVOLTAIC			SOLAR DYNAMIC		PMAD
	50%	66.7%	100%	30%	100%	100%
720 hours	X		X	X	X	X
4380 hours	X		X			
8760 hours	X		X	X	X	X
17520 hours	X		X			
43800 hours	X	X		X	X	X

Table 4-1. Summary of Evaluated Conditions. (ORU Perfectly Reliable)

		POWER OUTPUT			
		PV		SD	PMAD
		50%	100%	100%	100%
TIME	720 hours	X	X		
	8760 hours	X	X	X	X

Table 4-2. Summary of Evaluated Conditions. (Assembly Perfectly Reliable)

		POWER OUTPUT			
		PV		SD	PMAD
		50%	100%	100%	100%
TIME	720 hours	X	X		
	8760 hours	X	X	X	X

Table 4-3. Summary of Evaluated Conditions. (Improved MTBF)

To calculate the results, a computer program was designed on the Texas Instrument Explorer system using LISP. The program, written by Igor Vaks, is part of an effort for NASA in the Systems Engineering Department at Case Western Reserve University to develop an expert system capable of fault detection. Since LISP is not ideally suited for numerous calculations, it is slow for analytical programs. However, it is well suited to represent the data in corresponding pairs or triplets (i.e., power level with the discrete probability and/or

cumulative probability).

The results for the nominal cases are shown in Table 4-4.

PHOTOVOLTAIC

POWER OUTPUT	720 HOURS	4380 HOURS	8760 HOURS	17520 HOURS	43800 HOURS
100%	0.77525	0.20332	0.03742	0.00098	0
66.7%	0.98698	0.77215	0.46107	0.12091	0.00116
50%	**0.99359**	**0.89668**	**0.66169**	**0.22874**	**0.00307**

SOLAR DYNAMIC

POWER OUTPUT	720 HOURS	8760 HOURS	43800 HOURS
100%	0.89846	0.26434	0.00085
30%	0.9034	0.28256	0.00118

POWER MANAGEMENT AND DISTRIBUTION

POWER OUTPUT	720 HOURS	8760 HOURS	43800 HOURS
100%	0.99948	0.9358	0.34524

Table 4-4. Data for Model Nominal Cases.

The number in each entry represents the reliability of the corresponding system at the power level and time corresponding to that level. For example, at t = 720 hours, the PV module can provide at least 50% of its maximum power with a reliability of 0.99359. Also, at t = 8760 hours, the PV module can provide at least 50% power with a reliability of 0.66169. The criticality

where S = series system and P = parallel system,

$P_S(f)$ = the probability of failure of a series system,

$P_P(f)$ = the probability of failure of a parallel system.

When we make an ORU perfectly reliable, its MTBF approaches infinite; therefore, $P_P(f)$ is zero. However, we see that making the least reliable ORU (the ORU with the shortest MTBF) perfectly reliable produces the system with the lowest probability of failure. Since we need to minimize $P_S(f)$, we need to maximize $\prod_{i \in S} \exp[-t/MTBF_i]$. This is achieved by making the shortest MTBF approach infinite. In fact, if we rank the MTBFs from the shortest to the longest, and make them perfectly reliable one at a time, then we also produce systems which are ranked from the one with the smallest to the largest $P_S(f)$ regardless of time, the variation of the MTBFs, or the power levels. This insight helps in explaining why the SD and PMAD models act as they do.

Second, in any of the models, we expect the most critical ORUs to be those with the shortest MTBF, those ORUs not involved in a parallel system, and those with large quantities (more than two in this system). In the SD module, the most critical ORU was the SD controller (ORU 234) which had the shortest MTBF and was not in a

rankings for the perfectly reliable cases are given in Figures B-1 through B-3 in Appendix B. The criticality rankings for cases where the assemblies are perfectly reliable are given in Figures B-4 and B-5. The criticality rankings for cases where the MTBFs are varied are given in Figures B-6 through B-11. Since the rankings for the SD module and PMAD system do not change as time or the power level are varied, only the one year cases are given. From the data, there are several results worth noting.

ORU RESULTS

First, the criticality rankings of the ORUs for the SD module and PMAD system remain the same no matter what the time is, how much the MTBFs are varied, or what the power level is. Therefore, further examination of these models is not necessary beyond looking at the assemblies; and as expected, the rankings for the SD assemblies did not change as the parameters were varied. For additional insight to this observation, we examine the equations for computing the probability of failure.

$$P_S(f) = 1 - \prod_{i \in S} \exp[-t/MTBF_i] \qquad (6a)$$

$$P_P(f) = \prod_{i \in P} 1 - \exp[-t/MTBF_i] \qquad (6b)$$

parallel system. The next most critical ORUs all had the second shortest MTBF and were not part of a parallel system. At the bottom of the criticality rankings were the ORUs of the only parallel systems in the SD model. These results are not surprising since the SD model is primarily a series configuration.

The PMAD model has similar results but not for the same reasons. All PMAD ORUs are part of a parallel system. The most critical ORU, the power management controller (PMC)(ORU 302), does have the smallest MTBF. The MBSU (ORU 301) is the least critical as it is in a pure parallel system with a longer MTBF (i.e., the MBSU is not in series with another ORU). The ADCU and PDCU (ORUs 303 and 304, respectively) are evaluated as a series system first, then as a parallel system. This explains why they are in between the PMC and the MBSU. Also, note that the differences in the magnitude of the sensitivity ratios are minor which is expected in a series of parallel systems possessing similar MTBFs.

The PV model is more complex so no one characteristic is dominant. The PV source controller (PVSC)(ORU 144) has the shortest MTBF but at the 100% power level is 14th most critical at t = 720, 11th at t = 8,760 and 6th at t = 43,800 (66.7% power level). At the 50% power level, the PVSC is slightly more critical. The BCDU and battery

packs at the 100% level are the most critical at t = 720 and t = 8760; and under all conditions, the solar array blankets (ORUs 101 and 102) are very critical. The pattern seems to be that the power producing ORUs are the most critical, although at the lower power levels, the ESA is not as critical.

Third, certain ORUs in the PV model make drastic changes in their criticality ranking as time changes. The battery pack (ORU 152), the most numerous of the PV module's ORUs, is the most critical ORU at t = 720 and t = 8760 for the 100% power level; but at t = 43,800, it is the 22nd most critical. Similar results are found for the ORUs in the ESA to include the MIU (ORU 142). All drop in criticality at t = 43,800. For the 50% power level, the two IEA ORUs (ORUs 121 and 122) fall over time from the second most critical to the fourth least critical. However, the ESA ORUs start low in criticality at t = 720, rises significantly at t = 8760 (from 10th to 2nd) but drops back down to 11th at t = 43,800. The BCDU (ORU 151) and MIU also have similar patterns. For both power levels, the majority of the ORUs do not fluctuate significantly.

Fourth, in plotting the entire power profile for the battery pack, PVSC, BCDU and utility plate ORUs at t = 8760, the criticality ranking changes become more

clear (see Table 4-5).

EXCEEDANCE PROBABILITY

POWER OUTPUT	BCDU (ORU 151)	Utility Plate (ORU 140)	PVSC (ORU 144)	Battery Packs (ORU 152)
0	1	1	1	1
0.05555	0.97132	0.97705	0.97918	0.97222
0.08335	0.96848	0.97217	0.97447	0.97167
0.1111	0.9602	0.96283	0.96549	0.96631
0.1389	0.95131	0.95215	0.95518	0.96209
0.16665	0.94451	0.94112	0.9445	0.96094
0.19445	0.92084	0.92036	0.92448	0.93452
0.2222	0.89964	0.89631	0.90122	0.92618
0.25	0.8884	0.88268	0.88795	0.92224
0.2778	0.86405	0.86225	0.86808	0.90043
0.30555	0.82961	0.83306	0.83968	0.87131
0.33333	0.82688	0.82894	0.83548	0.87032
0.3611	0.75116	0.77047	0.77911	0.75875
0.3889	0.74271	0.76125	0.76979	0.75258
0.41665	0.73648	0.75037	0.75873	0.75097
0.44445	0.7136	0.7262	0.73457	0.72924
0.4722	0.6948	0.70295	0.71093	0.71792
0.5	0.68419	0.68388	0.69153	0.71559
0.5278	0.63639	0.63918	0.64692	0.65818
0.55555	0.60494	0.59884	0.6057	0.64436
0.58335	0.58756	0.57413	0.58078	0.63857
0.6111	0.55042	0.5386	0.54464	0.60389
0.6389	0.49797	0.48639	0.49154	0.56176
0.66665	0.49078	0.47551	0.48049	0.55925
0.69445	0.37754	0.38282	0.38932	0.39649
0.7222	0.35757	0.36074	0.36686	0.3827
0.75	0.34676	0.34286	0.34868	0.37966
0.7778	0.31632	0.31198	0.31727	0.34596
0.80555	0.28275	0.2732	0.27783	0.32314
0.83333	0.27039	0.25007	0.25431	0.32125
0.8611	0.21859	0.20527	0.20875	0.24339
0.8889	0.18021	0.1551	0.15773	0.22921
0.91665	0.16102	0.13001	0.13222	0.22211
0.94445	0.12129	0.09374	0.09533	0.18661
1	0.06169	0.03934	0.04	0.13334

Table 4-5. Data on Selected ORUs at t=8760 Hours.

This table demonstrates the reliability of the PV model at t = 8760 hours to attain at least a certain power output when the ORU (which heads the columns) is perfectly reliable. For example, the reliability that the system can provide at least 50% of its maximum power at t = 8760 hours is 0.68419 when all BCDUs are perfectly reliable and 0.69153 when both PVSCs are perfectly reliable. As can be seen, the battery pack ORU has a greater reliability than the BCDU at each power interval. The PVSC has a greater reliability than the utility plate at each power interval. However, this is not the case when the BCDU and battery pack ORUs were compared to the utility plate and PVSC ORUs. For example, the BCDU is more reliable than the utility plate in the interval 16.67% to 30.56% of maximum power whereas the opposite is true for the interval 30.56% to 50% of maximum power. In fact, the PVSC is greater than the BCDU more often than the utility plate is greater than the BCDU. To better understand this point, the ORU data in Table 4-5 is examined and the comparison between the ORUs is provided in Figures 4-1 through 4-3. A graphical comparison is also provided in Figures 4-4 through 4-7.

BCDU versus Utility Plate

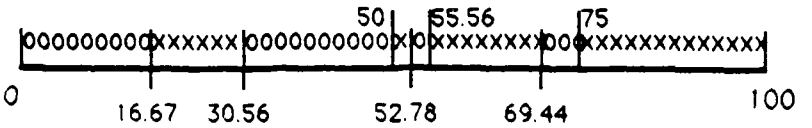

POWER OUTPUT
(% of max power)

BCDU more critical than utility plate in interval - xxxxx
utility plate more critical than BCDU in interval - ooooo

Figure 4-1. BCDU/Utility Plate Power Interval Comparison.

BCDU versus PVSC

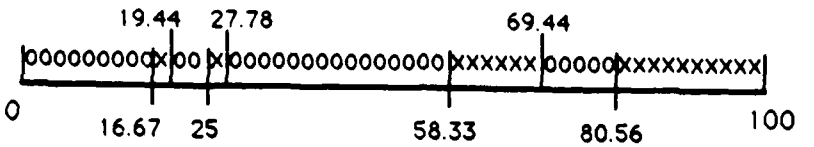

POWER OUTPUT
(% of max power)

BCDU more critical than PVSC in interval - xxxxx
PVSC more critical than BCDU in interval - ooooo

Figure 4-2. BCDU/PVSC Power Interval Comparison.

Battery Pack versus Utility Plate & PVSC

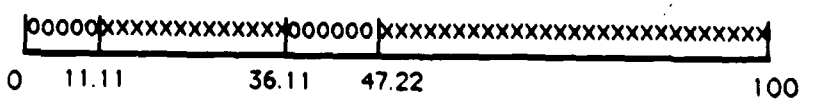

POWER OUTPUT
(% of max power)

Battery pack more critical than utility plate & PVSC - xxxxx
Utility plate & PVSC more critical than battery pack - ooooo

Figure 4-3. Battery Pack/Utility Plate & PVSC Power Interval Comparison

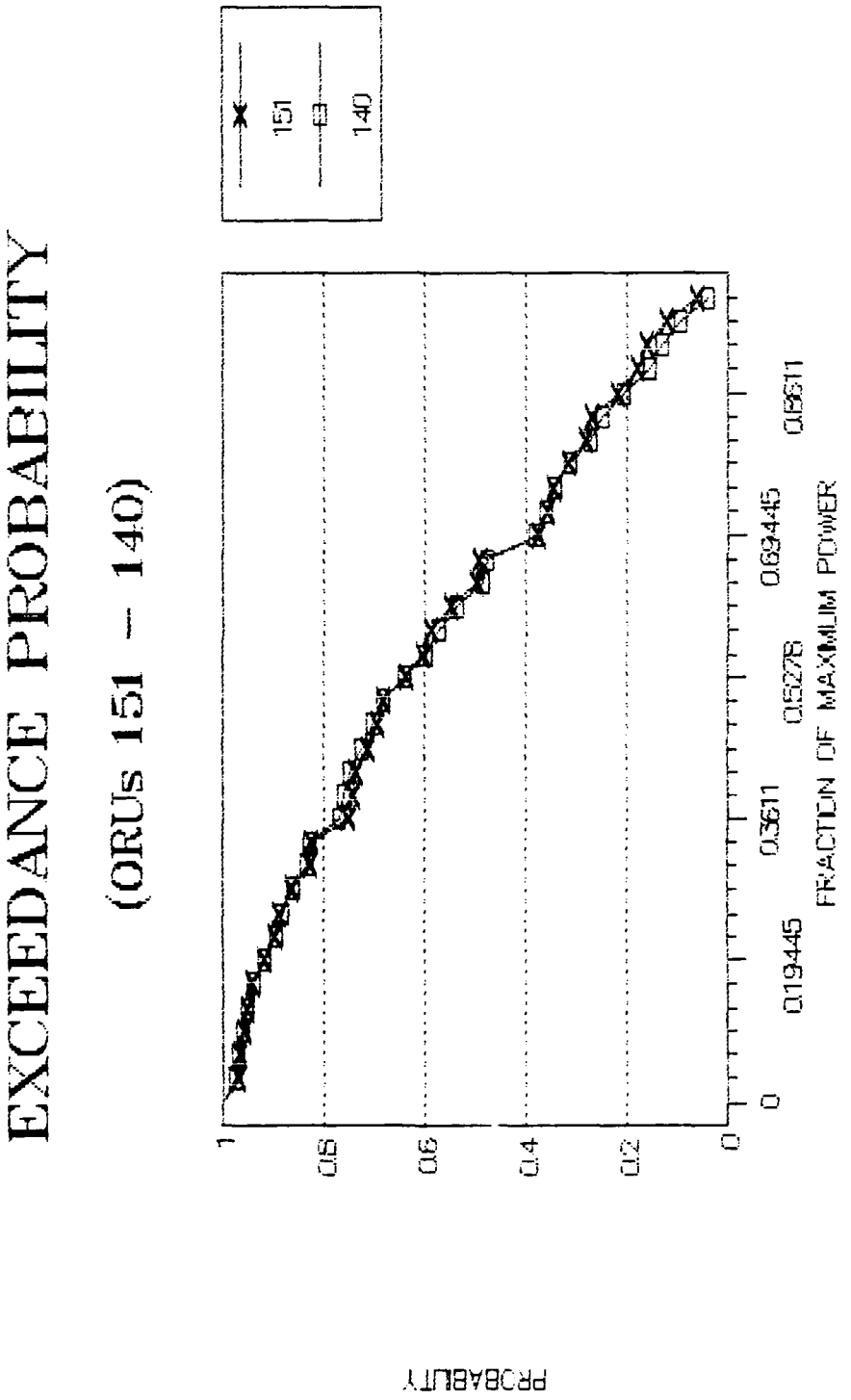

Figure 4-4. Exceedance Probability Plot (ORUs 151 & 140).

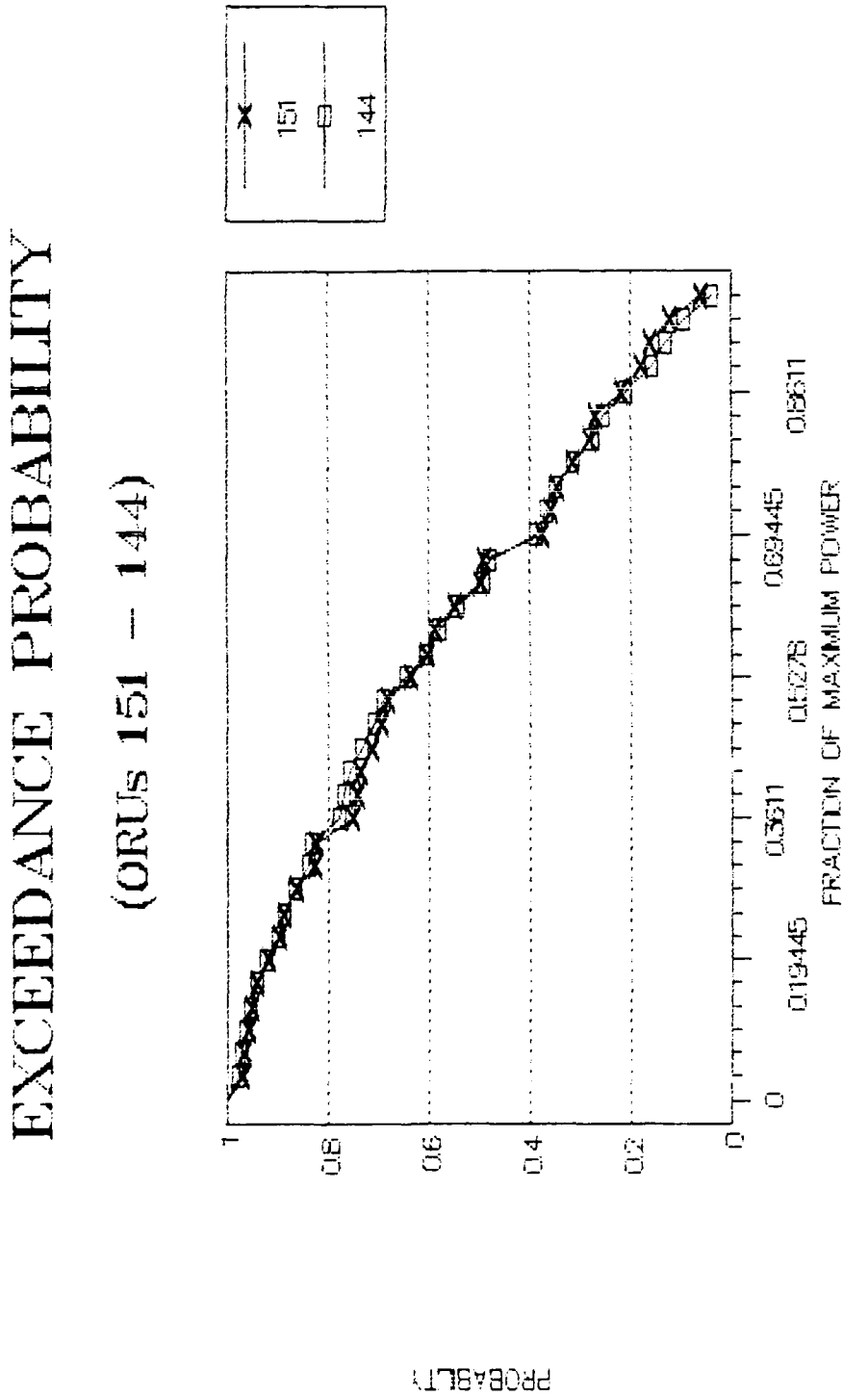

Figure 4-5. Exceedance Probability Plot (ORUs151 & 144).

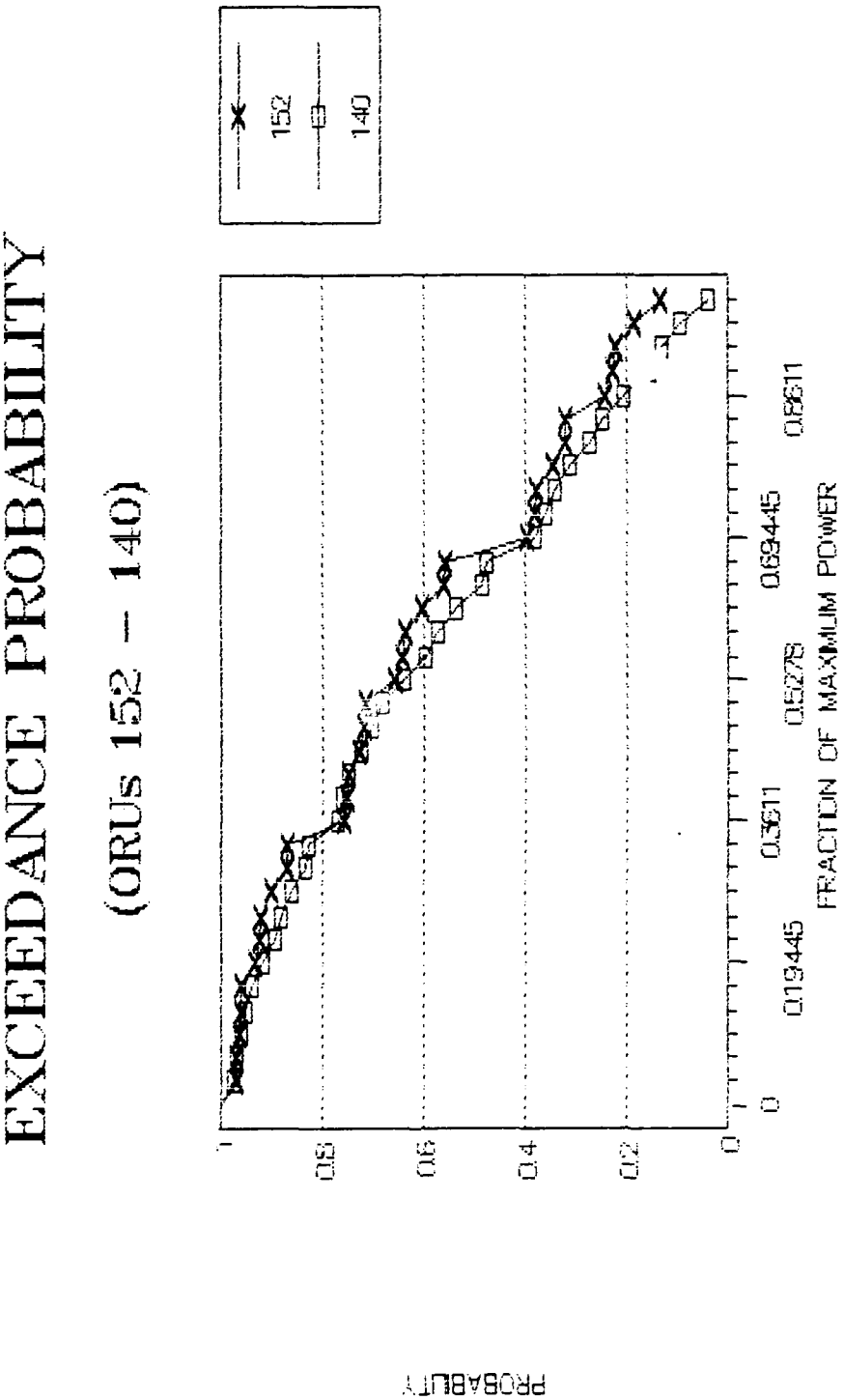

Figure 4-6. Exceedance Probability Plot (ORUs 152 & 140).

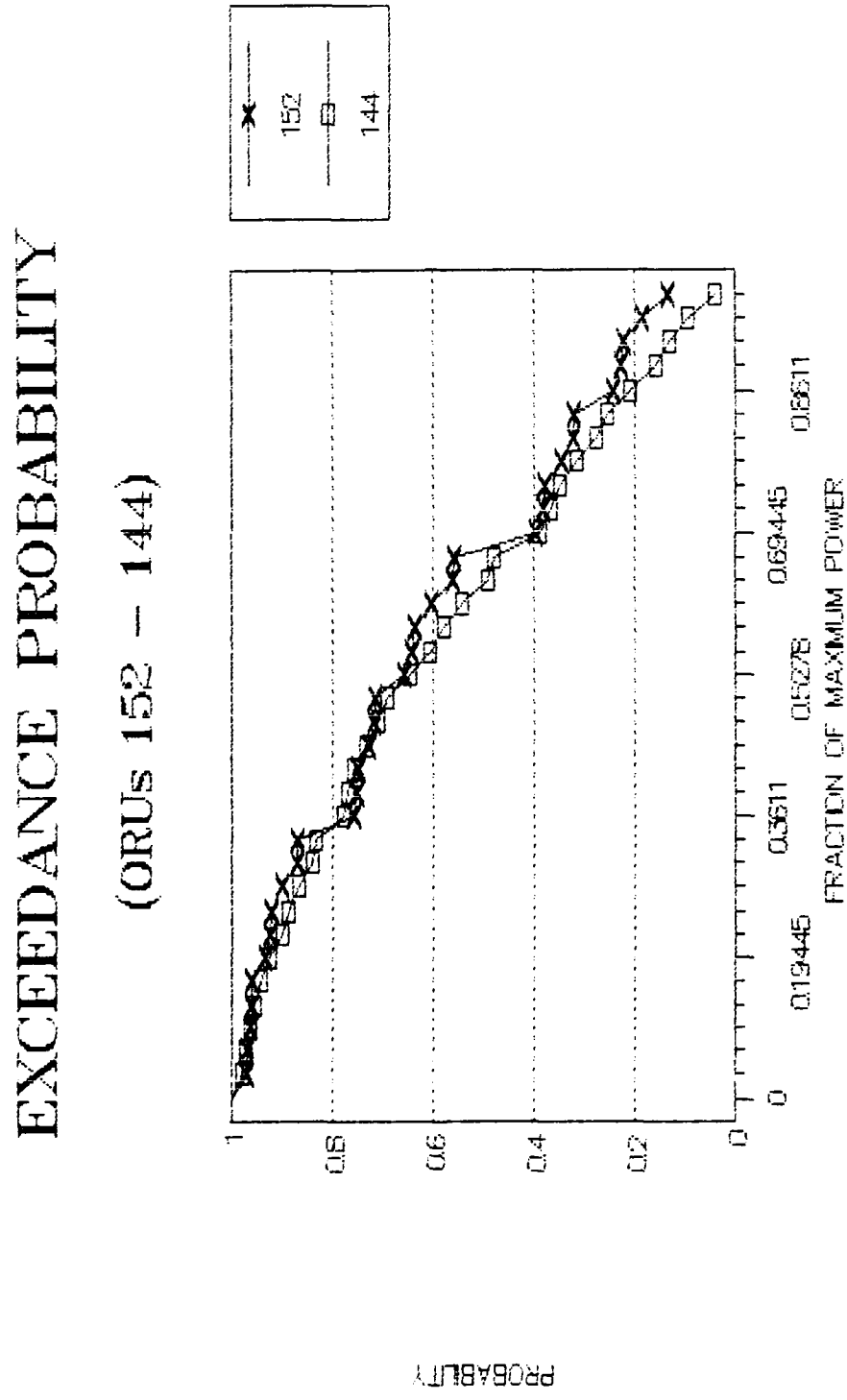

Figure 4-7. Exceedance Probability Plot (ORUs 152 & 144).

This tells us that when each ORU is perfectly reliable, one ORU has a higher probability than another in that specific interval. However, some ORUs do not have equal impact at each interval and may not be more critical than another ORU through the entire power spectrum. Since generally this phenomenon occurs much below the 100% interval, it may not be important. The importance of these "crossovers" could better be determined if the critical thresholds were known, i.e., what station functions are affected when the power falls below what level.

We do observe that the ORUs which seem to act irregularly (criticality rankings fluctuate significantly) are those modeled as part of the energy storage assembly (i.e., battery packs, BCDUs, utility plates and MIUs). As can be seen in Figures 4-4 through 4-7, the ORUs' reliabilities jump significantly at the 33.3% and 66.7% power levels. This is due to our assumption that the insolar model provides two-thirds of the power produced by the PV module and the eclipse model provides one-third. If we segment the exceedance plots into thirds, we note that each ORU possesses a plot whose pattern is similar in each segmented third. The only difference between each segment is that the rate that the reliability decreases increases as power increases.

Using Figure 4-7 as an example, we note that the plot for the PVSC varies more than the plot for the battery packs, i.e., the extremes for the PVSC are dispersed farther apart than the extremes for the battery packs. This greater dispersion by the PVSC ORU extremes combined with the larger decrease of reliability for the battery packs at the one-third and two-third points, provides an explanation for the "crossovers." The difference in the descents of the battery pack and PVSC plots seems to be caused by the number of ORUs in our model. There are 15 battery packs modeled and only two PVSCs modeled. As for the larger decrease at the segment divisions, the ESA ORUs seem to have a greater change at these points probably due to the fact they affect only one-third of the power while all other ORUs in someway affect 100% of the power. The key point is some ORUs in the PV model do not always remain relatively more critical than other ORUs at all levels as is the case in the SD and PMAD models.

Fifth, a comparison of the criticality rankings when a component is perfectly reliable and when its MTBF is improved provides more information. For instance, comparing the rankings at 100% power and t = 720, we notice that the ORUs are in the same relative order except for ORUs 103 and 142. ORU 142 is more critical in

the perfectly reliable case, but ORU 103 is more critical in the improved MTBF case. This is due to the MTBFs of each. The MTBF for ORU 142 is 87,600 hours (10 years) and the MTBF for ORU 103 is 131,400 hours (15 years). Since ORU 142 has a shorter MTBF, then being perfectly reliable will allow it to have a larger effect on the model. As the MTBFs increase, at some point ORUs 103 and 142 would have an equal impact; but in this work, all we can determine is that in fact ORU 142 has the possibility of having a greater impact on the PV module's performance than ORU 103. Not much can be said for the PV module at 50% power and t = 720 due to the miniscule differences between their impact on the power output. In general, there are just minor differences in the general rankings which are functions of the length of individual ORU MTBFs and their impact on a specific level of power.

ASSEMBLY RESULTS

First, when we examine the criticality rankings results when we made assemblies perfectly reliable, the receiver/PCU assembly is always the most critical. This is no surprise since this assembly is purely a series assembly. Even though the receiver/PCU ORUs have fairly long MTBFs, being a series system makes it vulnerable. Therefore, evidence indicates improvement on this

assembly's performance should be made first given that all assemblies use the same amount of resources. Added redundancy would be one method to do this. The EEA is the second most critical due to its ORUs having low MTBFs.

Second, when we examined the PV model at the 100% power level at one month and one year, the two most critical assemblies were the ESA and the SAA, respectively. This is due to the fact that these two assemblies are responsible for producing the power and determine what power levels exist. The better these assemblies are, the more likely the 100% power level can be obtained. If just one fails (there are four SABB ORUs and fifteen battery pack ORUs), then the system cannot produce 100% power. Taking this one step further, even though the SAA is responsible for producing more power than the ESA, there are just more ORUs that could fail and they have shorter MTBFs than the SAA ORUs. One might say that the ORUs that do not affect the power output levels have an equal impact at each level while the SAA and ESA specifically influence each power level differently.

However, when we examine the 50% power level at $t = 720$, the IEA is the most critical, but all assemblies generally affect the power output equally. This is probably due to the fact the nominal case reliability at

t = 720 is quite high (0.99359) and there is not much room to improve significantly. At t = 8760, the SAA is most critical and the ESA drops to fourth. This is due to the fact that the ESA has less impact on the system reaching 50%. The whole ESA could produce up to 66.7%. Therefore, for the same reason stated above for t = 720 at 100%, the SAA is the system whose performance should be improved with highest priority.

Third, when comparing the three models against each other on their effect to the EPS system, it is obvious the PMAD is the most reliable. This is due to: (1) there being fewer components in any path within the PMAD than there are in either the PV or SD model paths, and (2) there being greater redundancy in the PMAD.

Based on this ORU level analysis, the SD module is more likely to produce maximum power than the PV module. This in part is due to the fact there are just two power intervals. The reality that there are fewer components also helps. However, the fact that the SD is more likely to produce 100% power than the PV is misleading. The reverse analogy is not appropriate; that is, the PV module is not more likely to have a complete failure, or 0% output, than the SD module. Operators of the EPS will have to determine what are the key cutoff points in power level. for their uses. Perhaps the station can operate at

50% power for months. Perhaps the station has to operate at 90% power at all times; otherwise, life support systems could falter. Only the operators can make these determinations.

In Phase 1 as it stands now, the PV module is the only power producing system. In Phase 2, PV modules produce 60% of the EPS power, and SD modules produce the other 40%. Which system is more critical to the EPS is a function of the critical power thresholds and the impact of each module on the final outputs.

Finally, we will summarize the most critical ORUs and assemblies based on our test case. The battery pack was the most critical to the PV module for the higher power intervals while the sequential shunt unit was most critical at the 50% power level. The SD controller was the most critical at all power intervals to the SD module, and the power management controller was the most critical to the PMAD system. The energy storage assembly was the most critical assembly to the PV module at the 100% power level while the solar array assembly was the most critical at the 50% level. The receiver/PCU assembly was the most critical to the SD module at all power intervals.

POTENTIAL USE IN LOAD SCHEDULING

Obviously, our approach is useful in analyzing the reliability of the Space Station EPS. Other potential uses include 1) analysis of the same system at levels below the ORU level to assist in improving individual ORU reliability, 2) analysis of other complex space power systems and other similar power systems of a multi-modular design providing power to a small number of known loads, and 3) assisting in another area of scientific concern within the Space Station program such as load scheduling. By providing a tool that can determine what a system's reliability is in producing a certain level of power, it can be quite beneficial in selecting a good load schedule in terms of reliability.

The problem of load scheduling is being able to provide an "optimal" schedule. Due to the size of the problem and to fluctuating power requirements, finding the "optimal" schedule in a timely fashion may not be easy. There may be many "optimal" schedules which meet all constraints put into the problem (i.e., minimizing unused energy and varying the size of the energy storage assembly). Additional criteria may be needed to help reduce the set of candidate schedules further for ease and quality in the final solution. One of these criteria

is the reliability of the system in providing a certain level of power. To demonstrate this potential use, we provide a simple example where our approach can aid in the load scheduling problem.

SCHEDULING EXAMPLE

Suppose, according to a load schedule, the following load power profile is to be provided:

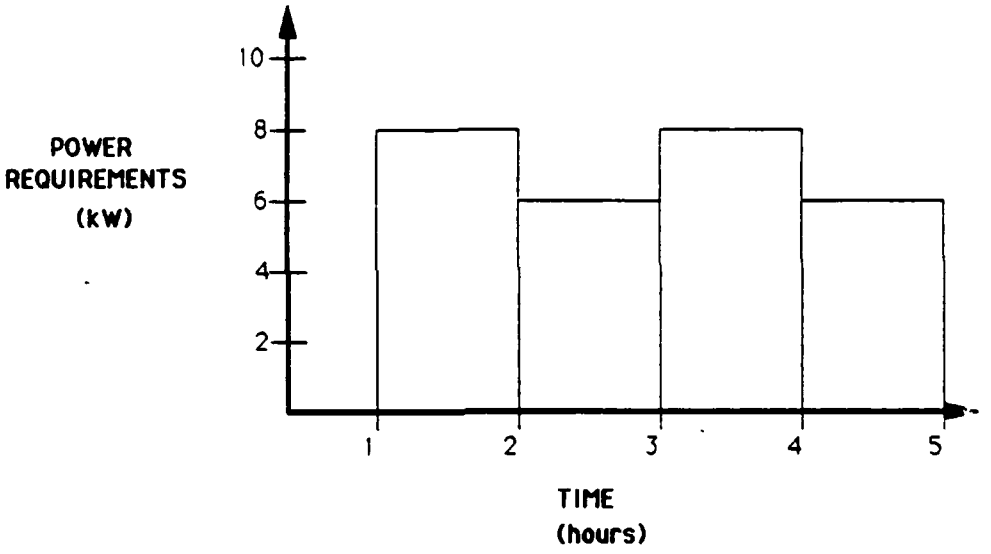

Figure 4-8. Example Load Power Profile.

This load needs 8 kW of power one hour into the mission for one hour. Two hours into the mission, this load needs 6 kW for one hour and so forth. Five hours into the mission, no additional power is needed.

The EPS we will use for this example has a simplified power spectrum given by Figures 4-9 and 4-10 which can be easily produced using the RBDs described in the previous

chapter. This is accomplished by determining the length of the time intervals desired, computing the exceedance probabilities for each interval, and recording the reliability for the power levels concerned (6 kW and 8 kW in our example).

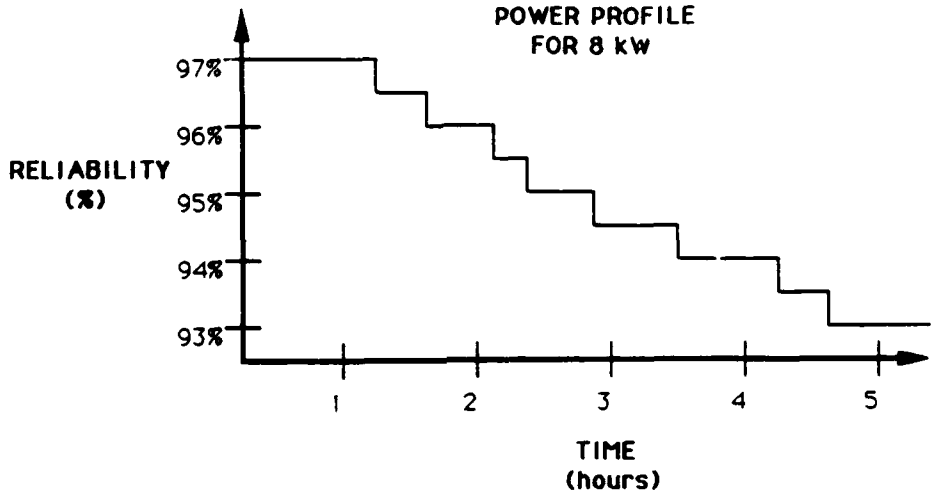

Figure 4-9. Example 8 kW Power Spectrum.

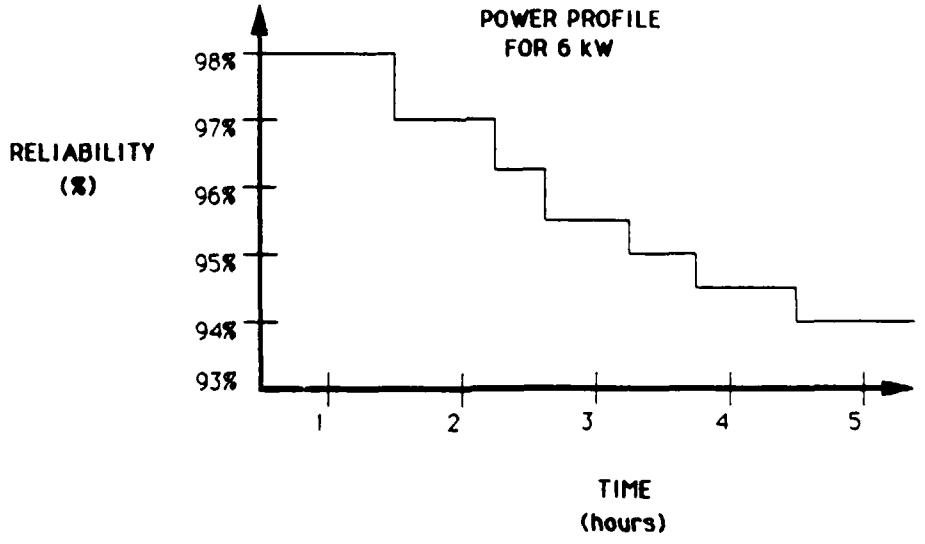

Figure 4-10. 6 kW Power Spectrum.

We use Figure 4-9 to explain the information provided. One hour into the mission, the power system will produce at least 8 kW of power with 97% reliability. Two hours into the mission, the power system will produce at least 8 kW with 96% reliability. Similar information is contained in Figure 4-10. During hours 2 and 3, the system will produce at least 6 kW of power with 95.5% reliability. Comparing this information with the load's power requirements, we see that the system can provide the required power with 96% reliability during the 1 to 2 hour time period and with 95.5% during the 2 to 3 hour time period. Each of these reliabilities are the result of determining the minimum reliability for that time period's power requirement. Table 4-6 provides the system reliabilities for each time period's power requirements.

TIME PERIOD (hours)	POWER REQ'TS	RELIA-BILITY
1 -2	8 kW	96%
2 -3	6 kW	95.5%
3 -4	8 kW	94%
4 -5	6 kW	94%

Table 4-6. System Reliability in Meeting Load Schedule Power Requirements

Therefore, as far as the system's ability to provide the load schedule's power requirements, this schedule has a reliability of 94% which is the minimum reliability during any time period. The following relationships define the computations:

$$R(I_i) = \min_{t \in I_i} R_W(t) \qquad (7)$$

$$R(T) = \min_{I_i \in I} R_W(I_i) \qquad (8)$$

where $i = 1,\ldots,n$;

W = the power levels;

I_i = the interval i;

I = set of all intervals

$= \{I_1, I_2, \ldots, I_n\}$; and

$R(T)$ = reliability of the load power profile during the period T. The reliability of the system to fulfill other "equally optimal" schedules' power requirements can be determined. This information can then discriminate between a set of "equally optimal" schedules and facilitate selecting a "more optimal" set of load schedules. The example above is in reality a multi-objective decision problem. The use of reliability results to discriminate between the set of "equally optimal" schedules is a lexicographic solution technique. There are other multicriteria methods including techniques for generating Pareto-optimal schedules [8]. In this area of load scheduling, our reliability approach

seems to be a useful tool.

One note of warning must be given at this point. In reality, over a period of four hours, the reliability of a power system will not decrease as fast as in our contrived example above. So many times, the method we used will not be useful; however, over longer time intervals (feasibly, a load could require several weeks or months to complete), reliability might decrease significantly enough where this approach would be useful.

CHAPTER 5 - SUMMARY AND CONCLUSIONS

CONCLUDING REMARKS

This work began as an effort to model the Space Station electrical power system in a series-parallel configuration. As the modeling process progressed, it became apparent that when certain ORUs failed, some power would be lost to the output, but not everything. The standard series-parallel approaches determine the reliability that the system works or does not work. Therefore, an analytical method had to be utilized to determine the reliability at different power levels. To accomplish this, we used a generalized case of capacity outage probability tables which we call the partitioned parallel connection. The partitioned parallel connection was the method that in essence defined the system's capabilities in terms of power outputs. Standard methods used most often define the component's capabilities using throughput capacities or percentage of maximum power output. Our method allows the system to define the effect components or assemblies have on the system. However, this method requires thousands of calculations for a complex system such as the EPS.

Since there were so many components, a computer program had to be developed to calculate the reliability. The number of power levels grew to such an amount that required a technique to reduce unnecessary calculations. The identification that exceedance probabilities could be used helped eliminate the calculations obstacle. Representing the output in terms of exceedance probabilities was the best way to display the reliabilities of what was a continuous power spectrum. At this point, our model had to be adjusted to separate the PV components that were needed during the insolar cycle and those needed during the eclipse cycle since the battery was assumed not needed during the insolar cycle. However, the problem was how to combine the two cycle models into one model.

Here the steady state assumption was the key. Since we assumed the system was at steady state whenever we wanted to evaluate it, we could then assume that the batteries would be fully charged. Also, we could assume that since the insolar cycle lasted two-thirds of each orbit, then the insolar model would provide two-thirds of the power on the average.

The problem encountered at this point was how to combine the PV's insolar and eclipse models. The summation connection was the provided remedy, but again

caused the number of power levels (thus the number of calculations) to combinatorially expand. These tools now allowed us to conduct a simple sensitivity analysis to identify critical ORUs that would be likely candidates to improve upon to enhance the system's performance.

The results provided no surprises except perhaps for the energy storage assembly's change in criticality. This phenomenon can be explained by its responsibility in determining the power levels and its relative influence at 100% power and 50% power. In order for the system to produce maximum power, the battery pack ORUs were the most critical in all cases where time was two years or less. However, since their influence on the system's ability to produce 50% maximum power is much less, the SAA ORUs became more critical. As for the SD model, the ORU with the shortest MTBF was the most critical since the SD model was much more simple being a series dominated system. The PMAD model's most critical ORU was the PVSC, the ORU with the shortest MTBF, although for slightly different reasons than used for the SD model.

The SD and PMAD models demonstrated that even though the test cases varied different parameters, the criticality rankings remained generally the same. However, since the PV model was more complex with much different relationships between components and

assemblies, the same was not true. A much closer look was needed to demonstrate how different ORUs are critical at one power level but not as critical at another. This phenomenon is more common with the power "producing" ORUs that utilize the partitioned parallel connection.

The most significant tool used in this work, although not an entirely new concept in the field of power systems reliability, is the partitioned parallel connection. It allows an analyst to define the power system without having to define each component's power characteristics. In many simulations, much time is spent trying to establish the states the system could generate. Most try to discretize a continuous system in the attempt to better understand the data and demonstrate how the system acts. In our model, only the MTBF and the failure output had to be defined for each block, as well as the type of block each ORU was. The partitioned parallel connection, and the other connection types, defined the other system characteristics which is what other system modelers are doing when they try to define each component's affect on the power output. This seems to be a more natural way of approaching the system modeling problem.

CONTRIBUTIONS

This work provides four contributions worth noting. First, by allowing the system to define its power output levels, computing the power profile can be done much faster using our approach. Second, using a computer package similar to the one developed in support of this work, our approach is much more flexible since our only tools are blocks and connections. Third, this is the only work to date which solely uses the ORU as the component level. Since the replacement policy is to use the ORU as the building blocks to the EPS, it is reasonable to do an analysis using the ORU as the reliability blocks also. Fourth, the power spectrum produced by our approach is much more realistic than previous attempts. Since we allow the system to define the intervals based on the characteristics of the model, the intervals are different sizes. Previous attempts define the intervals disregarding the system's characteristics initially. As mentioned earlier, our approach seems to be a more natural way to produce a power spectrum.

The concepts in this work were not complicated, yet it approached a systems problem using a slightly different approach. The partitioned parallel method seems well suited for modeling complex power systems from a systems perspective. After using this method, it is our

firm opinion that it is a viable tool to be considered by all space power system reliability analysts.

EXTENSIONS AND MODIFICATIONS

We made many assumptions in order to make our model work. Some could be eliminated with further efforts using the methods practiced in this work. To provide each component with a status other than being new at the beginning of the evaluated period is a minor variation in the exponential distribution. Adding the capability of repairing, maintaining, and replacing components at designated time periods would provide even better results and allow analysis of availability and maintainability. This type of extension is highly recommended. Modeling below the ORU level could add insight to the amount of redundancy needed to improve on those components that are most critical. Combining this model with a Bayesian model that could use these results as a prior distribution is in the making. Since the Space Station is still in flux as are the maintenance policies, an analysis on the cost effectiveness of scheduled replacement policies could be conducted. Additionally, since testing of the EPS components is ongoing, new data could be used in conjunction with our model to determine any changes in the reliabilities. Finally, we demonstrated how our

approach can be used in the load scheduling problem.

BIBLIOGRAPHY

[1] Allan, R.N.,et al;IEEE Tutorial Course Power System Reliability Evaluation, New York: Institute of Electrical and Electronic Engineers, Inc., 1982.

[2] Allen, William H., Poehle, Robert J., and Evatt, Thomas C., "Application of Advance Automation Techniques in the Space Station Electrical Power System," Proceedings of the Twenty-First Intersociety Energy Conversion Engineering Conference, August 25-29, Volume 3, 1986, pp. 1416-1422.

[3] Ang, Alfredo H-S. and Tang, Wilson H., Probability Concepts in Engineering Planning and Design, Volume 2: Decision, Risk, and Reliability, New York: Wiley & Sons, 1984.

[4] ARINC Research Corporation, UNIRAM Modeling of the NASA Space Station Electric Power System, prepared for NASA Lewis Research Center, 1988.

[5] Barton, John R. and Liffring, Mark E. "Autonomous Power System Test Bed Development," Proceedings of the Twenty-First Intersociety Energy Conversion Engineering Conference, August 25-29, Volume 3, 1986, pp. 1751-1756.

[6] Billinton, Roy and Allan, Ronald H.,Reliability Evaluation of Engineering Systems: Concepts and Techniques, New York: Plenum Press, 1983.

[7] Billinton, Roy and Allan, Ronald H.,Reliability Evaluation of Power Systems, Great Britain: Pitman Books Limited, 1984.

[8] Boyle, R.V., Coombs, M.G., and Kudija, C.T., "Solar Dynamic Power Option for the Space Station", Proceedings of the Twenty-Third Intersociety Energy Conversion Engineering Conference, July 31-August 5, Volume 3, 1988, pp. 319-328.

[9] Chankong, V. and Haimes, Y.Y., Multiobjective Decision Making: Theory and Methodology, Elsevier-North Holland, New York, 1983.

[10] Chankong, V., et al;"A Two-Level Structure for Advanced Space Power System Automation," report prepared for NASA Lewis Research Center, March 1989.

[11] Decker, D.K. and Vivian, Dr. J.M., "Energy Planning and Allocation for Multihundred Kilowatt Spacecraft", Proceedings of the Twenty-First Intersociety Energy Conversion Engineering Conference, San Diego, CA., August 25-29, Volume 3, 1986, pp. 2077-2080.

[12] DiFilippo, Denise, Space Power System Scheduling, M.S. Thesis, Case Western Reserve University, Cleveland, Ohio, October, 1988.

[13] Dolce, James L. and Faymon, Karl A., "Automating the U.S. Space Stations Electrical Power System", Optical Engineering, Volume 25, No.11, November 1986, pp. 1181-1185.

[14] Dunning, John W., Jr., "Space Station Power System Requirements", Proceedings of the Twenty-Third Intersociety Energy Conversion Engineering Conference, July 31-August 5, Volume 1, 1988, pp. 29-36.

[15] Faymon, Karl A., et al; "Lewis Research Center Power System Autonomy Program 1990 Demonstration", Proceedings of the Twenty-Second Intersociety Energy Conversion Engineering Conference, August 10-14, Volume 1, 1987, pp. 547-551.

[16] Fuhr, Kenneth H., "Failure Analysis of 3.5 Inch, 50 Ampere-Hour Nickel Hydrogen Cells Undergoing Low Earth Orbit Testing", Proceedings of the Twenty-Second Intersociety Energy Conversion Engineering Conference, August 10-14, Volume 2, 1987, pp. 889-892.

[17] Gombos, Frank J., and Dravid, Narayan, "An Integrated and Modular Digital Modeling Approach for the Space Station Electrical Power System Development", Proceedings of the Twenty-Third Intersociety Energy Conversion Engineering Conference, July 31-August 5, Volume 1, 1988, pp. 49-55.

[18] Haas,R.J., and Chawathe,A.K., "Space Station Nickel-Hydrogen Cell Design and Development", Proceedings of the Twenty-Third Intersociety Energy Conversion Engineering Conferenc, July 31-August 5, Volume 3, 1988, pp. 573-576.

[19] Hoffman, David, "RAM Simulation Model User's Guide," prepared for Space Station System Directorate of NASA Lewis Research Center, August 1988.

[20] Hoffman, David, "System Level RAM Modeling", Preliminary Information Report, prepared for Space Station System Directorate of NASA Lewis Research Center, October 6, 1987.

[21] Hudak, Ronald E., "Life Test Results of the Intelsat-V Nickel-Hydrogen Battery", Proceedings of the Twenty-Second Intersociety Energy Conversion Engineering Conference, August 10-14, Volume 2, 1987, pp. 897-899.

[22] Hwang, Warren C., Carter, Boyd J., and Badcock, Charles C., "Qualification of Space Batteries", Proceedings of the Twenty-Third Intersociety Energy Conversion Engineering Conference, July 31- August 5, Volume 1, 1988, pp. 1-2.

[23] McClure, John, Berman, Douglas, and Schweppe, Fred, "Autonomous Management of the Space Station Electric Energy System", Society of Photo-Optical Instrumentation Engineers, Space Station Automation II-Proceedings, October 28-30, 1986 pp. 90-97.

[24] McNamara,J.E., et al; "Photovoltaic Power Subsystem Design for Space Station", Proceedings of the Twenty-Third Intersociety Energy Conversion Engineering Conference, July 31- August 5, Volume 2, 1988,pp. 583-588.

[25] Miller, William D. and Jones, Ellen F., "Automated Space Power Distribution and Load Management", Proceedings of the Twenty-Second Intersociety Energy Conversion Engineering Conference, August 10-14, Volume 1, 1987, pp.544-546.

[26] Miller, William D. and Jones Ellen F., "Automated Power Management Within a Space Station Module", Proceedings of the Twenty-Third Intersociety Energy Conversion Engineering Conference, July 31-August 5, Volume 3, 1988, pp.395-399.

[27] Nored, Donald L. and Bernatowicz, Daniel J., "Electrical Power System Design for the U.S. Space Station", Proceedings of the Twenty-First Intersociety Energy Conversion Engineering Conference, August 25-29, Volume 3, 1986, pp.1416-1422.

[28] Pages, Alain and Gondran, Michel. System Probability: Evaluation & Prediction in Engineering, New York : Springer-Verlag, 1986.

[29] Rice, Robert R., "Space Station Power System Selection", Proceedings of the Twenty-First Intersociety Energy Conversion Engineering Conference, August 25-29, Volume 3, 1936, pp.1886-1891.

[30] Rocketdyne Division of Rockwell International, Systems Engineering and Integration, Power System Description Document, prepared for Space Station Freedom Electric Power System WP-04, SE-02, October 28,1988.

[31] Sheskin, Theodore J., "Allocating Energy to Experiments on the Space Station", Proceedings of the Twenty-Second Intersociety Energy Conversion Engineering Conference, August 10-14, Volume 1, 1987, pp.345-349.

[32] Singh,C., et al; "Reliability Models for Space Station Power System", Proceedings of the Twenty-Second Intersociety Energy Conversion Engineering Conference, August 10-14, Volume 1, 1987, pp. 268-273.

[33] Singh, C., et al; " A Simulation Model for Reliability Evaluation of Space Station Power Systems", Proceedings of the Twenty-Third Intersociety Energy Conversion Engineering Conference, July 31- August 5, Volume 2, 1988, pp. 595-598.

[34] Smithrick, John J., "Effect of Leo Cycling at Shallow Depths of Discharge on Mantech IPV Nickel-Hydrogen Cells", Proceedings of the Twenty-Third Intersociety Energy Conversion Engineering Conference, July 31-August 5, Volume 2, 1988, pp. 447-451.

[35] Teren, Fred, "Space Station Electric Power System Requirements and Design," Proceedings of the Twenty-Second Intersociety Energy Conversion Engineering Conference, August 10-14, Volume 1, 1987, pp.39-47.

[36] Turnquist, Scott R., and Twombly, Mark A., Space Station Electrical Power System Availability Study, Prepared for Lewis Research Center, ARINC Research Corporation, Annapolis, Maryland, November, 1988.

[37] Vogt, S.T. and Proeschel, R.A., "Space Station Photovoltaic Power Module Design", Proceedings of the Twenty-Third Intersociety Energy Conversion Engineering Conference, July 31-August 5, Volume 3, 1988, pp.567-572.

APPENDIX A - SPACE STATION ELECTRICAL POWER SYSTEM COMPONENT DESCRIPTIONS

PHOTOVOLTAIC MODULE (PV)

SOLAR ARRAY ASSEMBLY - converts solar insolation to DC electrical power during sunlit portion of orbit.

101,102 RIGHT or LEFT SOLAR ARRAY BLANKET and BOX

-structure that houses the large area silicon solar cells used in converting solar energy into electrical energy. The solar cells are fixed to an accordion-folded flexible blanket stored in a box during launch.

103 MAST/CANISTER

-support mechanism that deploys and provides support for the solar blanket. The canister houses the mast mechanism during launch.

104 SEQUENTIAL SHUNT UNIT

-provides control of solar array voltage by shunting array current that exceeds the load demand.

BETA GIMBAL ASSEMBLY - provides structural support, structural attachment, articulation for sun P&T and the transfer of electrical signals and power to and from the station PV power module.

111 GIMBAL ROLL RING SUBASSEMBLY

-delivers electric power command signals and data from solar array assembly through the beta gimbal assembly to the IEA. The power and data that flows through this subassembly is destined for the electrical equipment assembly to be converted, stored and distributed as required.

112 GIMBAL BEARING SUBASSEMBLY

-provides rotational capabilities and structural support for the roll ring subassembly, drive motor subassembly and PV array. It provides path between the power generation device and the transition structure while allowing for orientation to the sun.

113 GIMBAL DRIVE MOTOR SUBASSEMBLY

-controls the position, velocity and acceleration of the beta gimbal. It provides control commands to the gimbal drive motors. It imparts drive torque to the bearing subassembly via the ring gear enabling the beta gimbal to rotate.

114 STATION GIMBAL TRANSITION STRUCTURE

-positions the beta gimbal as designed.

INTEGRATED EQUIPMENT ASSEMBLY - provides structural attachment for energy storage and electrical equipment assemblies requiring on-orbit maintenance and cooling.

121 INTEGRATED EQUIPMENT ASSEMBLY STRUCTURE

-serves as the structure to which utility plates, thermal manifolds and electrical cables are attached.

122 CABLE SET AND TRAY

-provides cabling connecting components requiring data or power. It integrates the PV cable set to the truss and the structural framework.

HERMAL CONTROL ASSEMBLY - acquires and transfers excess heat from PV module and rejects it to space.

131 RADIATOR PANEL

-provides the medium to reject excess heat acquired by the utility plates. It consists of nine panels, a condenser section that actually rejects the heat into space, and an evaporator section that interfaces with the main condenser. Its design allows for two panels to fail before affecting ORUs on the utility plates.

132 GN_2 CANISTER

-contains nitrogen gas used to pressurize the bellows which are used to provide a high contact force evenly distributed over the contact area between the condenser and radiator panels.

133 PRESSURIZATION UNIT

-regulates the pressure of the nitrogen gas in the radiator panels to ensure continual and maximum contact between the condenser and radiator panels.

134 INTERCONNECT PLUMBING

-piping that connects the elements of the thermal control assembly and provides a vessel for the transport of excess heat and heat transport fluids. It includes piping taking the heat from the utility plates and connects the heat acquisition, heat transport and heat rejection components.

135 CONDENSER/INTERFACE SUBASSEMBLY

-receives super-heated ammonia vapor from the utility plates and releases heat to the evaporator of the radiator panels. It condenses the vapor into sub-cooled liquid which enters the cold end pumping chamber of the rotating fluid management device (RFMD).

136 CONDENSER MOUNT STRUT

-provides a mounting location for the condenser so it will be in contact with the radiator panels.

137 ACCUMULATOR

-regulates the amount of liquid ammonia in the RFMD of the pump unit. It is part of the heat transport subassembly that is activated when transients arise

in the various heat transfer processes. The accumulator volume is controlled by the vapor pressure of the ammonia.

138 THERMAL CONTROL PUMP UNIT

-provides force to maintain proper fluid flow in the thermal control assembly.

139 THERMAL SUPPORT STRUCTURE

-provides the support framework for the thermal control assembly.

140 UTILITY PLATES

-provides surface to mount battery packs and electronic equipment ORUs. It provides thermal, electrical and fluid interfaces between energy storage assembly ORUs and the PV electrical equipment ORUs. The plates are mounted to the integrated equipment assembly.

ELECTRICAL EQUIPMENT ASSEMBLY - conditions and controls electrical power and provides electrical interface to PMAD and Solar Dynamic (SD) modules.

141 DC SWITCHING UNIT (DCSU)

-regulates and controls the source power so input power is always within acceptable limits. It provides the power switching function for interconnection of solar array and battery source power to the main inverter units (MIUs) for

conversion to 20kHz AC power. DCSUs are always used in redundant pairs.

142 MAIN INVERTER UNIT (MIU)

-converts DC power obtained by the solar array or energy storage assembly to 20kHz AC power. MIUs are always used in redundant pairs.

143 MAIN BUS SWITCHING UNIT (MBSU)

-allows AC power to find the best path to PMAD. It is a combination of remote bus interface (RBIs) switches. It provides switching between redundant AC busses. MBSUs are always used in redundant pairs.

144 PV SOURCE CONTROLLER (PVSC or PVC)

-provides communication between the PMC and the PV module functional controllers. It controls the generation, storage and regulation of the PV source power. It controls and monitors the PV wings. It can operate PV module in the event of certain PMAD failures which increases system reliability. PVCs are always used in redundant pairs.

145 POWER DISTRIBUTION and CONTROL UNIT (PDCU)

-provides lower voltage AC power to PV module electrical equipment. It functions similarly to a wall outlet. PDCUs are always used in redundant pairs.

ENERGY STORAGE ASSEMBLY - stores, conditions, controls and distributes electrical power produced by solar arrays.

151 BATTERY CHARGE/DISCHARGE UNIT (BCDU)

-controls charge and discharge rates of the battery packs. In conjunction with commands from the PVC, measures and compares parameters and adjusts the charge rates to match the target charge rate values given by the PVC. It regulates current flow to the battery and boosts battery voltage to the level of the DC bus voltage. It isolates the battery pack from both the charge/discharge unit and the control power bus to protect the batteries against downstream faults. It consists of a battery controller, charge regulator, discharge regulator and DC fault interrupters and DC cables. One BCDU is used with every three battery packs. Peak power output is 6.5 kW.

152 NiH_2 BATTERY PACK

-meets all energy storage requirements for the station, including safety, performance, commonalty and modularity. It is a nickel hydrogen rechargeable battery consisting of thirty 81 A-hr cells in series.

401 ALPHA GIMBAL

-provides solar array and SD pointing on the alpha axis. It allows for passage across its assembly for data and electrical energy. It is not a part of the PV module.

SOLAR DYNAMIC MODULE (SD)

CONCENTRATOR ASSEMBLY - acquires and concentrates radiation into receiver.

201 REFLECTIVE SURFACE SUBASSEMBLY

-offset parabolic design of 19 hexagonal truss panels of lightweight graphite epoxy construction with multiple triangular reflective facets mounted in the hexagonal panels. It reflects incoming solar radiation through the solar dynamic receiver aperture.

202 CONCENTRATOR STRUCTURE STRUT SET

-provides framework to provide a fixed reference distance between the reflector vertex and the receiver aperture and firmly supports the reflector.

203 CONCENTRATOR CONTROLS CABLE SET

-provides connections within the concentrator for commands and data.

204 SUN SENSOR

-provides the sensing aperture used in determining the optimal angle for solar insolation.

205 INSOLATION METER

-measures solar insolation intensity data which is used to determine the adjustment the two-axis fine-pointing mechanism should make.

206 TWO-AXIS FINE-POINTING MECHANISM

-provides vernier-pointing capability and acts as the structural transition between the interface structure and reflector support strut set.

HEAT REJECTION ASSEMBLY - acquires and transfers excess heat waste from SD module and rejects it to space so as to maintain appropriate SD module component and electrical equipment within required temperature limits during active modules operations.

211 RADIATOR PANEL DEPLOYMENT SUBASSEMBLY

-provides the heat rejection function for SD module heat rejection assembly by radiating heat into space. It consists of eight panels, a deployment mechanism and the support structure.

212 HOT INTERCONNECT LINES

-fluid lines with disconnects that provide the flow path between the power control unit (PCU) assembly and the radiator array subassembly. Two pairs of lines exist.

213 COLD INTERCONNECT LINES

-two pairs of fluid lines with disconnects that provide the flow path between the SD utility plate and the PCU assembly.

214 PUMP INTERCONNECT LINES

-fluid lines with disconnects that provide the flow path between the radiator array subassembly and the fluid management units. Two pairs of lines exist.

215 UTILITY PLATE

-contains electronics cooling cold plate, thermal interface with electronics ORUs and fluid interfaces with other coolant management subassembly ORUs. Under all operating conditions the utility plate coolant outlet temperature remains less than 20°C.

216 FLUID MANAGEMENT UNIT

-contains all of the active components for each loop of the closed Brayton cycle (CBC) heat rejection assembly.

RECEIVER/POWER CONTROL UNIT (PCU) - make up the power generation subsystem. It exchanges heat from the heat source, stores thermal energy and converts thermal energy in the cycle working fluid to electrical energy.

221 RECEIVER

-admits concentrated solar flux through its aperture. It consists of 82 tubes carrying the working fluid that absorbs the solar energy. It serves as the heat source heat exchanger and thermal energy storage device for the SD module.

222 ENGINE CONTROLLER

-controls operation of the PCU.

223 PARASITIC LOAD RADIATOR

-performs the function of an electrical sink for excess power. It provides effective speed control for the turbo-alternator rotor while managing the excess power in a way that allows fast response to changes in user demand.

224 CONTROL VALVE ACTUATOR

-provides a closed-center, three-way diverter valve design. It isolates the accumulator from the compressor allowing pressure to be stored until needed for peak power operation.

225 PCU POWER CABLE SET

-provides power connections within and from the PCU.

226 PCU SIGNAL/DATA CABLE SET

-provides signal and data connections within the PCU.

ELECTRICAL EQUIPMENT ASSEMBLY - contains most of the major electric components required to operate and control the SD module and electric power it generates.

231 FREQUENCY CHANGER UNIT

-solid state power electronic component which converts the mid-frequency, 3-phase AC power from the SD alternator at its output to 20 kHz single phase as power at its output for transmission to the

SD module/PV module interface.

232 LINEAR ACTUATOR, OUTER

-in conjunction with the inner linear actuator translates and rotates the reflective surface subassembly independently of the receiver/PCU assemblies resulting in a low-gimbaled mass and modest coarse and fine-pointing parasitic power requirements.

233 LINEAR ACTUATOR, INNER

-in conjunction with the outer linear actuator translates and rotates the reflective surface subassembly independently of the receiver/PCU assemblies resulting in a low-gimbaled mass and modest coarse and fine-pointing parasitic power requirements.

234 SD CONTROLLER

-controls the total operation of the SD module excluding the PCU operations. It includes controls for concentrator pointing, beta gimbal pointing, radiator deployment/retraction, fluid pumps and overall SD supervisory control.

BETA GIMBAL ASSEMBLY - accounts for the seasonal motion of the sun and procession of the orbit plane, the beta gimbal rotates the SD module a nominal +52 degrees about the beta axis.

241 GIMBAL ROLL RING SUBASSEMBLY

-delivers electric power from the electrical equipment assemblies (output from the frequency changer unit) and data signals from the SD module controller, across the rotating interface to be delivered to and received from the PV module.

242 GIMBAL BEARING SUBASSEMBLY

-provides the structural path between the power generation device and the transition structure while allowing for rotation for orientation to the sun. It consists of a pair of bearings, wing gear and housings.

243 GIMBAL DRIVE MOTOR/CONTROLLER SUBASSEMBLY

-controls the position, velocity and acceleration of the beta gimbal. It provides control commands to the beta gimbal drive motors. It provides the position of the beta gimbal, drive motor status and health monitoring status to the SD controller. It provides torque to point and slew the attached power generation device.

244 STATION GIMBAL TRANSITION STRUCTURE

-positions the beta gimbal within the 5-meter truss so that it is centered within an outboard face of the 5-meter cube and positioned into the cube interior to allow for proper clearance of the

interface structure assembly with the transverse boom.

INTERFACE STRUCTURE/INTEGRATION HARDWARE ASSEMBLY - provides structural attachment and cabling for SD components.

251 INTERFACE STRUCTURE ASSEMBLY

-high rigidity interface structure to which all other SD module assemblies are ultimately attached. It supports the receiver assembly, the PCU assembly and the Heat Rejection assembly as well as the SD equipment box subassembly. It provides part of the interface between the Receiver/PCU/Heat rejection assemblies launch package and the shuttle.

252 SD CABLE SET

-conducts 20kHz AC, single phase power from the output of the frequency changer in the SD module to intermediate control equipment such as an RBI and from there to the SD module/PV module interface.

POWER MANAGEMENT AND DISTRIBUTION MODULE (PMAD)

301 MAIN BUS SWITCHING UNIT (MBSU)

-serves as the primary tie point for utility power feeder protection and supplies utility power to the distribution system. It turns internal RBIs on and off under normal operation and interrupts faults and reconfigures the system as necessary. MBSUs are always used in redundant pairs.

302 POWER MANAGEMENT CONTROLLER (PMC)

-primary controller of PMAD system. It provides overall power system coordination and EPS data flow. It is the interface between the power system and the data management system network and interfaces with subordinate controllers via the PMAD control bus. It conducts built-in test functions. It controls functions for power distribution system coordination and monitoring of power generation system. It has data management/communications functions with external systems and ground to include providing DMS with specific power system data that has been received from the lower level control processors and actual sensor data. It coordinates and commands the lower level control processors in order to provide users power.

303 AC/DC CONTROL UNIT (ADCU)

-converts AC power to DC power.

304 POWER DISTRIBUTION CONTROL UNIT (PDCU)

-serves as the final distribution point to all user loads and is always used in redundant pairs.

APPENDIX B - PRESENTATION OF DATA

CRITICALITY RANKING FOR PV

(720 HOURS – 100% POWER)

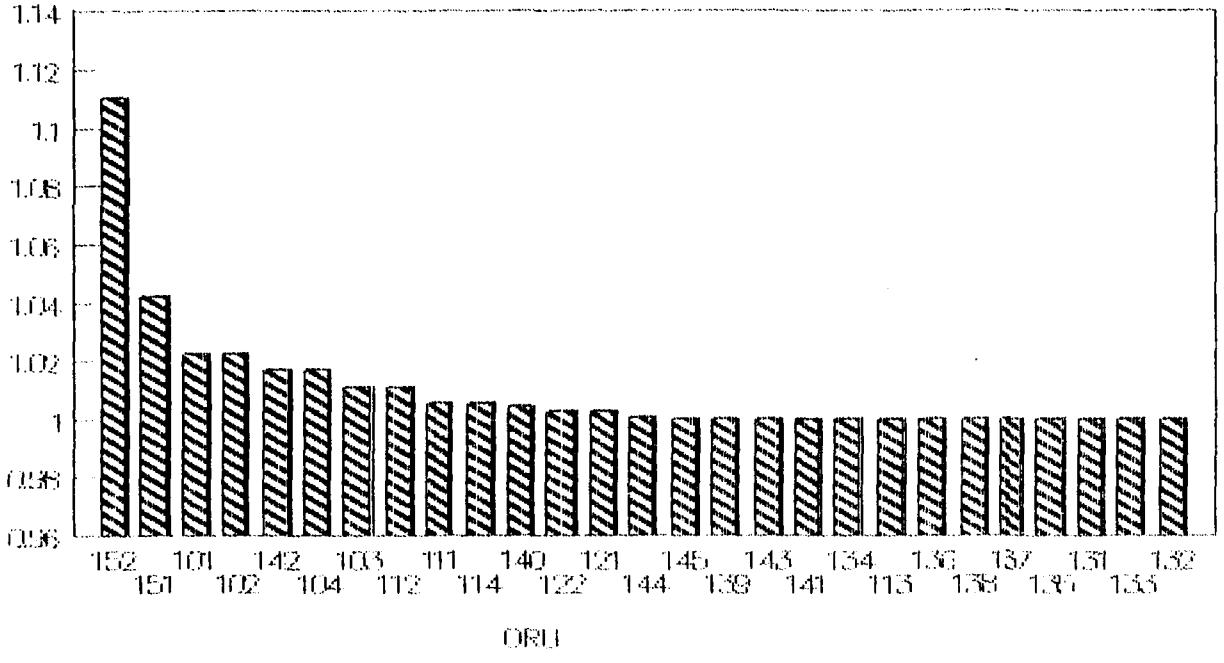

Figure B-1a. Criticality Ranking for PV Model (Perfect Reliability).

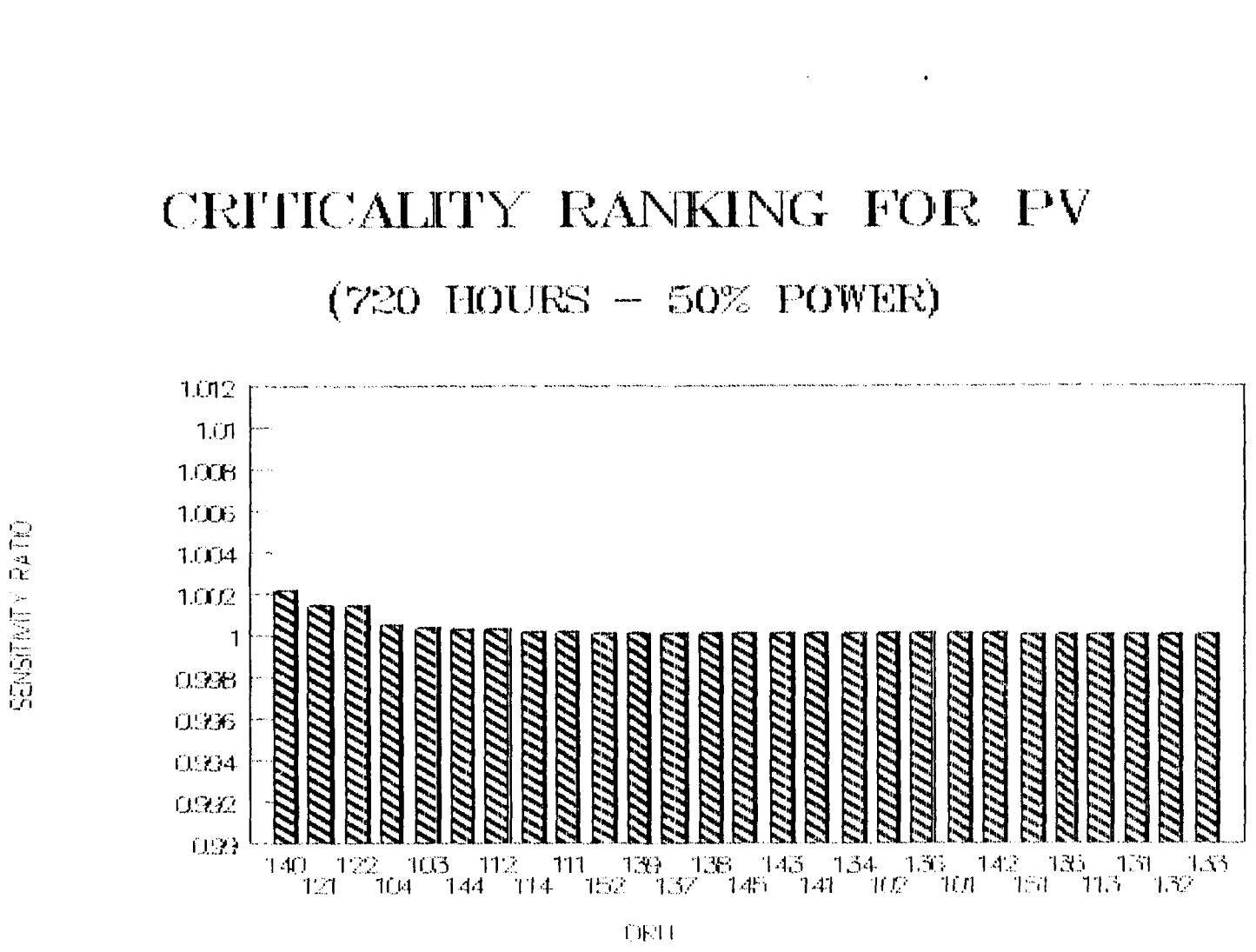

Figure B-1b. Criticality Ranking for PV Model (Perfect Reliability).

CRITICALITY RANKING FOR PV

(4380 HOURS – 100% POWER)

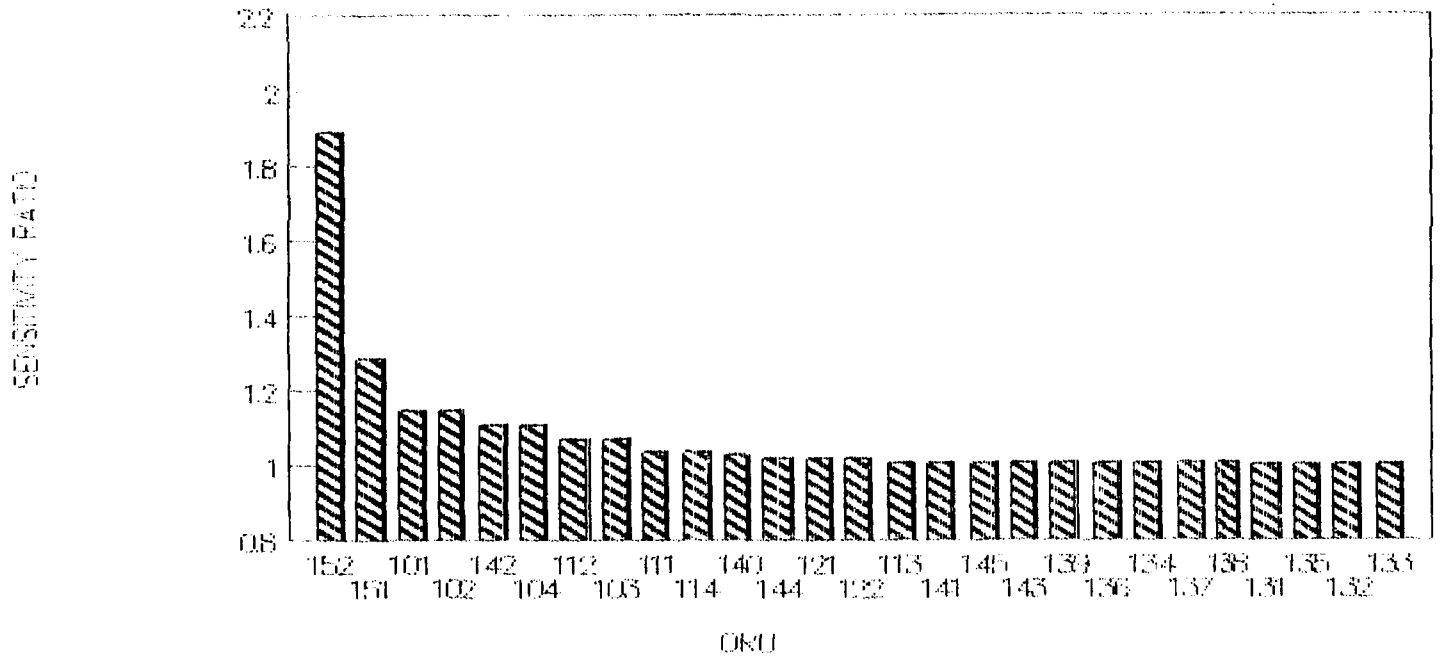

Figure B-1c. Criticality Ranking for PV Model (Perfect Reliability).

CRITICALITY RANKING FOR PV

(4380 HOURS – 50% POWER)

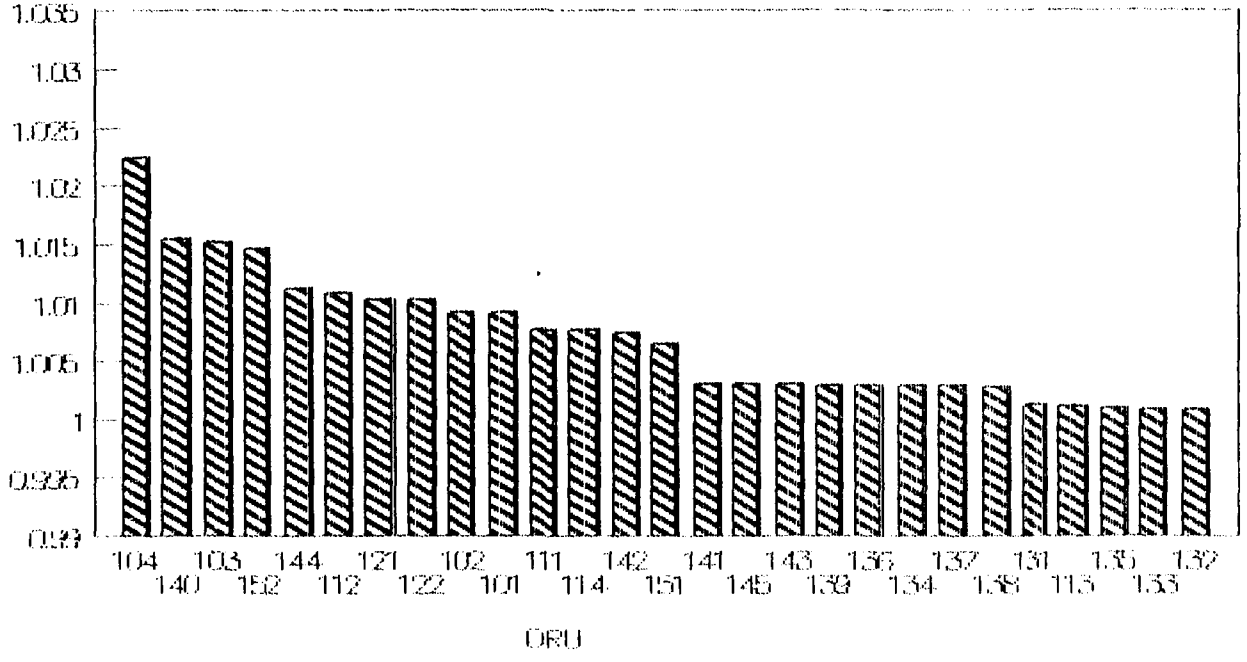

Figure B-1d. Criticality Ranking for PV Model (Perfect Reliability).

CRITICALITY RANKING FOR PV

(8760 HOURS – 100% POWER)

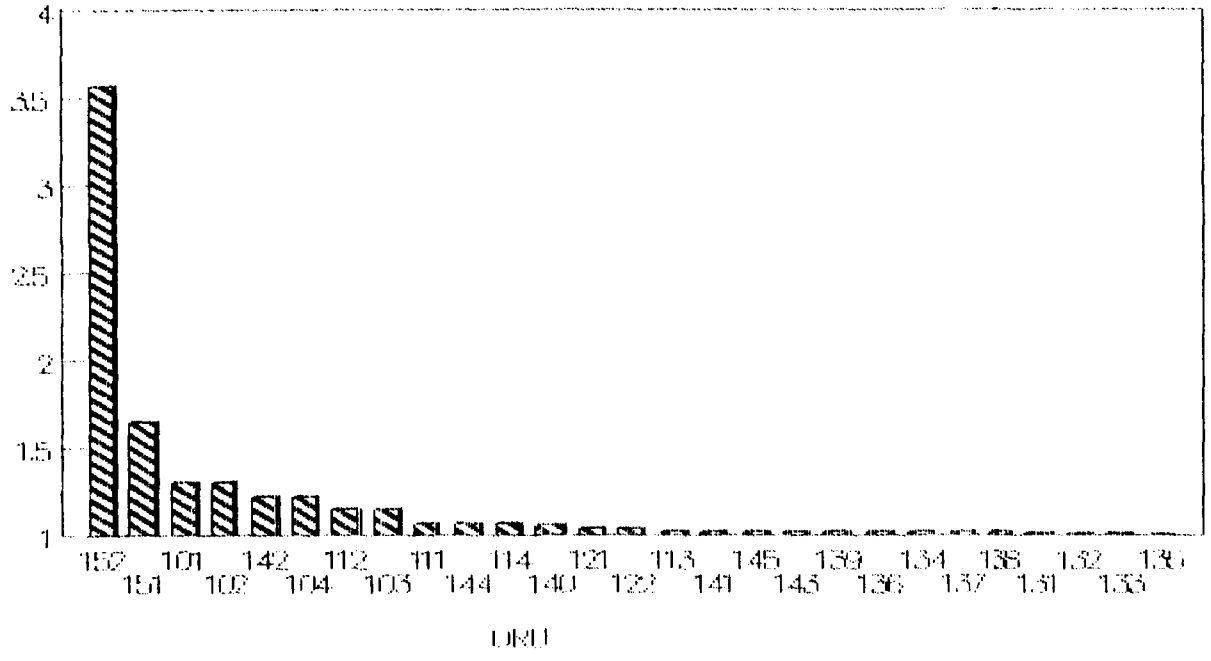

Figure B-1e. Criticality Ranking for PV Model (Perfect Reliability).

CRITICALITY RANKING FOR PV

(8760 HOURS – 50% POWER)

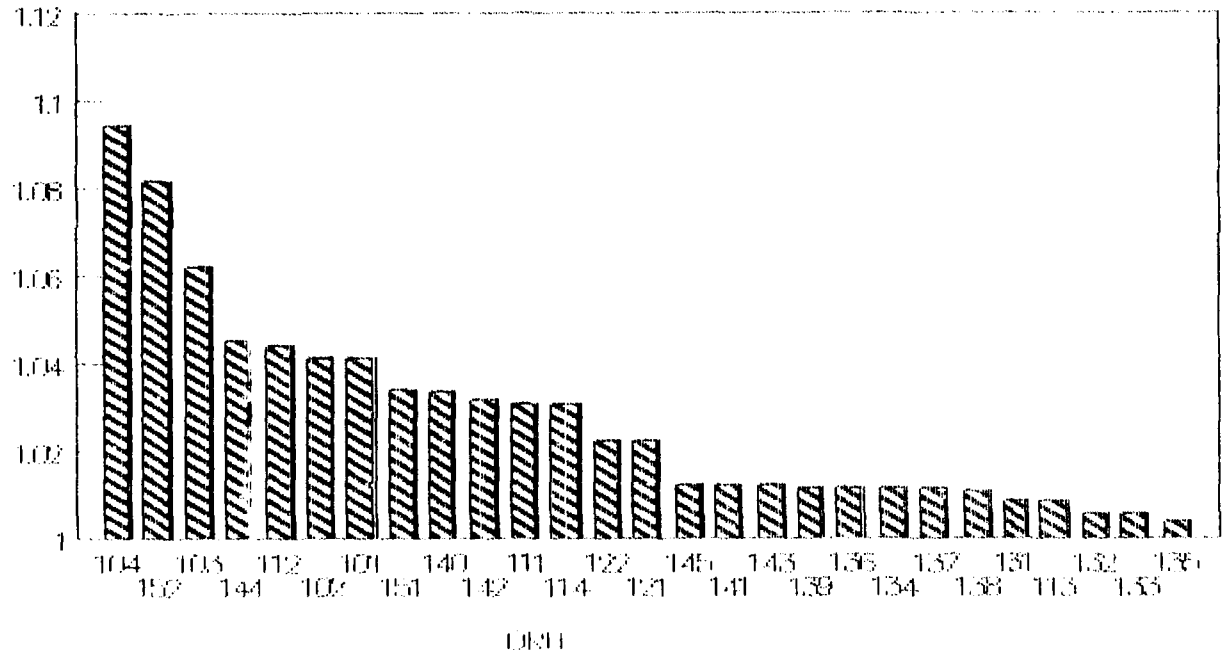

Figure B-1f. Criticality Ranking for PV Model (Perfect Reliability).

CRITICALITY RANKING FOR PV

(17520 HOURS – 100% POWER)

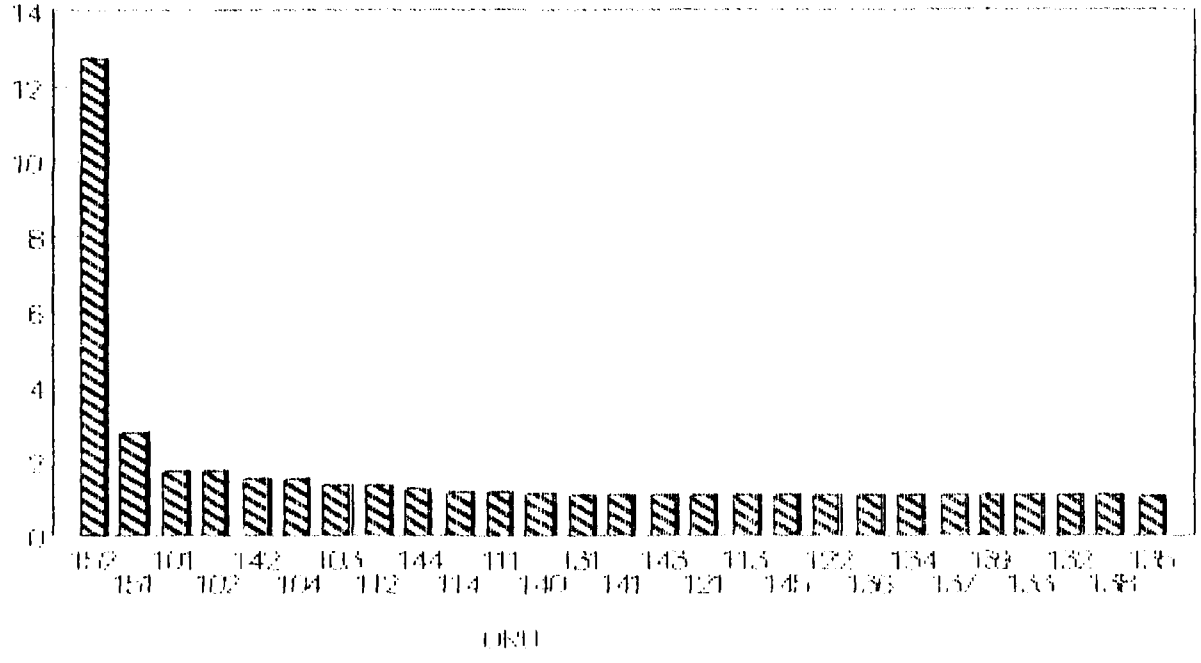

Figure B-1g. Criticality Ranking for PV Model (Perfect Reliability).

CRITICALITY RANKING FOR PV

(17520 HOURS – 50% POWER)

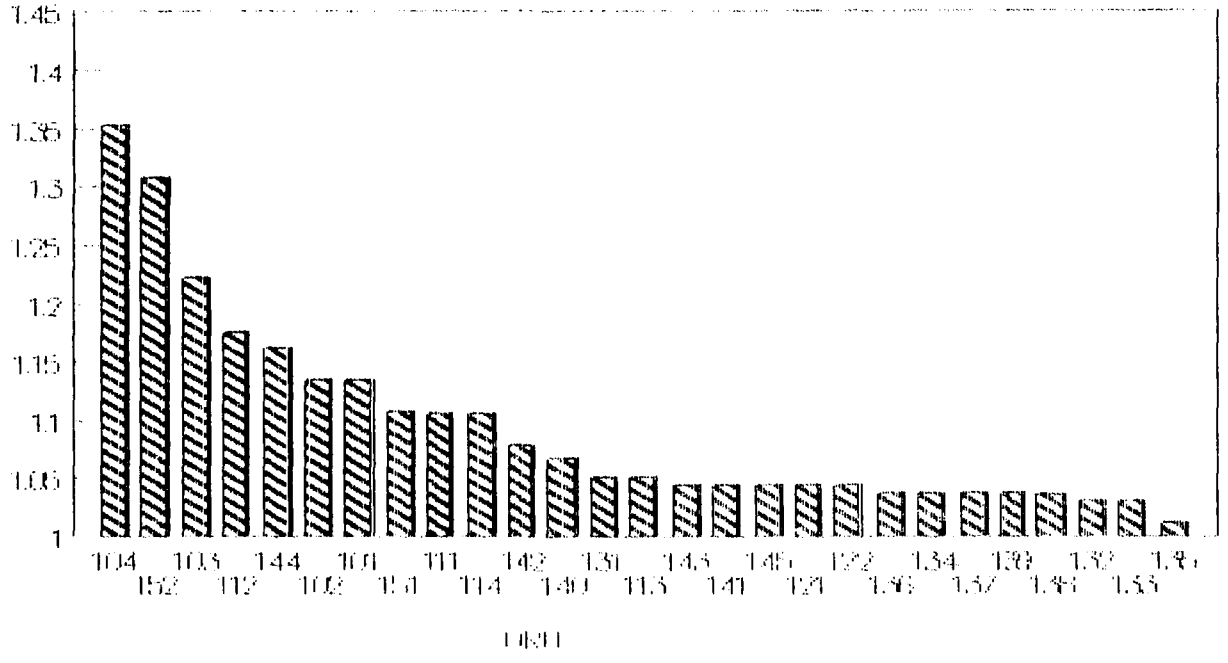

Figure B-1h. Criticality Ranking for PV Model (Perfect Reliability).

CRITICALITY RANKING FOR PV

(43800 HOURS – 66.7% POWER)

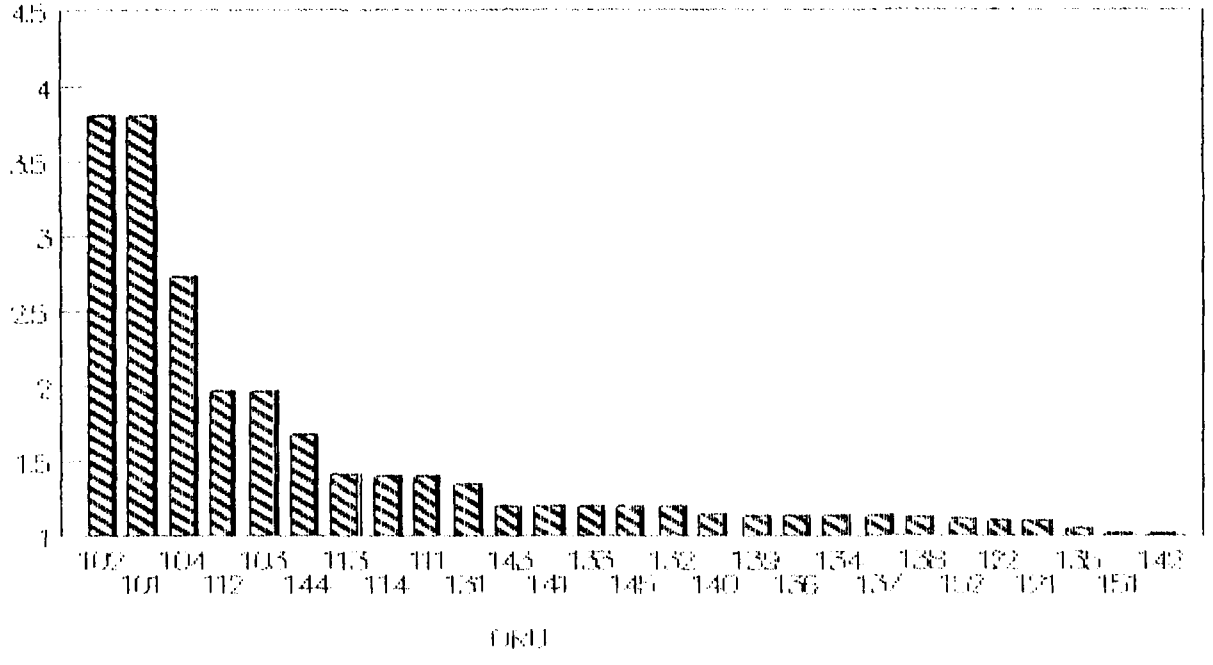

Figure B-1i. Criticality Ranking for PV Model (Perfect Reliability).

CRITICALITY RANKING FOR PV

(43800 HOURS – 50% POWER)

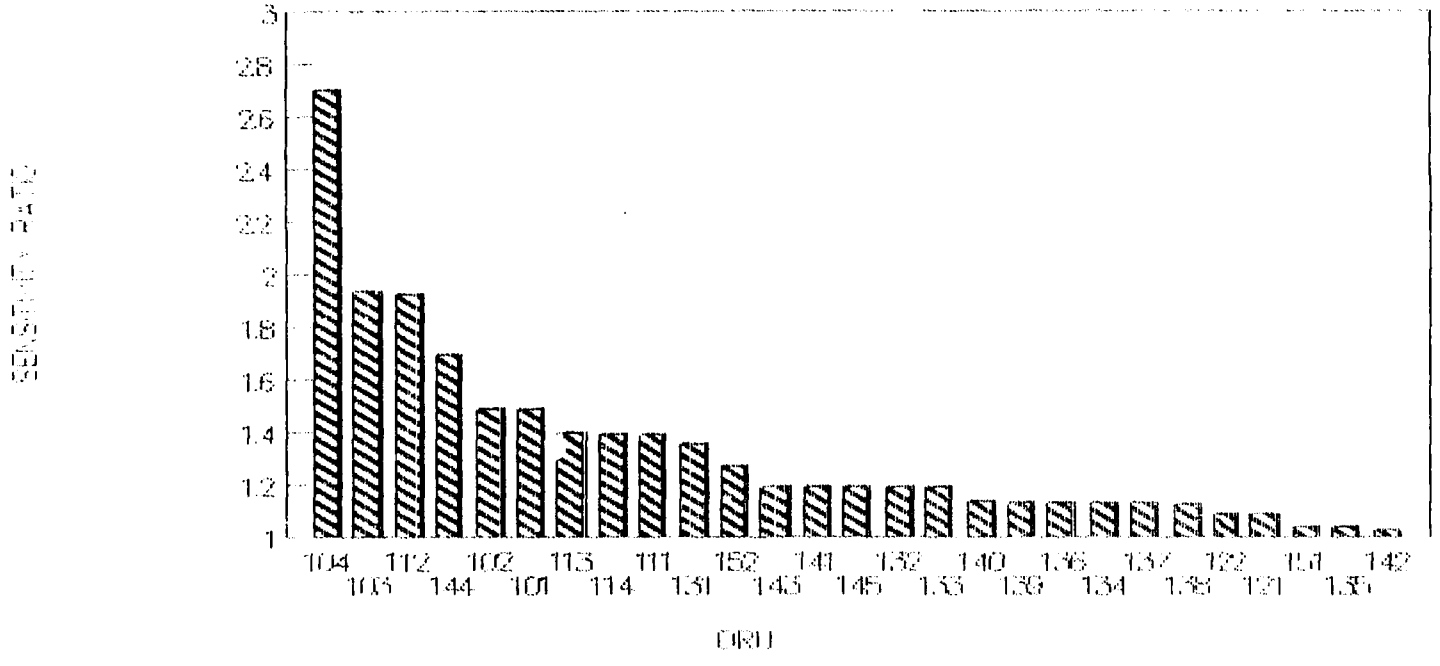

Figure B-1j. Criticality Ranking for PV Model (Perfect Reliability).

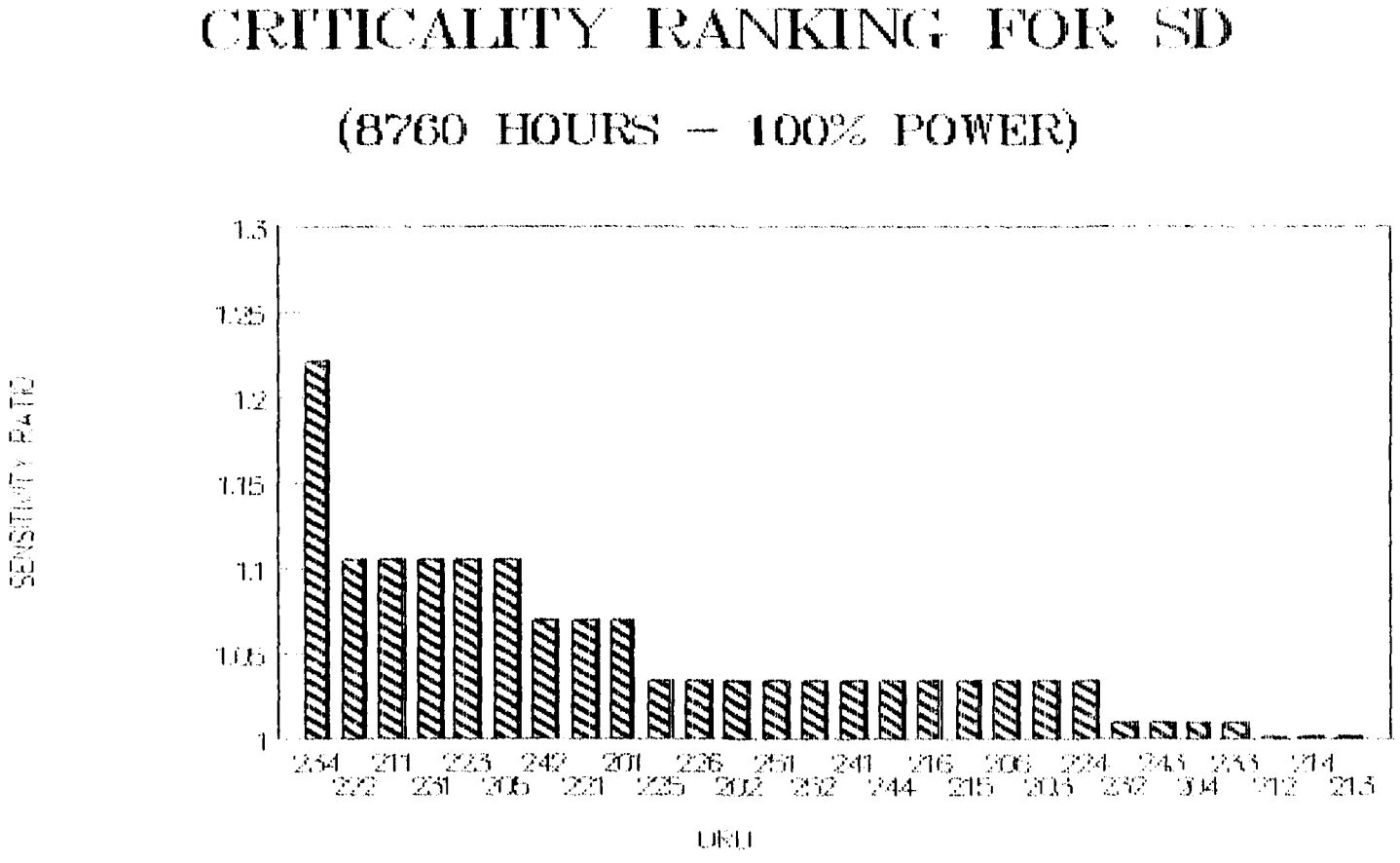

Figure B-2. Criticality Ranking for SD Model (Perfect Reliability).

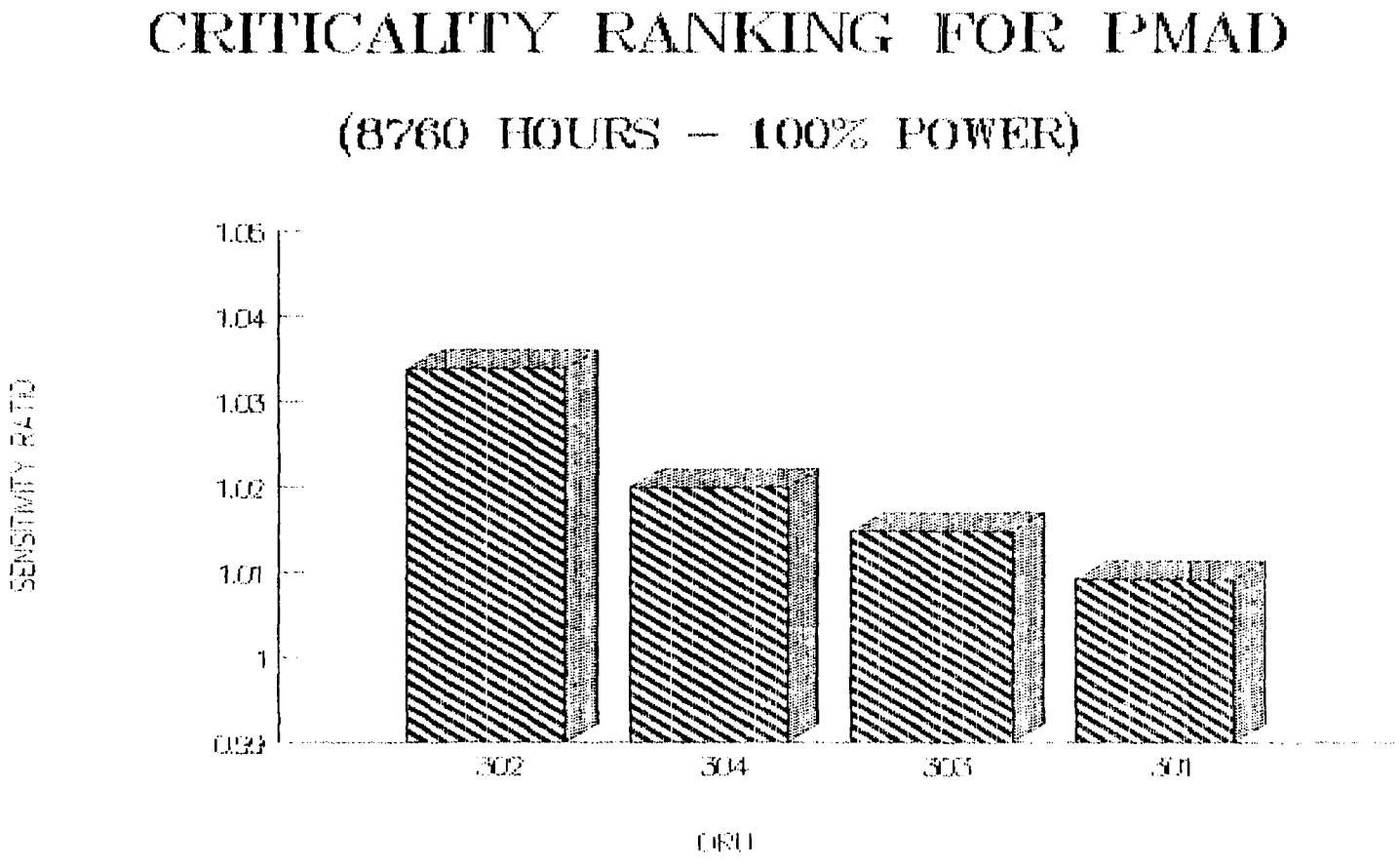

Figure B-3. Criticality Ranking for PMAD Model (Perfect Reliability).

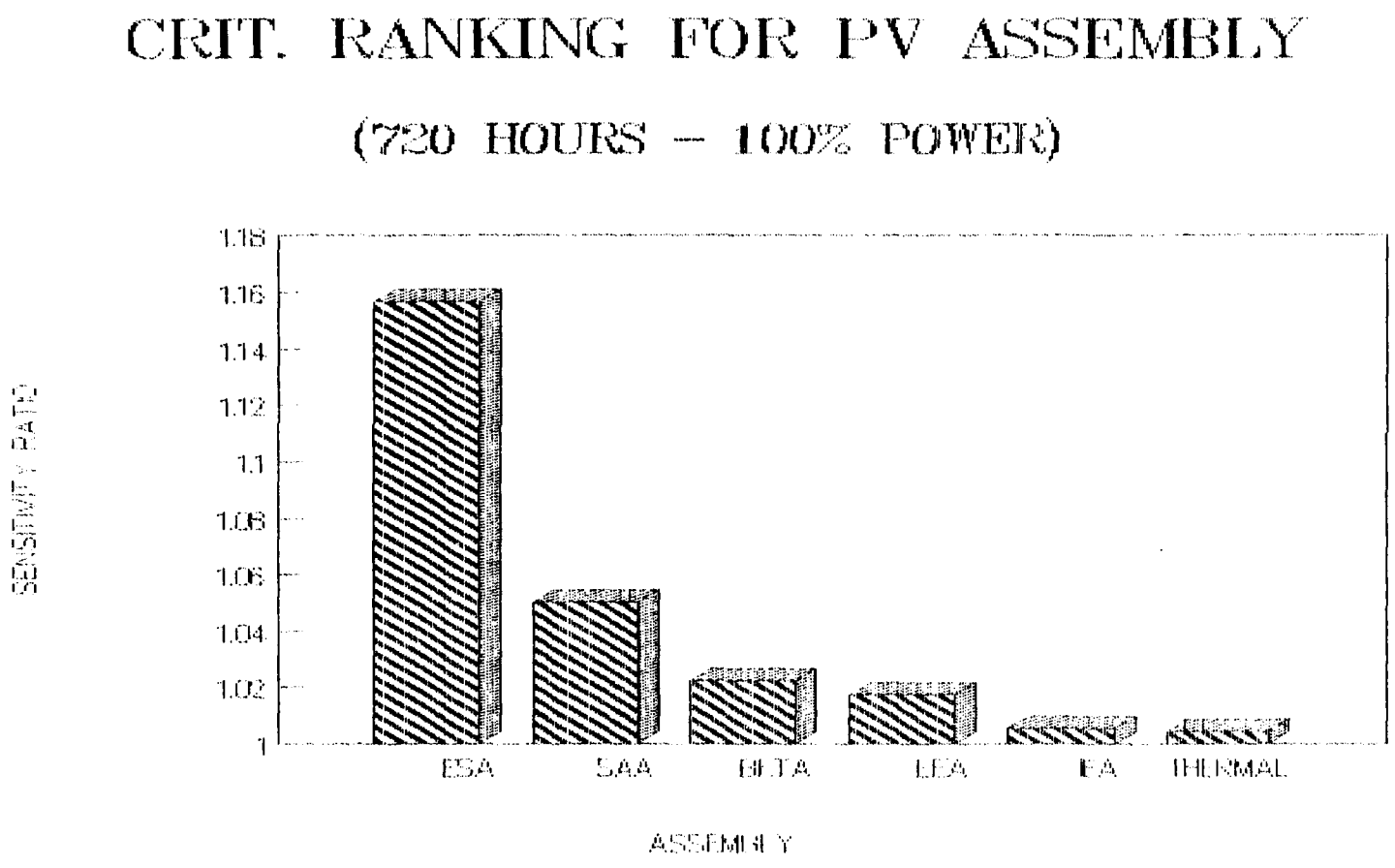

Figure B-4a. Criticality Ranking for PV Assemblies (Perfect Reliability).

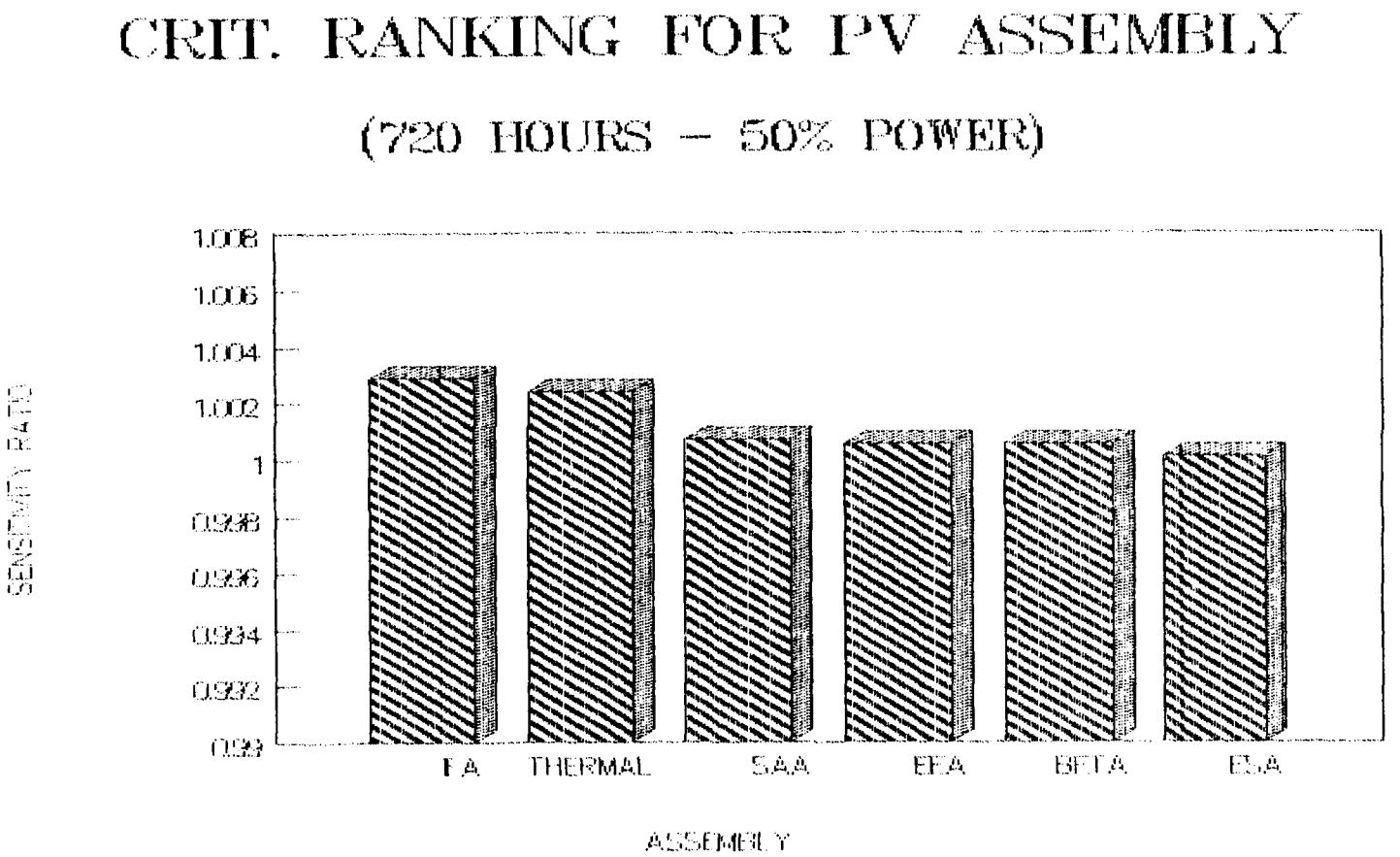

Figure B-4b. Criticality Ranking for PV Assemblies (Perfect Reliability).

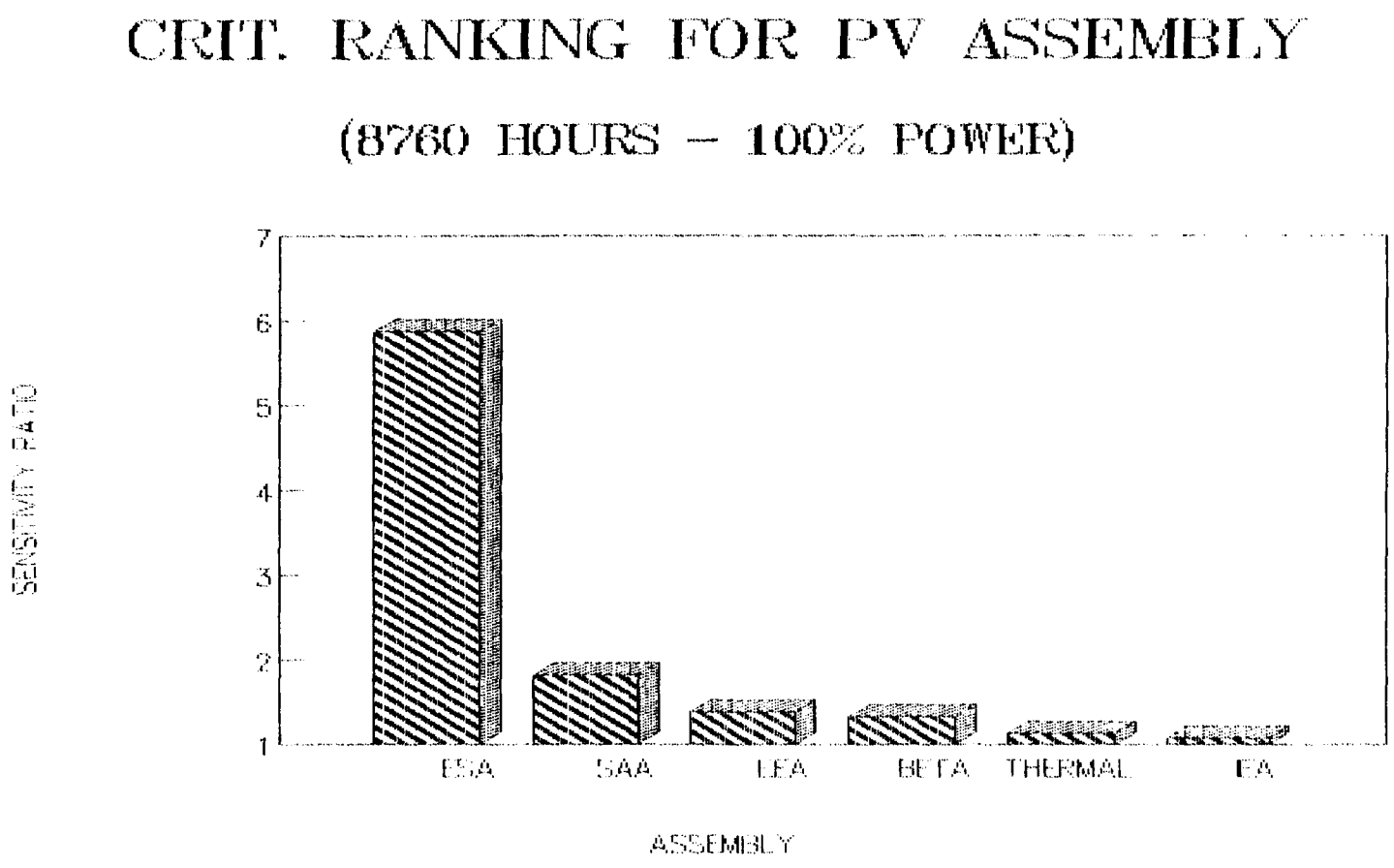

Figure B-4c. Criticality Ranking for PV Assemblies (Perfect Reliability).

CRIT. RANKING FOR PV ASSEMBLY

(8760 HOURS – 50% POWER)

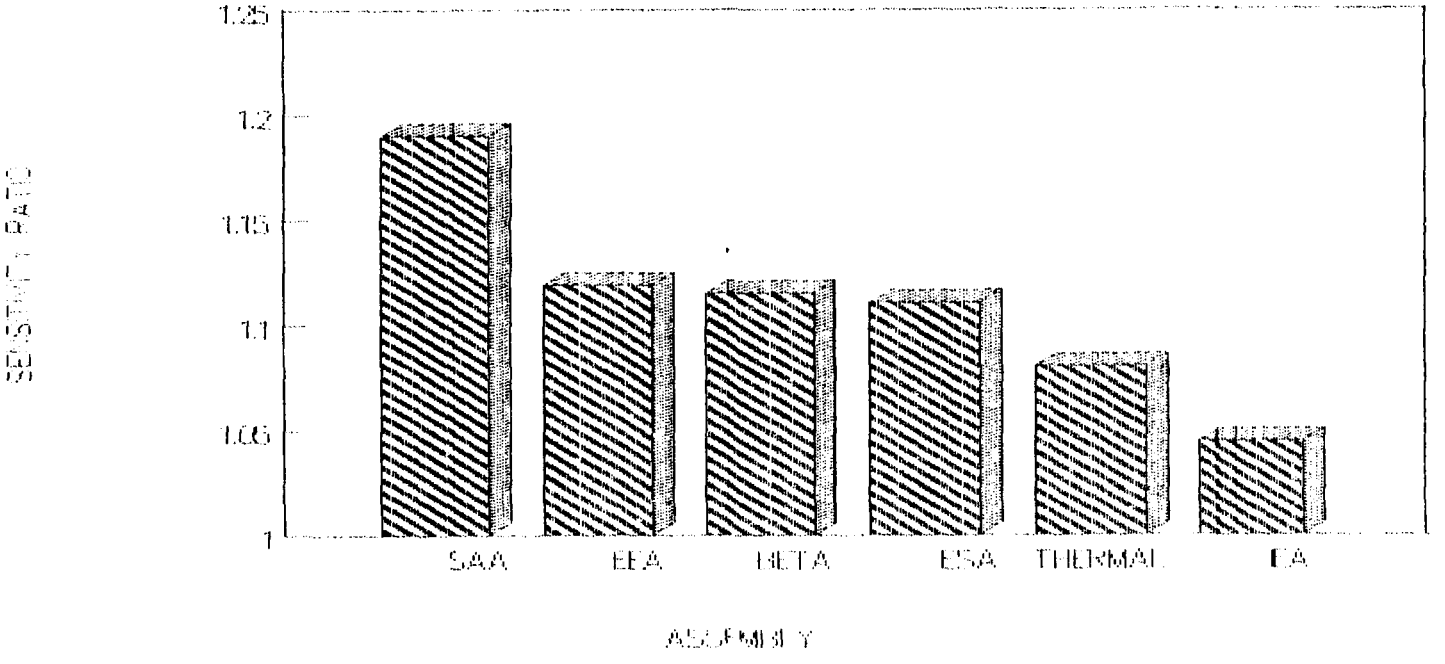

Figure B-4d. Criticality Ranking for PV Assemblies (Perfect Reliability).

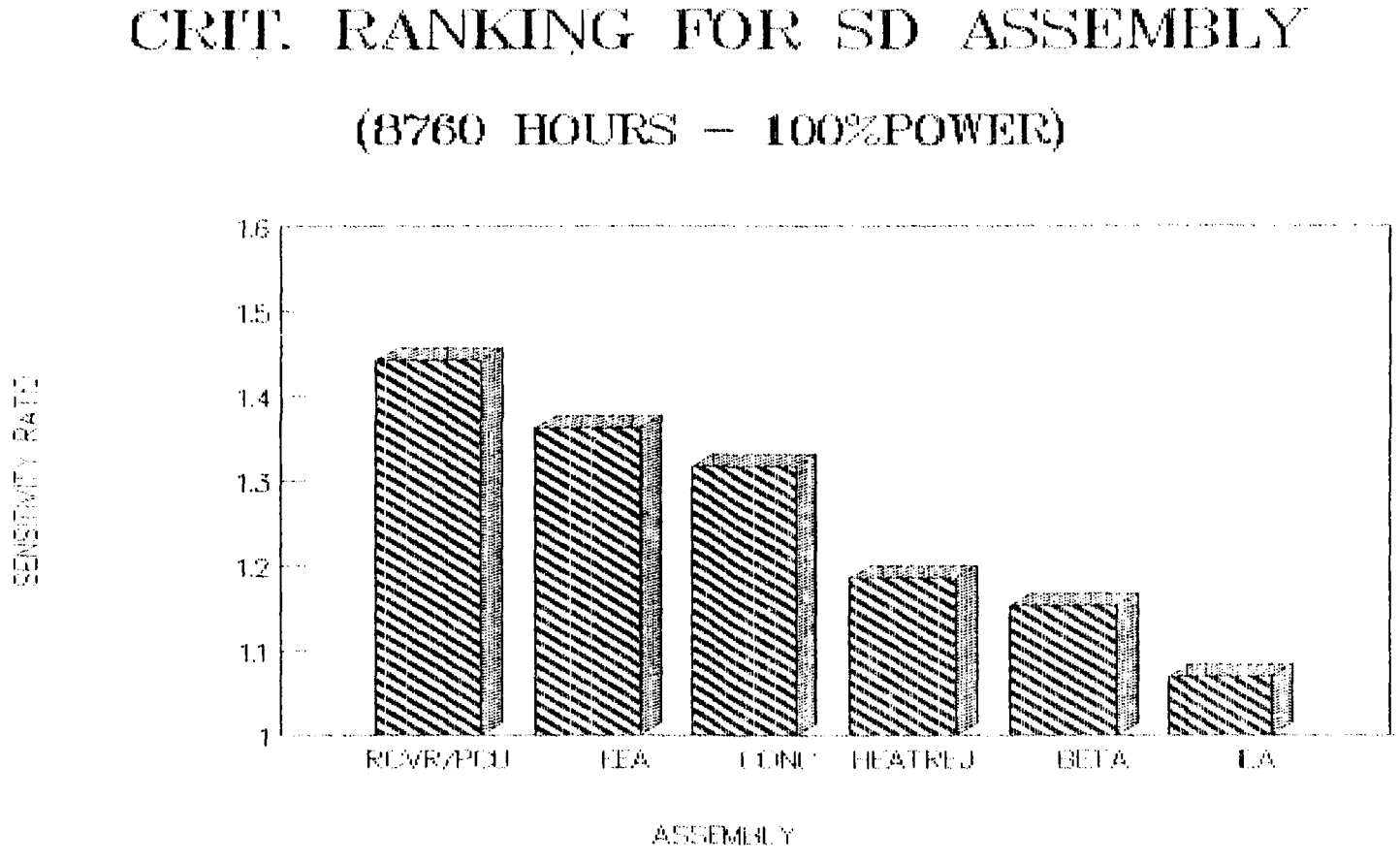

Figure B-5. Criticality Ranking for SD Assemblies (Perfect Reliability).

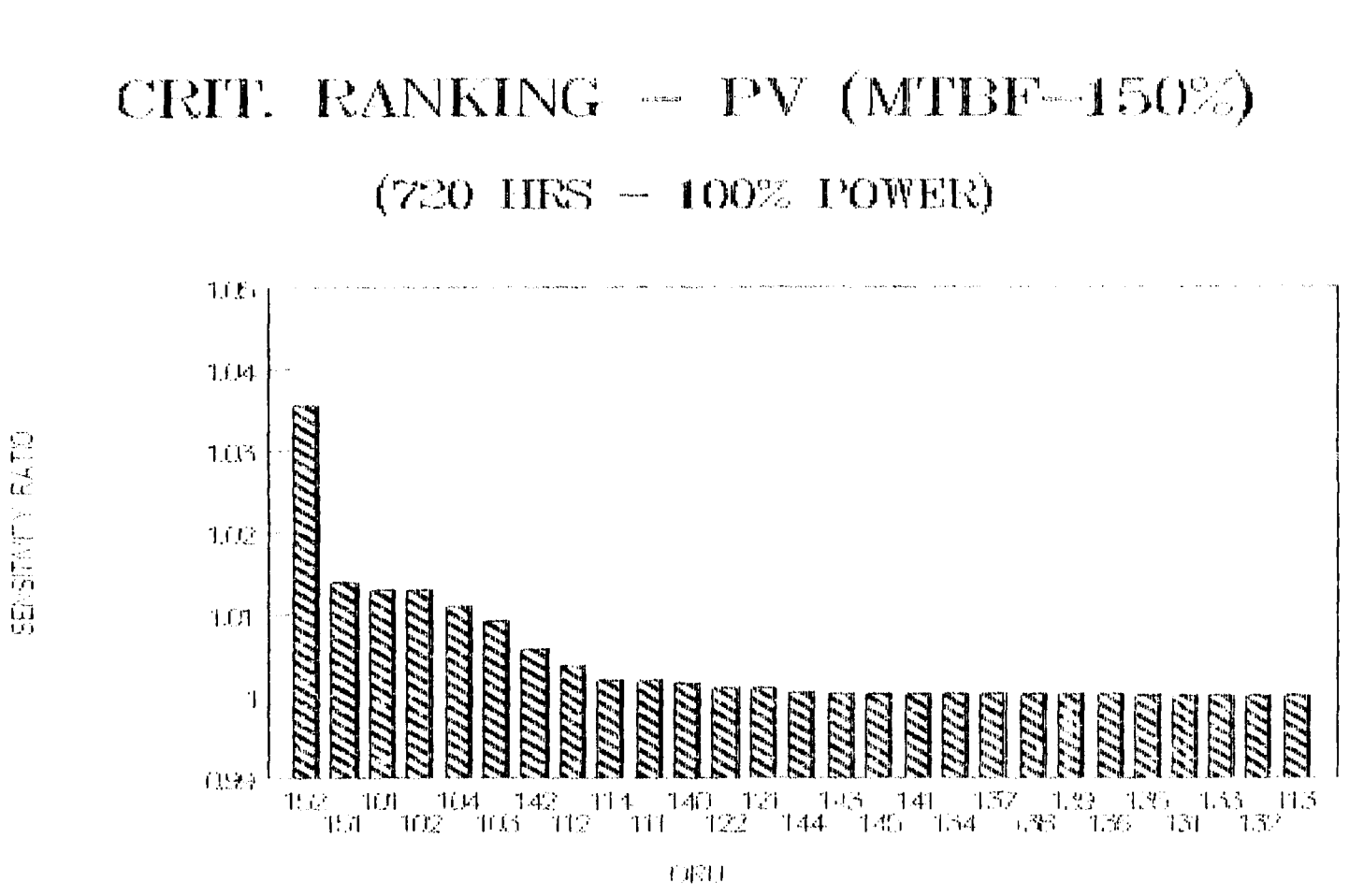

Figure B-6a. Criticality Ranking for PV Model (150% MTBF).

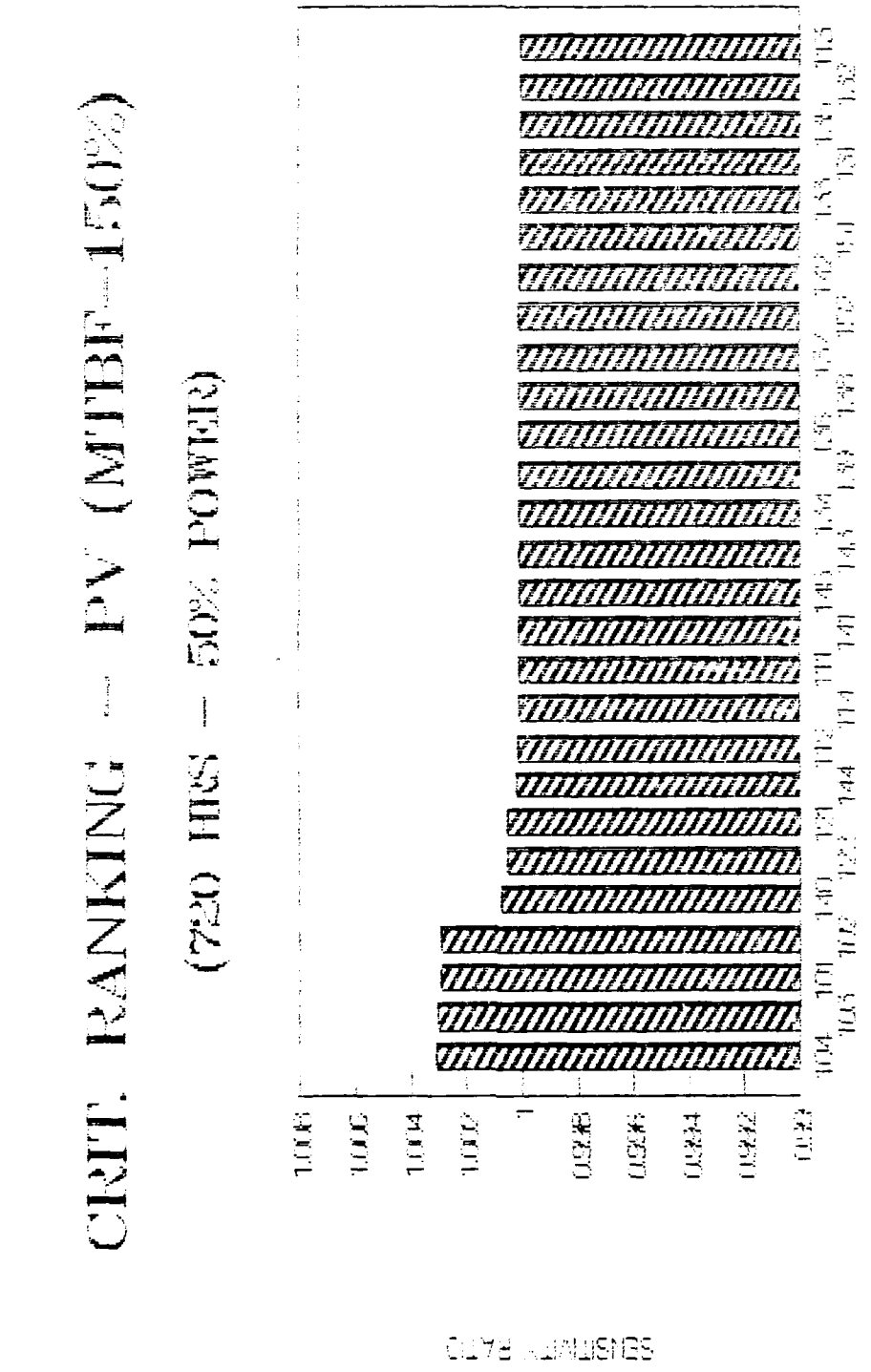

Figure B-6b. Criticality Ranking for PV Model (150% MTBF).

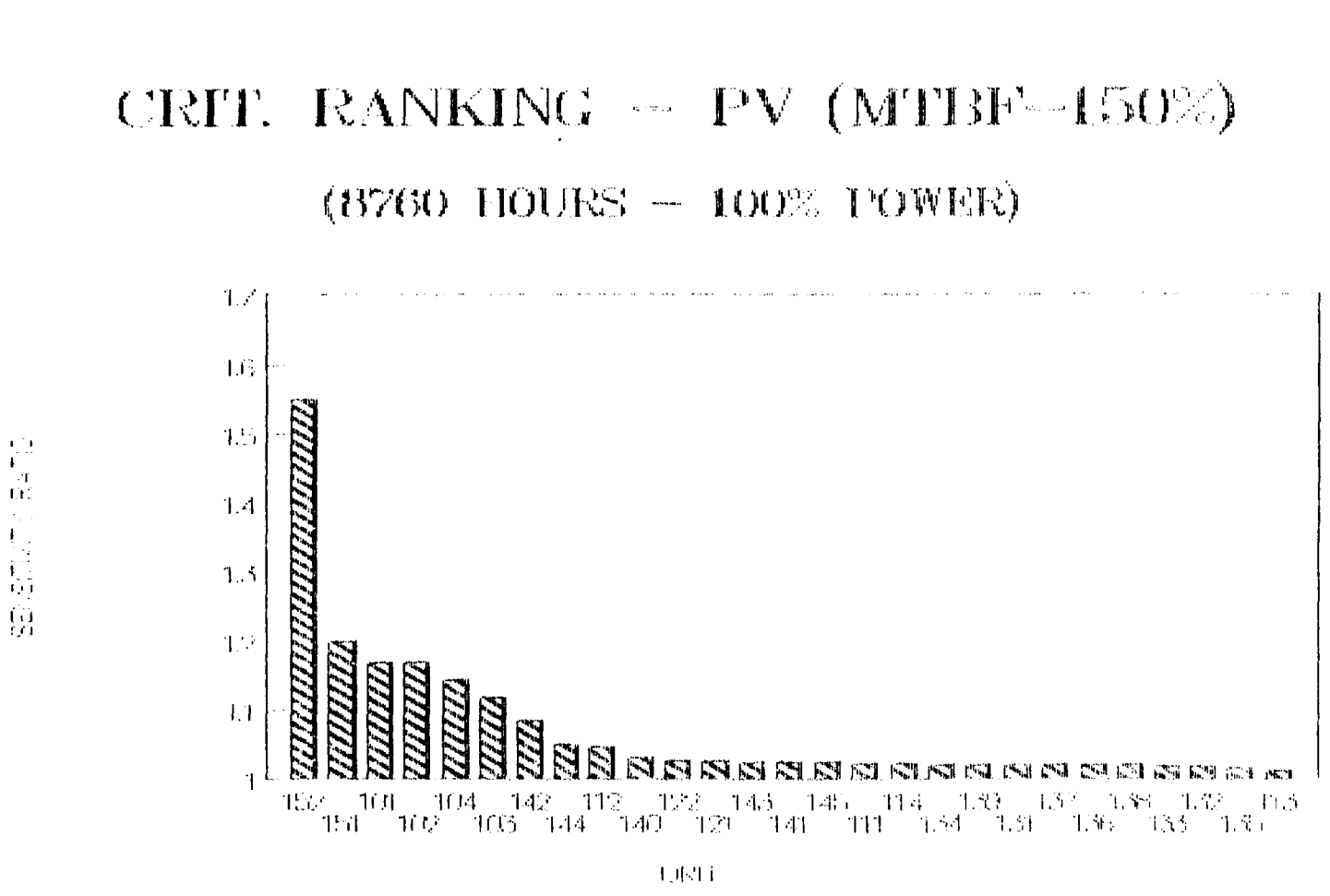

Figure B-6c. Criticality Ranking for PV Model (150% MTBF).

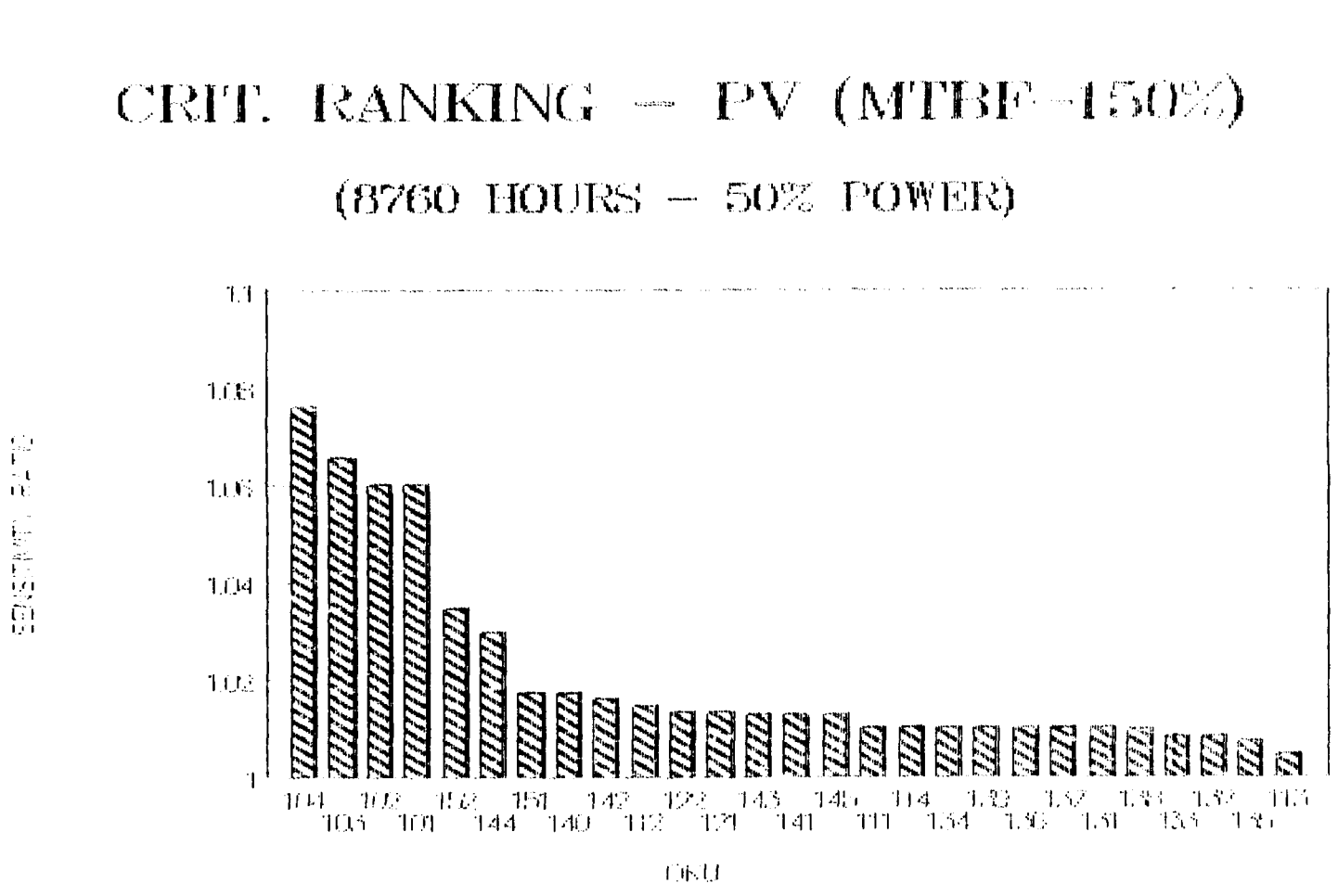

Figure B-6d. Criticality Ranking for PV Model (150% MTBF).

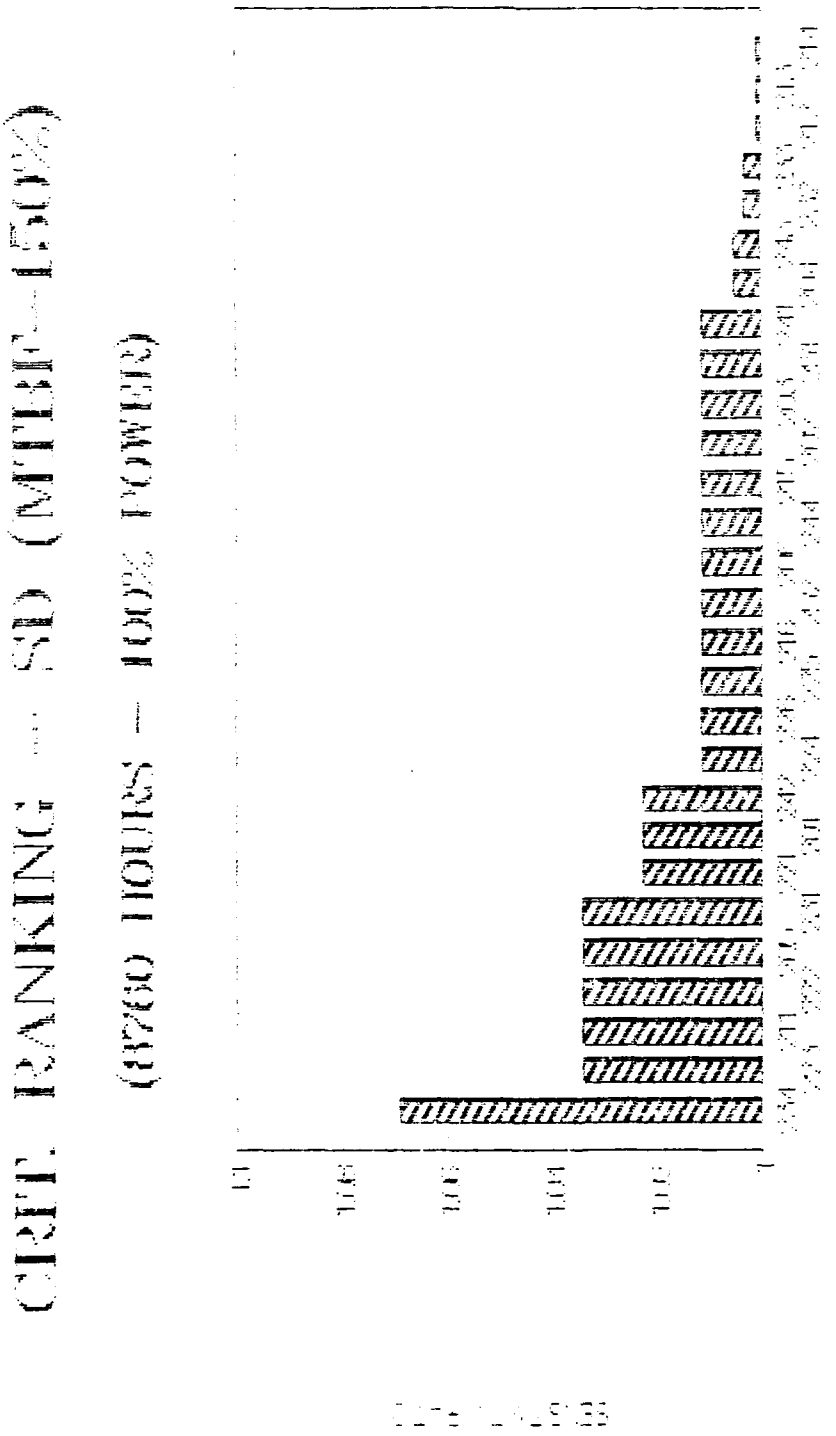

Figure B-7. Criticality Ranking for SD Model (150% MTBF).

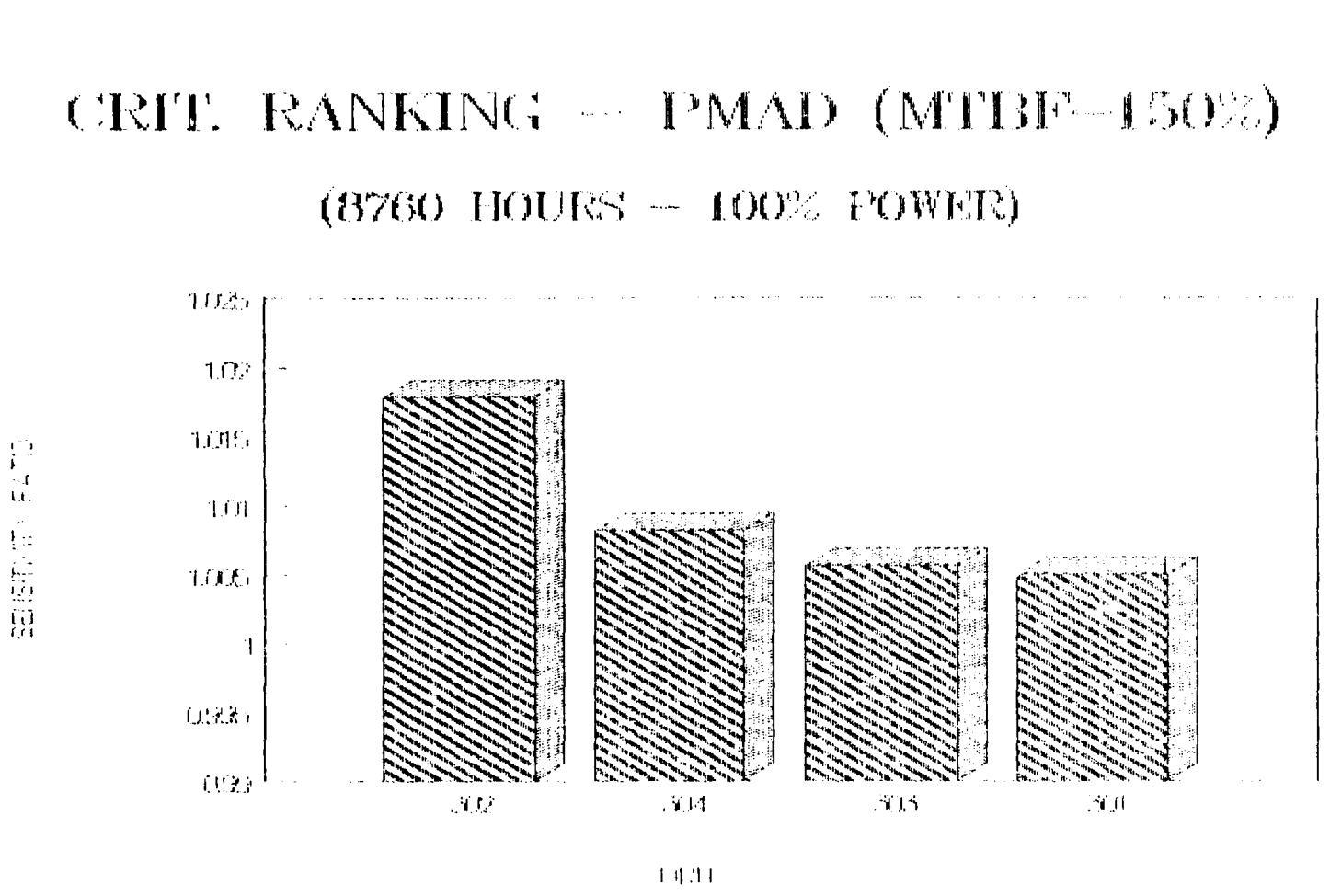

Figure B-8. Criticality Ranking for PMAD Model (150% MTBF).

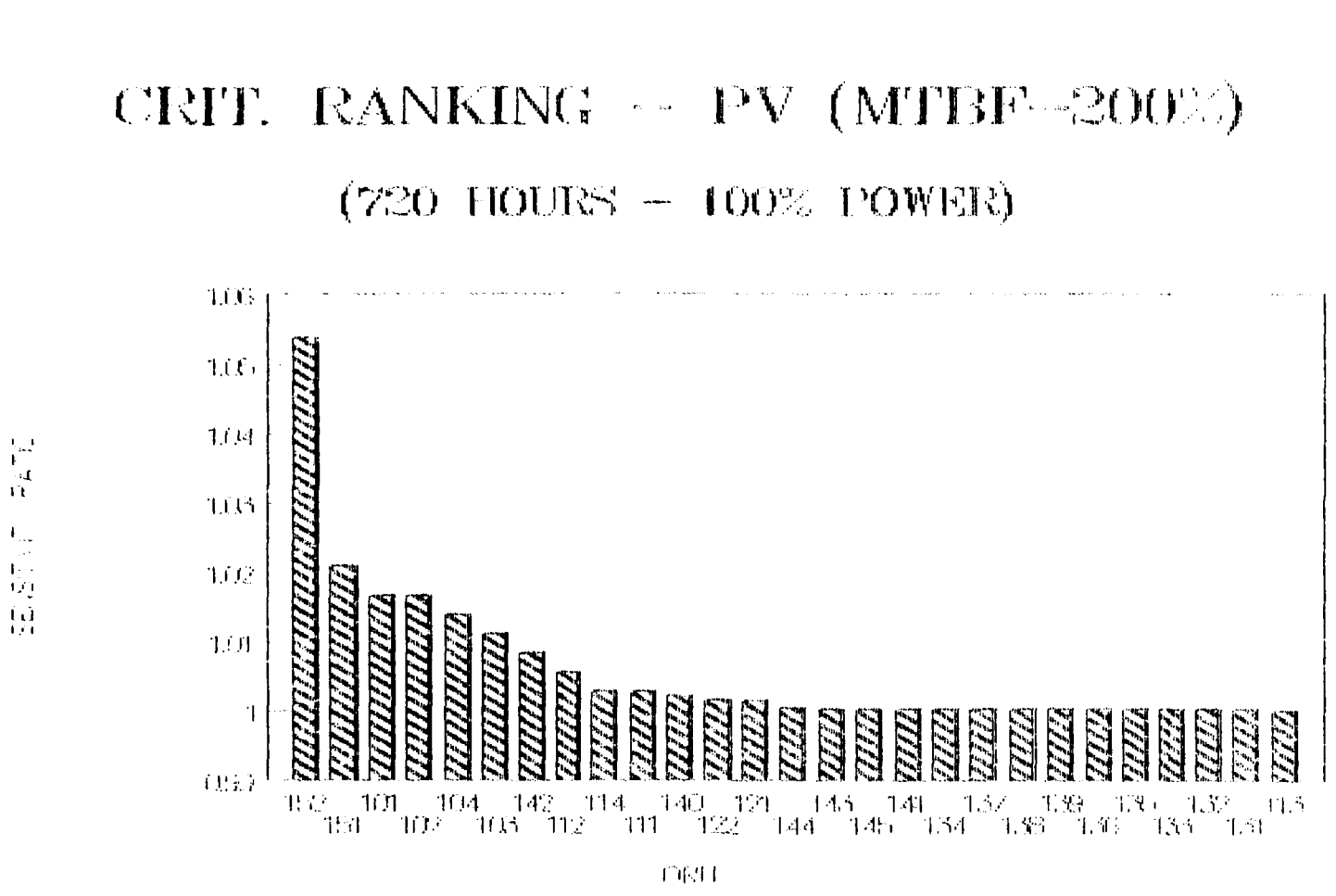

Figure B-9a. Criticality Ranking for PV MOdel (200% MTBF).

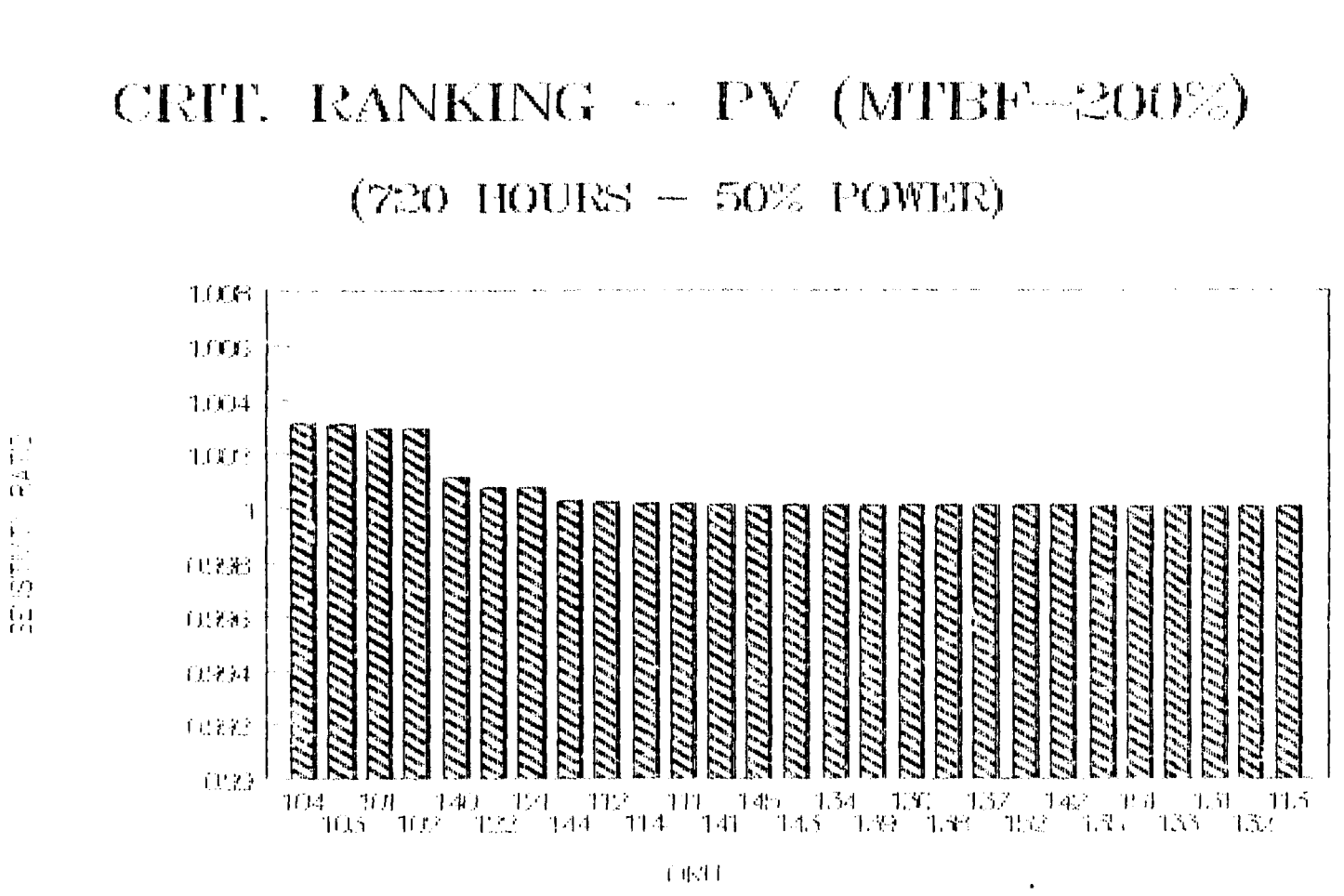

Figure B-9b. Criticality Ranking for PV Model (200% MTBF).

CRIT. RANKING — PV (MTBF=200%)

(8760 HOURS — 100% POWER)

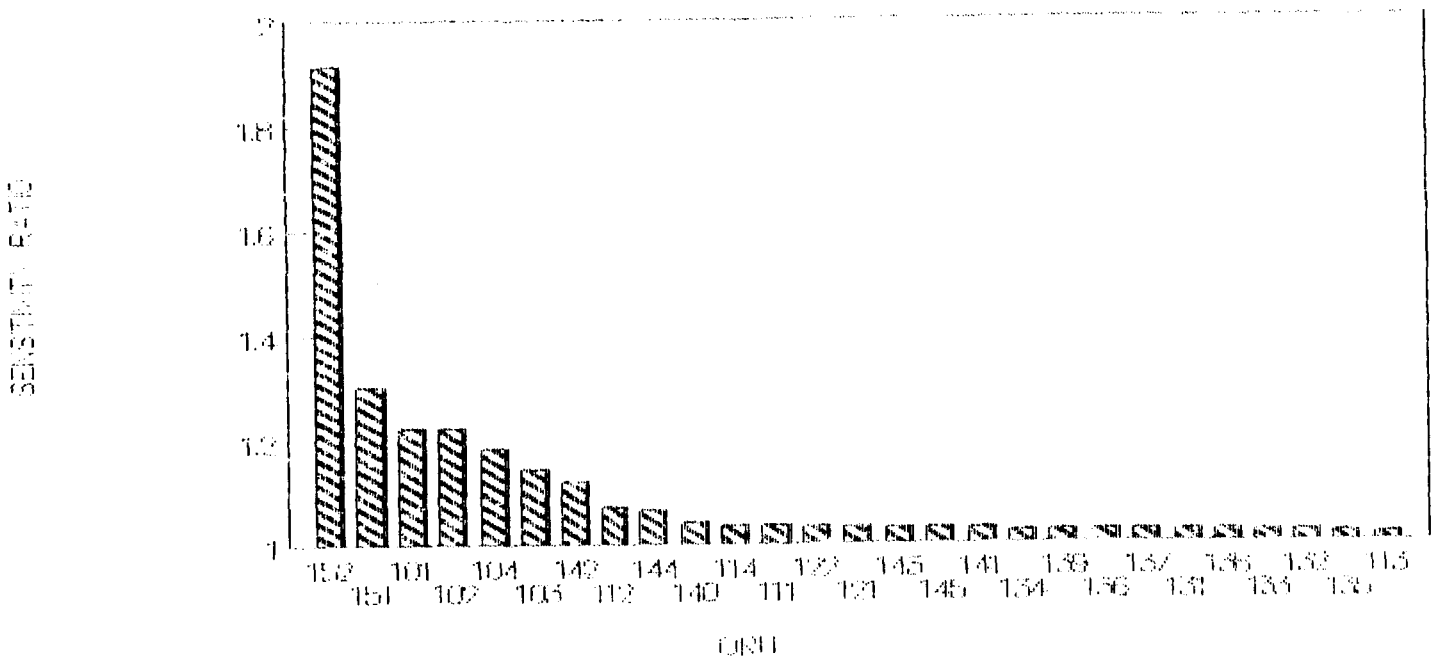

Figure B-9c. Criticality Ranking for PV Model (200% MTBF).

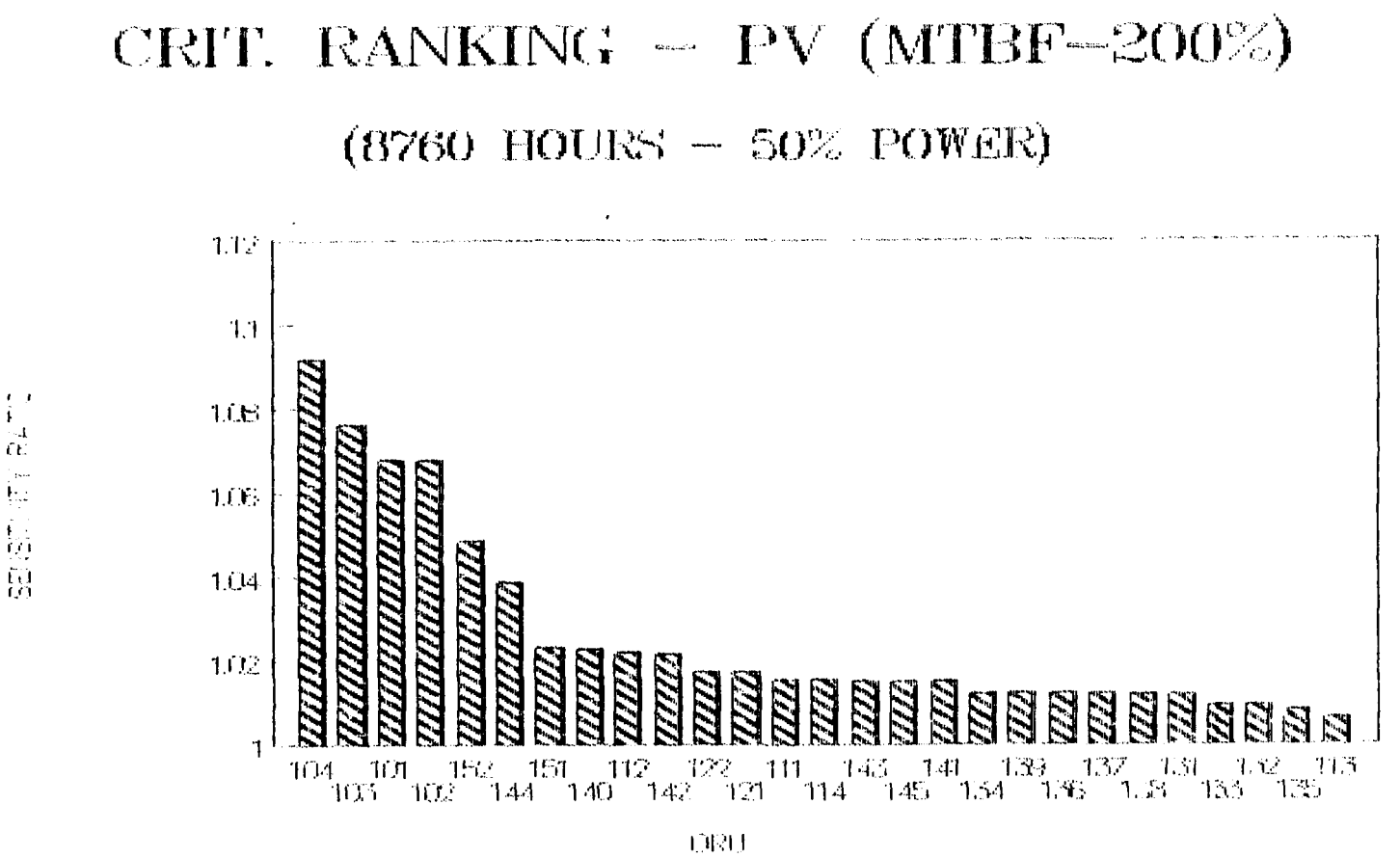

Figure B-9d. Criticality Ranking for PV Model (200% MTBF).

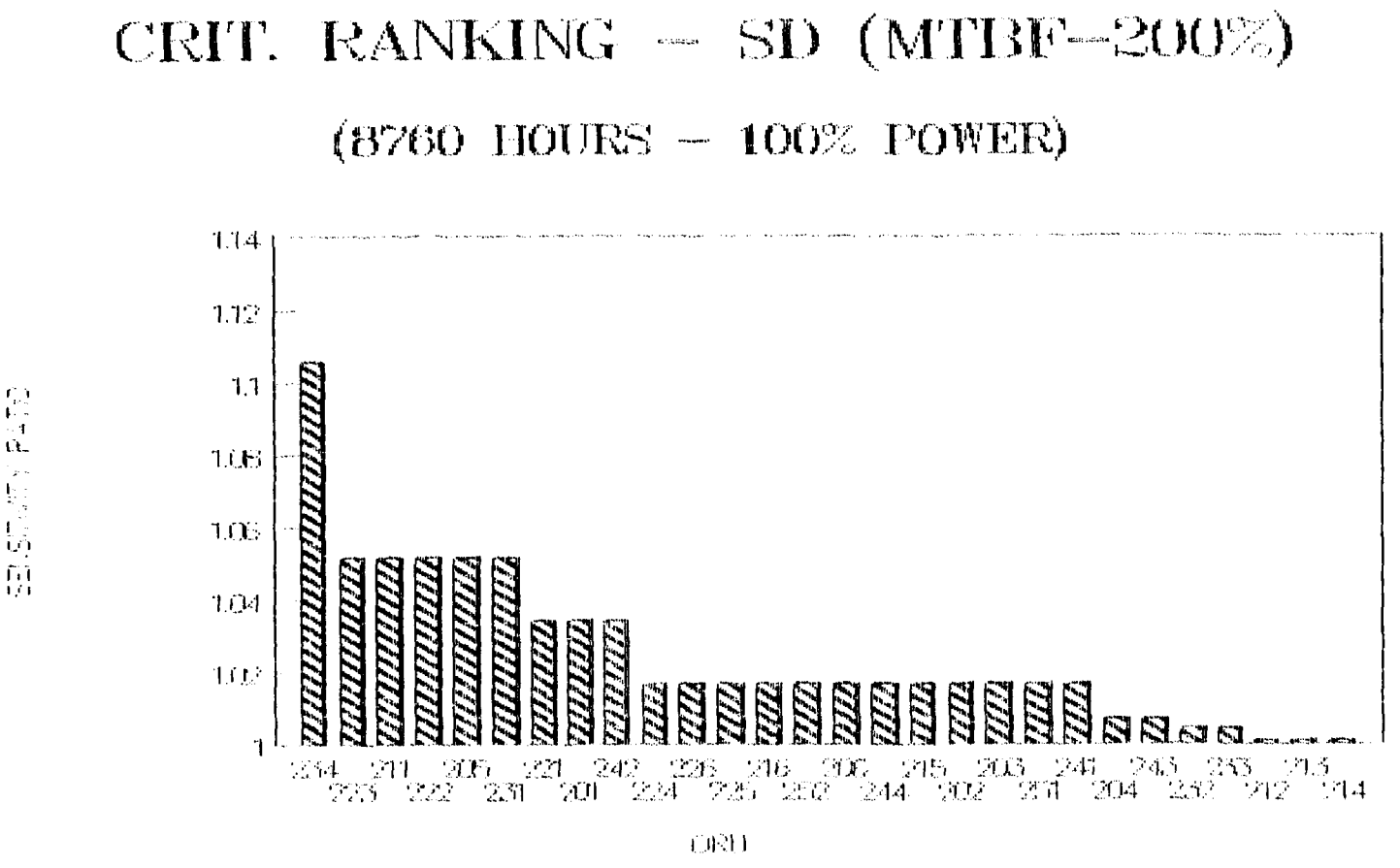

Figure B-10. Criticality Ranking for SD Model (200% MTBF).

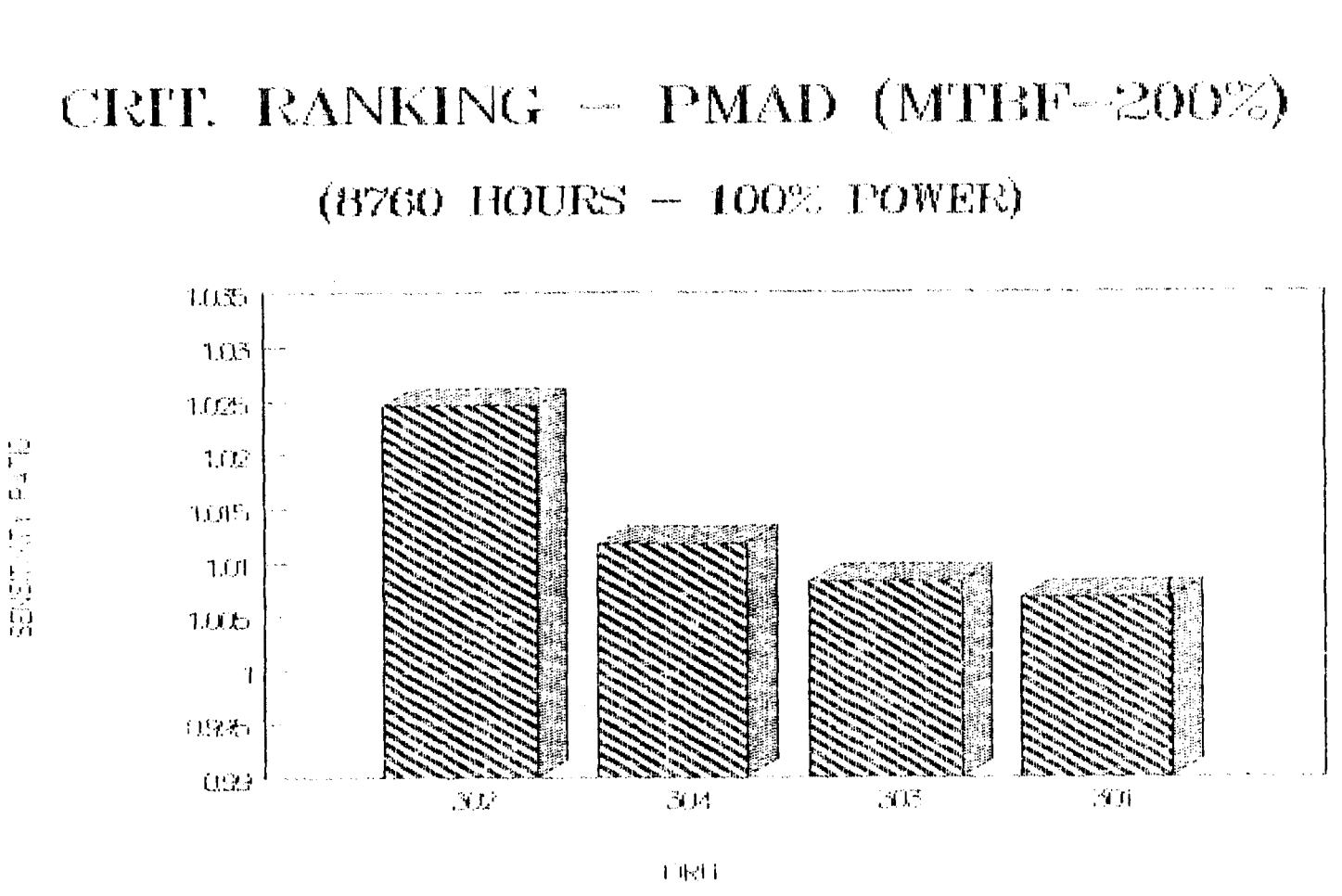

Figure B-11. Criticality Ranking for PMAD Model (200% MTBF).

APPENDIX C - ABBREVIATIONS

AC	alternating current
ADCU	AC to DC control unit
BCDU	battery charge/discharge unit
BGA	beta gimbal assembly
CNDSR	condenser
DC	direct current
EEA	electrical equipment assembly
EPS	Electrical Power System
ESA	energy storage assembly
GIM	gimbal
HRA	heat rejection assembly
IBM	International Business Machines
IEA	integrated equipment assembly
SABB	solar array blanket and box
IS/IHA	interface structure/integration hardware assembly
LeRC	Lewis Research Center
MBSU	main bus switching unit
MIU	main inverter unit
MTBF	mean-time-between-failure
NASA	National Aeronautics and Space Administration
ORU	orbital replacement unit
PCU	power control unit
PDCU	power distribution control unit
PMAD	power management and distribution
PMC	power management controller
PSDD	Power System Description Document
PVSC	photovoltaic source controller
PC	personnel computer
PV	photovoltaic
RAM	reliability, availability, and maintainability
RBD	reliability block diagram
SAA	solar array assembly
SSU	sequential shunt unit
SD	solar dynamic
TCA	thermal control assembly